A Study of Nonlinear Negative Capacitance

By

CHARLES LESTER WRIGHT, JR.

CYRUS O. HARBOURT

August 16, 1965

Technical Report No. 5

LABORATORIES FOR ELECTRONICS AND
RELATED SCIENCE RESEARCH
College of Engineering-Electrical Engineering
THE UNIVERSITY OF TEXAS
AUSTIN, TEXAS 78712

The University of Texas' Laboratories for Electronics and Related Science Research are interdisciplinary laboratories in which graduate faculty members and graduate candidates from numerous academic disciplines conduct research.

Research conducted for this technical report was supported in part by the Department of Defense's JOINT SERVICES ELECTRONICS PROGRAM (U. S. Army, U. S. Navy, and the U. S. Air Force) through the Research Grant AF-AFOSR 766-65. This program is monitored by the Department of Defense's JSEP Technical Advisory Committee consisting of representatives from the U. S. Army Electronics Laboratories, U. S. Army Research Office, Office of Naval Research, and the U. S. Air Force Office of Scientific Research.

Additional support of specific projects by other Federal Agencies, Foundations, and The University of Texas is acknowledged in footnotes to the appropriate sections.

THE UNIVERSITY OF TEXAS

LABORATORIES FOR ELECTRONICS AND RELATED SCIENCE RESEARCH

A STUDY OF NONLINEAR NEGATIVE CAPACITANCE

Technical Report No. 5

By

CHARLES LESTER WRIGHT, JR.*

CYRUS O. HARBOURT+

August 16, 1965

*Research Engineer Assistant III, Candidate for Ph.D. degree in Electrical Engineering

+Associate Professor of Electrical Engineering

ABSTRACT

An analytical study is made of the behavior of a certain class of RLC networks which contain a theoretical nonlinear negative capacitance along with various possible combinations of constant parasitic elements that are certain to be present in any physical realization of this type of capacitance. The theoretical capacitor is defined in terms of its charge-voltage relationship, i.e., $e = -aq + bq^3$, where e is the voltage across the terminals of the capacitor, q is the charge associated with the capacitor, and a and b are arbitary, positive, real constants.

This study is directed toward an evaluation of the usefulness of a nonlinear negative capacitance in a network to accomplish either amplification or oscillation or switching.

In order for a network to be useful as an amplifier, its small-signal model must be stable. Therefore, for this part of the study the nonlinear capacitor is represented by a linear, negative capacitance. Of the twenty-four networks defined for this study only two are found to be possibly stable. Both of these networks, and only these networks, have a positive capacitor in series with the assumed negative capacitor.

Singular point analysis discloses that any of the defined networks may have two stable equilibrium points. This is the basic criterion for a bistable device, so the conclusion is that nonlinear capacitance, like nonlinear resistance, can be used effectively to construct a switching circuit. Phase plane plots of one of the second order networks are included to illustrate switching from each stable singularity to the other.

It is proven by phase plane methods that none of the second order systems can support a sustained oscillation. An argument based on energy relationships and on the nonoscillatory nature of the second order networks is presented to show that none of the third order networks can serve as oscillators. Hence, the results here indicate that, unlike negative resistance, negative capacitance cannot be used as the mechanism by which oscillation is induced in a passive network which contains dissipative elements.

A nonlinear negative capacitance has been realized by means of a transistor negative impedance converter circuit. From analysis of the negative impedance converter, the lumped model of the negative capacitance is predicted to be a nonlinear, frequency-dependent resistor in series with a nonlinear, frequency-dependent negative capacitor. The locus of the tip

of the complex impedance, as a function of frequency, is predicted in this analysis; this locus was subsequently verified by AC steady state measurements in the laboratory. Although not considered in the analytical study, the effect of unavoidable stray capacitance was seen in the experimental results.

The square wave response of the negative impedance converter is also obtained, and a relationship between the steady state square wave response and the values of the model is derived.

TABLE OF CONTENTS

CHAPTER I

NONLINEAR NEGATIVE CAPACITANCE

1.1 Introduction

The concept of a negative circuit element is not new. J. L. Merrill first reported the idea of using active circuit elements (i.e., vacuum tubes) to control the voltage-current relationship at a pair of terminals in order to make the impedance seen at that terminal pair equal to the negative of an impedance placed elsewhere in the network.[1] This impedance converter, or, more descriptively, negative impedance converter, was used to obtain negative resistance which was successfully used in telephone repeater amplifiers.

As transistors became reasonably reliable for mass production, it was only natural that transistor negative impedance converters be considered. J. G. Linvill wrote a classic paper on transistor NIC's (negative impedance converters);[2]

---

[1] J. L. Merrill, "Theory of Negative Impedance Converters," Bell System Technical Journal, Vol. 30 (Jan., 1951), pp. 88-109.

[2] J. G. Linvill, "Transistor Negative Impedance Converters," Proc. IRE, Vol. 41 (June, 1953), pp. 725-729.

this paper is primarily concerned with negative resistance, as is a later paper by Linvill[3] which describes the use of negative resistance as a circuit element to realize various transfer functions of an RC filter. Other examples of the use of negative resistance include a nonlinear phase shift circuit reported by Barbiere.[4]

On a more theoretical basis, Larky[5] presented a method whereby the effect of undesirable parasitic elements associated with the NIC might be reduced or possibly eliminated. Lundry[6] furnished some basic relationships in terms of the four terminal network parameters concerning the analysis of NIC's as well as their practical realization.

The preceding references all refer to a negative impedance obtained by means of an NIC. However, the concept of negative linear capacitance (and negative linear inductance) has been used in the analysis of solid-state masers.[7]

---

[3] J. G. Linvill, "RC Active Filters in Which the NIC Uses Transistors," Proc. IRE, Vol. 42 (March, 1954), pp. 555-564.

[4] R. G. Barbiere, "A Graphical Analysis of a Nonlinear RC Phase Shift Feedback Circuit," Proc. IRE, Vol. 43 (June, 1955), pp. 673-683.

[5] A. I. Larky, "Negative Impedance Converters," Trans. IRE, PGCT (Sept., 1957), pp. 124-131.

[6] W. R. Lundry, "Negative Impedance Circuits--Some Basic Relations and Limitations," Trans. IRE, PGCT (Sept., 1957), pp. 32-139.

[7] R. L. Kyhl, et al., "Negative L and C in Solid State Masers," Proc. IRE, Vol. 58 (June, 1961), p. 1157, with correction Proc. IRE, Vol. 60 (July, 1962), p. 1608.

Much work has also been done concerning negative elements in general without regard to how they might be realized. An article by Manley and Rowe[8] gives some general energy relationships for any nonlinear elements; then Rowe[9] extends this paper to include small signal analysis of nonlinear circuit elements.

Finally, McDonald and Brachman[10] discuss nonlinear capacitance specifically, although their article is restricted to the charging of a theoretical nonlinear positive capacitor.

Various describing-function-type approaches have been devised in order to apply some of the theory of linear circuits to the study of nonlinear systems, e.g., in a paper by Thomsen and Schlesinger[11] an approximate solution of a network which contains nonlinear reactive elements is obtained by use of some of the concepts of linear network theory.

---

[8] J. M. Manley and H. E. Rowe, "Some General Properties of Nonlinear Elements. Part I--General Energy Relations," Proc. IRE, Vol. 44 (July, 1956), p. 904.

[9] H. E. Rowe, "Some General Properties of Nonlinear Elements. Part II--Small Signal Theory," Proc. IRE, Vol. 46 (May, 1958), p. 850.

[10] J. R. McDonald and M. K. Brachman, "The Charging and Discharging of Nonlinear Capacitors," Proc. IRE, Vol. 43 (June, 1955), p. 741.

[11] J. S. Thomsen and S. P. Schlesinger, "Analysis of Nonlinear Circuits Using Impedance Concepts," Trans. IRE, PGCT, CT 2 (Sept., 1955), p. 271.

In Linvill's[12] paper the NIC that is described is used to obtain a negative resistance. A plot of the input terminal impedance phasor shows that the terminal impedance is not pure negative resistance, but that parasitic reactance must be associated with the resistance. This parasitic reactance is capacitive for low frequencies and is inductive for high frequencies (above about 50 KC). For a certain range of frequencies (about 40 KC to 100 KC) the reactance is small compared to the negative resistance. Outside this range of frequencies the reactance is not small and the NIC could not be considered even as a first approximation as an ideal negative resistance.

In the preceding discussion reference has been made to nonlinear positive and negative resistance, nonlinear positive capacitance and linear negative reactance. To this writer's knowledge no work has been reported concerning a physical nonlinear capacitor that is negative for some values of charge and/or voltage. The primary objective of this paper is to contribute to the theory of nonlinear negative capacitance (NNC) circuits. This is done in two parts; in the first part the behavior of a class of networks which contain an NNC is studied, and in the second part an NNC is produced in the laboratory by means of an NIC circuit. The first step in this study is to obtain the basic power and energy relationships for the NNC, as well as the

---

[12]Linvill, "Transistor NIC," p. 725.

natural response of simple two element networks containing only the NNC and one each positive linear R, L, or C. In this step one sees the differences as well as the similarities between the solutions of these networks and the well known solutions of the corresponding networks which contain only linear positive elements.

If a useful property of this capacitance could be established this would be an important addition to the circuit theory of the NNC. Therefore, the next step is to study the response of a broader class of networks which contain an NNC to discover whether its presence in these networks makes them particularly suitable to perform certain fundamental and useful network functions. There is no doubt that the ideal NNC will not be physically realizable but will have parasitic elements associated with it; therefore, for this part of the analysis various combinations of R and L are used in conjunction with the NNC to represent lumped models of a potentially realizable capacitance.

The results of the preceding analysis depend on the way the NNC is defined. Since it is a capacitance it can be defined by the charge voltage relationship at its terminals. This charge-voltage characteristic must be hypothesized since no single element is presently known to exhibit a characteristic with the desired properties. Negative capacitance is obtained in this work from an active network. There is some indication

that single devices possessing negative incremental capacitance may eventually be developed.[13] Consequently, any characteristic that is assumed will be an approximation of an actual characteristic. A cubic charge-voltage relationship is chosen to represent the NNC in portions of the analysis; in other parts a piecewise linear curve is used. It is felt that for some actual NNC the piecewise linear characteristic might be a better approximation than the cubic curve.

A study of nonlinear negative capacitance must include data on a physically realizable capacitance as well as on a theoretical one. Therefore, an anlysis of a transistor negative impedance converter is presented and a prediction is made of the lumped model of the realizable NNC. This model is subsequently verified by both AC steady state and square wave transient measurements. Measurement of the charge voltage characteristic of this capacitance is discussed and waveforms of the NIC currents and voltages are shown under small signal and large signal operation.

1.2 Definitions and Basic Circuit Analysis of Nonlinear Negative Capacitance

The term "nonlinear negative capacitance" is very general and can be construed as an electric circuit element

---

[13] C. O. Harbourt, "Lumped Models for Negative-Parameter Electrical Devices," to be published in IEEE Transactions on Circuit Theory.

which dissipates no power, which is characterized by the voltage across its terminals and the charge that has entered the terminals, and which has a charge-voltage characteristic that is nonlinear and that has a negative slope for some values of charge and voltage.

For purposes of this theoretical study the charge-voltage characteristic that is used to describe the NNC has two semi-infinite regions in which the capacitance is positive; in one finite region the capacitance is negative. Such a characteristic may be expressed analytically as

$$e = -aq + bq^3, \tag{1.1}$$

where e is the voltage across the terminals, q is the charge that has been deposited on one of the plates of the theoretical capacitor, and a and b are constants. This characteristic is shown in Fig. 1.1. Note that if $b = 0$ the value of the linear capacitor is $-1/a$.

For the characteristic of Eq. (1.1), e is a single-valued function of q, so the capacitance is expressed as a function of q, i.e.,

$$C = \frac{1}{de/dq} = \frac{1}{-a + 3bq^2}. \tag{1.2}$$

Assume that the charge delivered to the NNC is a periodic function of time with period T. Then the average power delivered to the NNC is

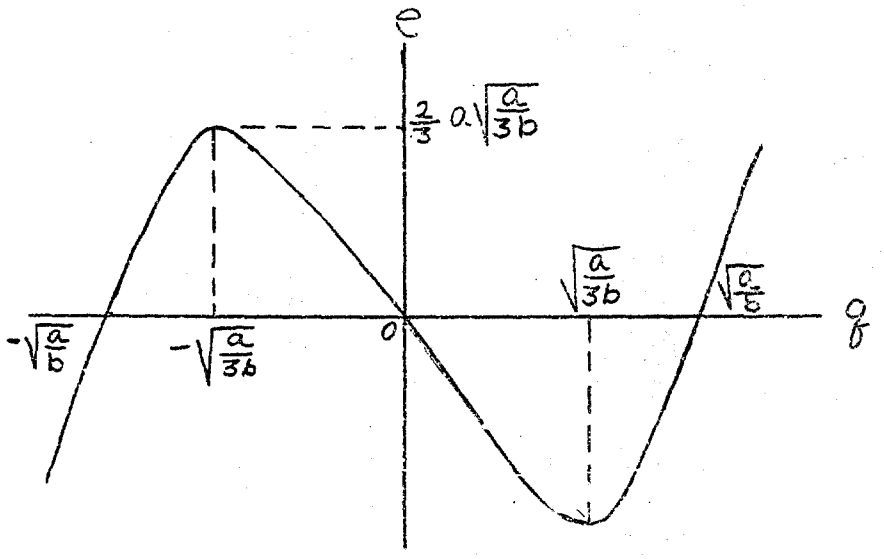

Fig. 1.1. Characteristic of NNC

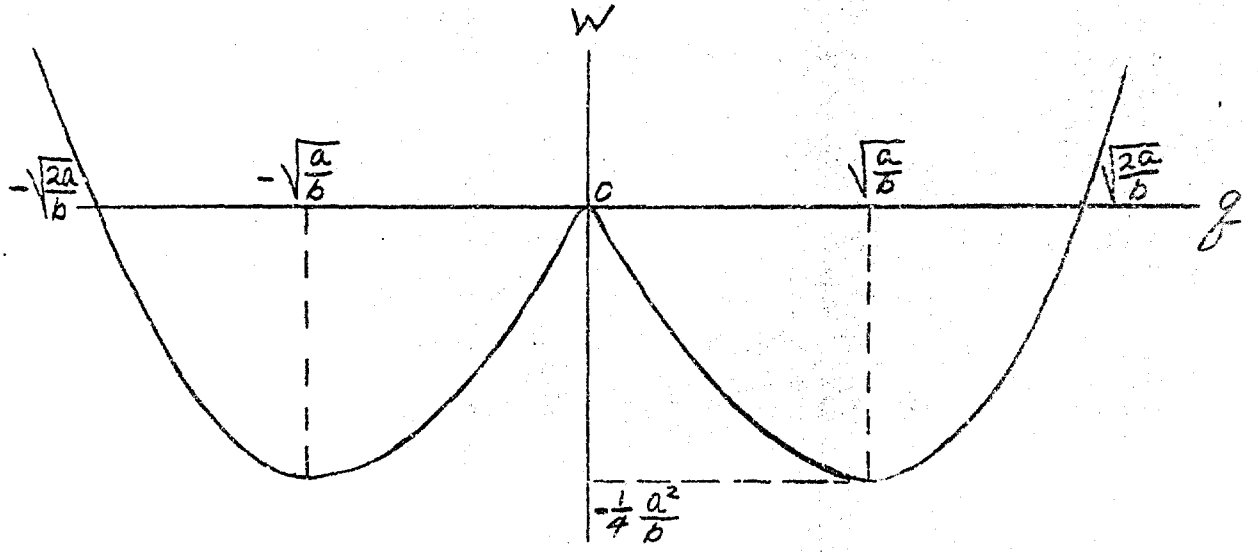

Fig. 1.2. Plot of Instantaneous Energy Stored vs. Charge

$$P_{ave} = \frac{1}{T}\int_0^T e\,i\,dt$$

$$= \frac{1}{T}\int_{q(0)}^{q(T)} (-aq + bq^3)\,dq$$

$$= \frac{1}{T}\left/ -\frac{aq^2}{2} + \frac{bq^4}{4}\right/_{q(0)}^{q(t)} . \qquad (1.3)$$

Since q is periodic, q(T) = q(0) and the value of the integral [Eq. (1.3)] is zero.

The average power can be shown to be zero for any device for which the voltage across the terminals of the device is a function of the charge that has been delivered to the device; i.e., for q periodic

$$P_{ave} = \frac{1}{T}\int_0^T e\,i\,dt = \frac{1}{T}\int_0^T e\frac{dq}{dt}\,dt = \frac{1}{T}\int_{q(0)}^{q(T)} e\,dq .$$

Now, if e is a function of q, the integration can be performed, and the upper and lower limits are identical, so the value of the integral is zero. Naturally this does not imply that the average power dissipated by a resistor is zero, for the voltage across the resistor is not a function of the charge that has been delivered to the resistor, but is a function of the time rate of change of the charge flowing through the resistor. The energy associated with the NNC is given by the time integral of power:

$$W = \int p\,dt = \int (-aq + bq^3)\,dq = \frac{-aq^2}{2} + \frac{bq^4}{4} + W(q=0) \qquad (1.4)$$

Equation (1.4) is shown plotted in Fig. 1.2.

In order to further characterize the behavior of the NNC consider the combination of the NNC with one each positive, linear R, L, C, as shown in Fig. 1.3.

First consider the circuit of Fig. 1.3(a). The homogeneous equation for this circuit is

$$R\,dq/dt - aq + bq^3 = 0,$$

or

$$\frac{dq}{dt} - \frac{a}{R}q = -\frac{b}{R}q^3 \tag{1.5}$$

This is a form of the Bernoulli[14] equation; the substitution $x = 1/q^2$ leads to a linear equation, for

$$\frac{dx}{dt} = \frac{dx}{dq}\frac{dq}{dt} = -\frac{2}{q^3}\left(\frac{a}{R}q - \frac{b}{R}q^3\right),$$

and

$$\frac{dx}{dt} + \frac{2a}{R}x = \frac{2b}{R}. \tag{1.6}$$

The solution of Eq. (1.6) is

$$x = e^{-\frac{2a}{R}t}\int \frac{2b}{R}e^{\frac{2a}{R}t}\,dt + Ke^{-\frac{2a}{R}t}$$

$$= e^{-2a/Rt}\,\frac{b}{a}e^{\frac{2a}{R}t} + Ke^{-\frac{2a}{R}t}.$$

$$1/q^2 = \frac{b}{a} + Ke^{-\frac{2a}{R}t}$$

$$q^2 = \frac{1}{\frac{b}{a} + Ke^{-\frac{2a}{R}t}}. \tag{1.7}$$

---

[14] W. J. Cunningham, Introduction to Nonlinear Analysis (New York: McGraw-Hill Book Company, Inc., 1958), p. 60ff.

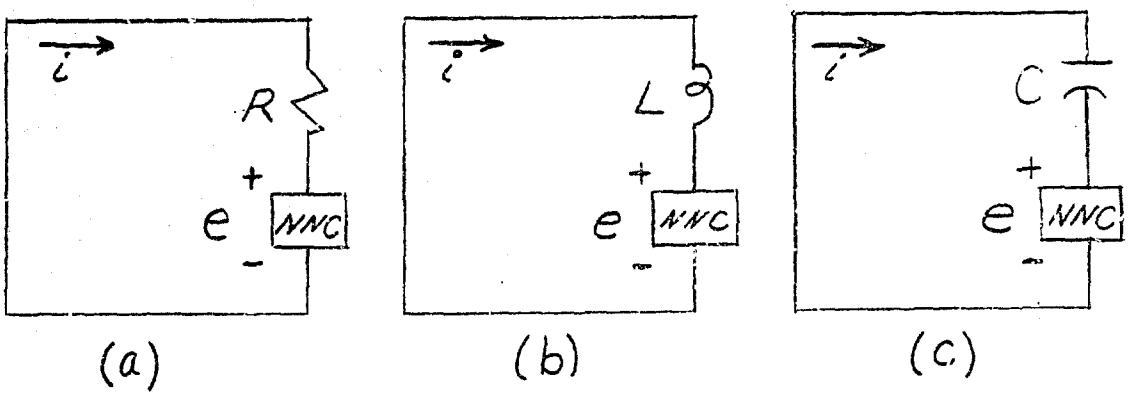

Fig. 1.3. Simple Circuits Containing NNC

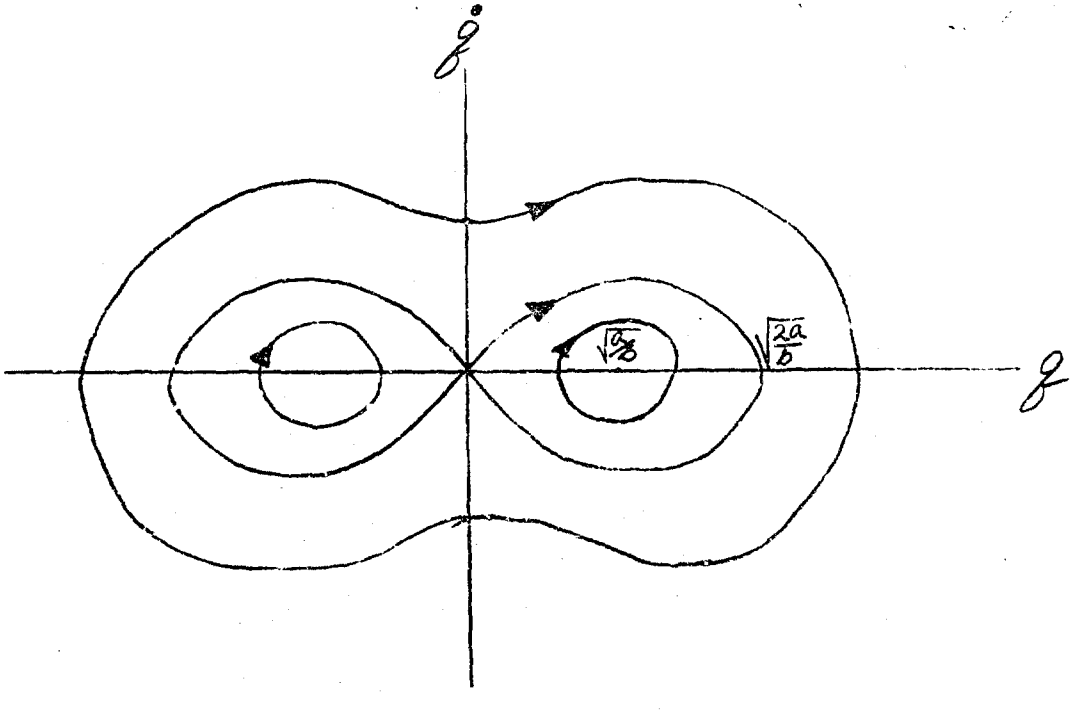

Fig. 1.4. Phase Portrait of Network of Fig. 1.3(b)

Note, from Eq. (1.7), that, if the initial value of q is zero then the constant of integration must be infinite and $q \equiv 0$. Also, regardless of non-zero initial conditions, the final value of $q = \pm\sqrt{\frac{a}{b}}$, which is the point of zero voltage across the NNC (see Fig. 1.1). From Eq. (1.7) the current is found to be

$$i = \frac{dq}{dt} = \frac{\frac{Ka}{R} e^{-\frac{2a}{R}t}}{\left[\frac{b}{a} + K e^{-\frac{2a}{R}t}\right]^{3/2}} . \tag{1.8}$$

Equation (1.8) indicates that the current in the circuit of Fig. 1.3(a) decays to zero, as is expected in a source free RC circuit, but the decay is obviously more complex than in the corresponding linear RC case.

The homogeneous equation from the circuit of Fig. 1.3(b) is

$$\frac{d^2q}{dt^2} = \frac{a}{L} q - \frac{b}{L} q^3 . \tag{1.9}$$

Singular point analysis discloses that the location and type of the three singular points of Eq. (1.9) are:

1. $q = \sqrt{\frac{a}{b}}$, $\dot{q} = 0$; center.

2. $q = 0$, $\dot{q} = 0$; saddle.

3. $q = -\sqrt{\frac{a}{b}}$, $\dot{q} = 0$; center.

Equation (1.9) can be integrated once if the substitution $dq/dt = p$, $d^2q/dt^2 = p\,dp/dq$ is made. The resulting equation after integration is

$$\left(\frac{dq}{dt}\right)^2 = \frac{a}{L}\left(q^2 - \frac{b}{2a}q^4 + C_1^2\right). \tag{1.10}$$

A boundary condition must be specified. When $dq/dt = 0$, q is at its maximum value, say Q_0, and

$$C_1^2 = -Q_0^2 + \frac{b}{2a}Q_0^4.$$

Equation (1.10) becomes

$$\left(\frac{dq}{dt}\right)^2 = \frac{a}{L}\left[q^2 - Q_0^2 - \frac{b}{2a}\left(q^4 - Q_0^4\right)\right]. \tag{1.11}$$

Equation (1.11) constitutes one form of a solution to Eq. (1.9) since $\dot{q}$ may be plotted versus q for various values of maximum charge, Q_0. However, the solution will be carried further. A plot of Eq. (1.11) has the form shown in Fig. 1.4. Note from Eq. (1.11) that $\dot{q}$ is imaginary for small values of q if $Q_0^2 < 2a/b$. It will now be shown that Eq. (1.11) can be put into the form of an elliptic integral.

Rewrite Eq. (1.11) as

$$\frac{dq}{dt} = \pm\sqrt{\frac{a}{L}\left[q^2 - Q_0^2 - \frac{b}{2a}\left(q^4 - Q_0^4\right)\right]} \tag{1.12}$$

Let $q(0) = Q_0$; hence $\dot{q}(0) = 0$. Choose the (-) sign for the radical so that $\dot{q} < 0$ for t small. Assume

$q = Q_0 \cos\phi$; $dq = -Q_0 \sin\phi\, d\phi$, and

$q^2 - Q_0^2 = -Q_0^2 \sin^2\phi$, Eq. (1.12) becomes

$$\frac{dq}{dt} = -\sqrt{\frac{a}{L}}\sqrt{\frac{b}{2a}Q_0^2 \sin^2\phi\left(Q_0^2\cos^2\phi - \frac{2a}{b} + Q_0^2\right)}\,.$$

Separate variables and rearrange terms to get

$$\int_0^t dt = \int_0^{\phi} \frac{d\phi}{\sqrt{\frac{b}{2}\left(Q_0^2 - \frac{a}{b}\right)}\sqrt{1 - \frac{Q_0^2}{2\left(Q_0^2 - a/b\right)}\sin^2\phi}} \quad , \tag{1.13}$$

or

$$t = \frac{u(\phi, k)}{\sqrt{\frac{b}{2}\left(Q_0^2 - a/b\right)}} \quad , \text{ where} \tag{1.14}$$

$$k^2 = \frac{Q_0^2}{2\left(Q_0^2 - a/b\right)} \quad . \tag{1.15}$$

The relationship between u and φ is $\operatorname{cn} u = \cos\varphi$ where $\operatorname{cn} u$ is the elliptic cosine of u. From Eq. (1.14) it is seen that $Q_0^2 \geq a/b$ is necessary for t to be real. This requirement may also be seen from the phase portrait since the phase trajectory must encircle at least one of the centers, located on the abscissa at $\pm\sqrt{\frac{a}{b}}$. However Eq. (1.15) indicates that $\frac{1}{2} < k^2 < \infty$; if

$$Q_0^2 > \frac{2a}{b} \text{, then } \tfrac{1}{2} < k^2 < 1 \text{;}$$

$$\frac{a}{b} < Q_0^2 < \frac{2a}{b} \text{, then } k^2 > 1 \text{;}$$

$$Q_0^2 = \frac{2a}{b} \text{, then } k^2 = 1 \text{.}$$

First consider the case where $Q_0^2 \geq 2a/b$ so that $\frac{1}{2} \leq k^2 \leq 1$; then

$$\xi = Q_0 \operatorname{cn} u = Q_0 \operatorname{cn}\left[\sqrt{\tfrac{b}{2}\left(Q_0^2 - \tfrac{a}{b}\right)}\, t\right],$$

$$\dot{\xi} = \xi = Q_0 \frac{d \operatorname{cn} u}{du}\frac{du}{dt} = -Q_0\sqrt{\frac{b}{2}\left(Q_0^2 - \frac{a}{b}\right)}\operatorname{sn} u \operatorname{dn} u \,. \tag{1.16}$$

This is obviously the case where the phase trajectory encircles all three singular points. Next assume that $a/b < Q_o^2 < 2a/b$ so that $k^2 > 1$. In this case the identity (for $k^2 > 1$)

$$cn(u|k^2) = dn[uk|1/k^2]$$

may be used to make the charge depend on an elliptic function whose parameter is less than one. So

$$q = Q_0 \, dn\, u'$$

$$i = \dot{q} = -Q_0^2 \sqrt{\frac{b}{2c}} \, (k')^2 \, sn\, u' \, cn\, u' \tag{1.17}$$

Where $u' = uk = Q_0\sqrt{\frac{b}{2c}}\, t$, and the elliptic functions of Eq. (1.17) depend on the parameter

$$k' \text{ with } (k')^2 = \frac{1}{k^2} = \frac{2(Q_0^2 - a/b)}{Q_0^2}$$

The phase trajectory in this case encircles only one center. Note that the average value of dn u' is not zero (unless $k^2 = 1$); this establishes the nonzero average value required of q for this case.

Thus analytical expressions have been established for the expected oscillation of the lossless LC circuit.

The homogeneous equation for the network of Fig. 1.3(c) is a nonlinear algebraic equation:

$$q/c - aq + bq^3 = 0 \tag{1.18}$$

which is satisfied by

$$q = 0, \text{ or } q^2 = \frac{1}{b}(a - 1/c) \tag{1.19}$$

Equation (1.18) is of little value in determining the behavior of the NNC in Fig. 1.3(c), since the solution of this equation yields only three isolated values of charge. The solution does not reveal how or whether the charge changes from one value to another nor does it lend any insight into the stability of the circuit.

C H A P T E R I I

PROPERTIES OF NETWORKS WHICH CONTAIN A NONLINEAR NEGATIVE CAPACITANCE

2.1 Definition of Networks to Be Studied

The NNC has been introduced in the preceding chapter by presentation of some voltage and power relationships as well as source-free circuit responses. It is now desirable to consider the possibilities of the theoretical NNC as a circuit element. It is axiomatic that the idealized NNC discussed in Chapter I can never be obtained in practice; one would expect some dissipation in any practical NNC (obtained, e.g., by a negative impedance converter) as well as parasitic positive capacitance; at some frequencies an inductive effect might be noted at the terminals of the NNC.

This uncertainty about the lumped model of a realizable NNC prompts one to consider the ideal NNC in several circuit configurations, assuming that one or more of the circuits will approximate the NNC throughout some range of frequencies and/or some voltage level. In order to simplify the analysis that follows, the cubic curve that has been used to define the capacitor will be replaced by a piecewise linear characteristic.

Active networks are used basically for one of three purposes: as amplifiers, as oscillators, as on-off devices; viz., switching circuits; therefore each of the following networks will be studied with regard to its usefulness for any of these three functions. The type of networks to be studied will be defined as follows:

1. The basic three-element networks will consist of one each +R, +L, and piecewise linear C.
2. The networks will be studied with resistive, capacitive and inductive loads.

In order to be acceptable as an amplifier the natural frequencies of the network must be adjustable so that the network appears dissipative; i.e., initial energy stored in any of the reactive elements of the network must be ultimately dissipated by resistive elements of the network. In linear network terminology this simply says that all the poles of the network function must be in the left half of the complex frequency plane. If the network is to be useful as an oscillator, then initial energy stored in any of the reactive elements must result in a sustained oscillation. If a network is to be suitable as a switching circuit, it will be necessary that the network have two stable states. It must be possible to trigger the network from one stable state to the other by application of an appropriate voltage or current.

2.2 Basic Networks and Amplification

The basic networks are shown without loads in Fig. 2.1(a). These one-port-networks represent all possible combinations of one each R, L, and (piecewise linear) C.

The first part of the study will be concerned with the effect of negative capacitance on the small signal stability of the networks shown in Fig. 2.1(b). It is assumed here that the capacitance is always negative and linear, this may be accomplished by proper biasing, operation in a limited frequency range, or restraint on the magnitude of the signal source.

If each of the networks of Fig. 2.1(a) is placed in the configuration of Fig. 2.1(b), it is seen that there are twenty-four possibilities. It turns out that twelve of these possibilities are second order networks and twelve are third order networks. Since linear network theory applies to the amplification study, all twenty-four networks may be conveniently investigated in this respect.

The system used to identify each of the twenty-four networks is as follows: each network will be denoted by an integer (one through eight) followed by a letter (R, L, or C). The integer indicates one of the networks of Fig. 2.1(a) and the letter indicates the load that is placed on this network [see Fig. 2.1(b)].

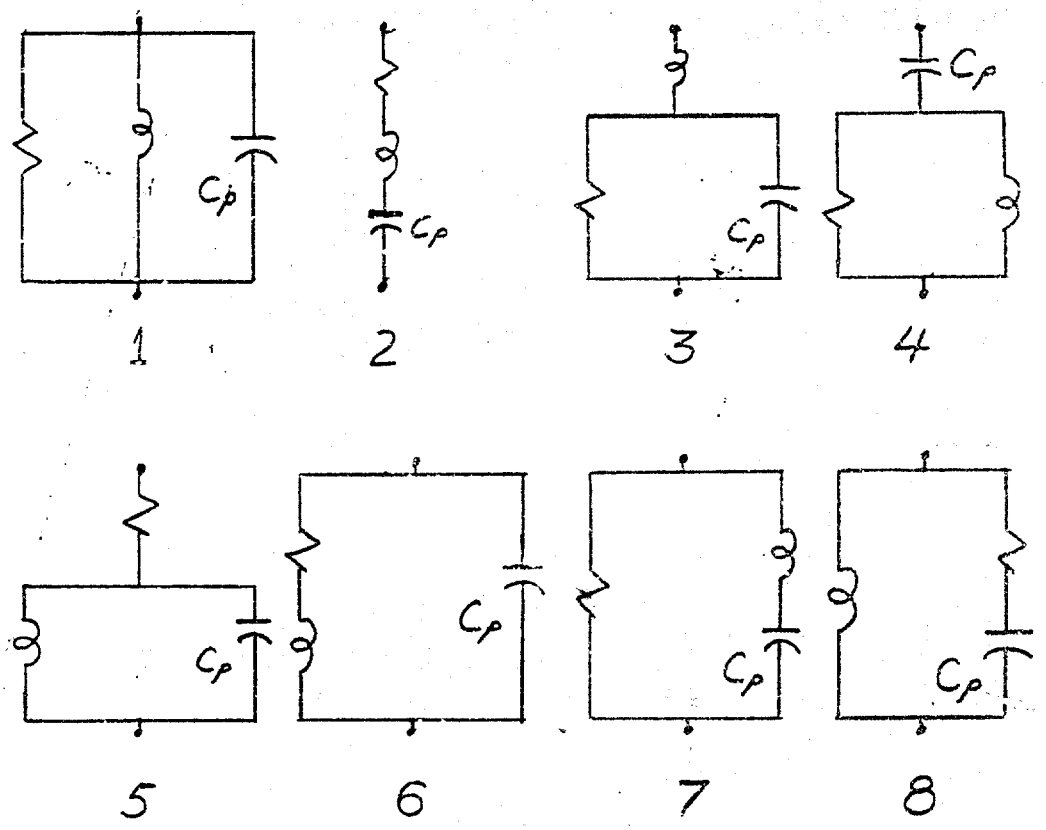

Fig. 2.1(a). Basic Networks

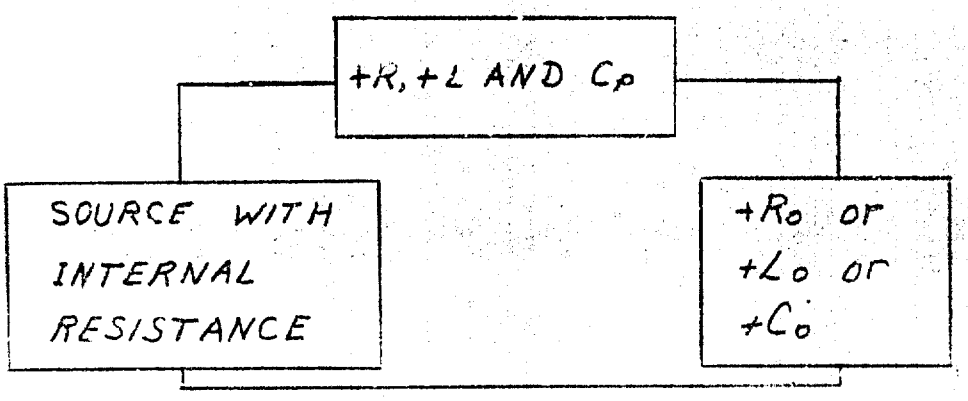

Fig. 2.1(b). General Network Used to Study the Effect of Negative Capacitance

The characteristic equations of the networks are found and then inspected for possible right-half plane poles. The only networks that could be considered as small signal linear amplifiers are networks 2C and 4C (see Fig. 2.2). The poles of both 2C and 4C will all be in the left half of the complex frequency plane if $C_o \leq C$; this condition insures that the total series capacitance is non-negative. Properties of these networks may be explained as follows. Consider networks 2C and 4C with their voltage sources reduced to zero, and with $L = 0$ in 2C and $L = \infty$ in 4C. Both of these networks then become the RC circuit of Fig. 2.3. First, assume that the RC circuit is driven between terminals a and b; this is the case where the negative capacitance with dissipation is placed in parallel with the series RC circuit made up of R_g and C_o. If the elements are adjusted so that $R = R_g$ and $C_o = C$ then the AC impedance between terminals ab is

$$Z_{ab}(j\omega) = \frac{R}{2} + \frac{1}{2R\omega^2C^2} .$$

At low frequencies the magnitude of this impedance is higher than the magnitude of the $R_g - C_o$ combination alone; hence the voltage V_{ab} is higher with the lossy negative capacitance included then it is without the capacitance. In this sense the negative capacitance may be considered to accomplish voltage amplification. However, another effect is also seen; note that Z_{ab} is real for all frequencies. The negative capacitance

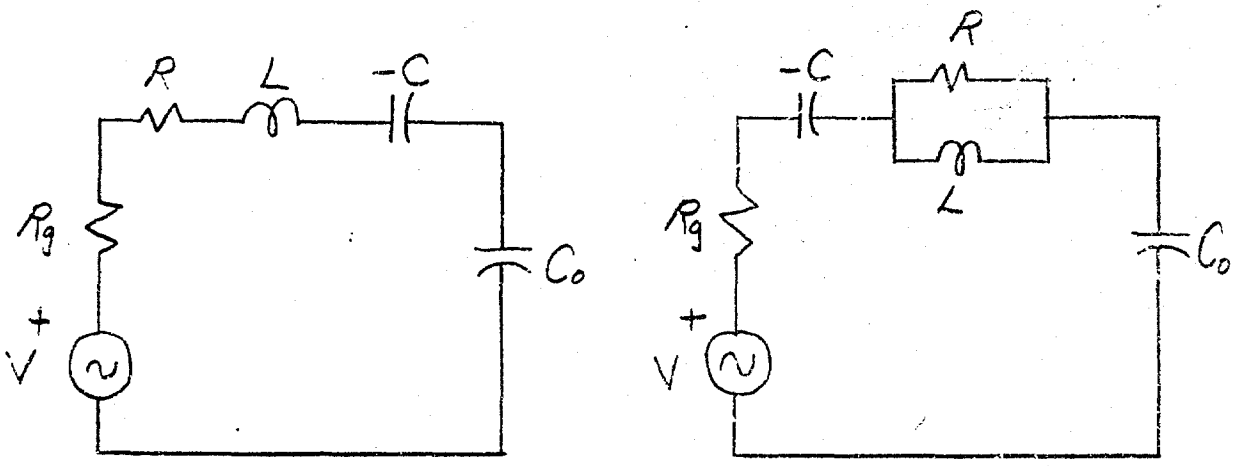

Fig. 2.2. Possible Small Signal Linear Amplifiers

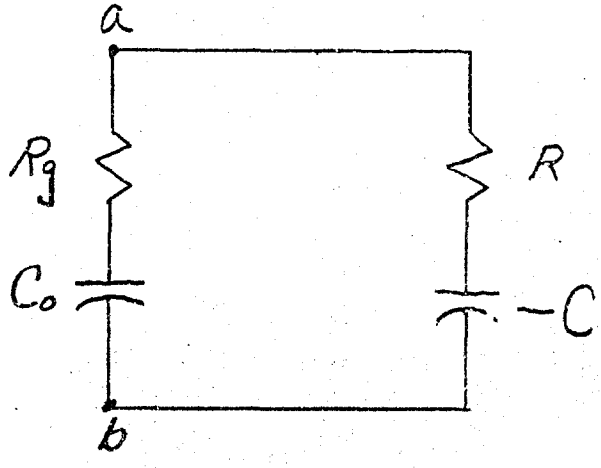

Fig. 2.3. RC Circuit

cancels the effect of the positive capacitor as far as phase shift between the current and voltage at the input terminals.

Thus the negative capacitance may be used to cancel the effect of capacitive reactance at terminals ab. Obviously if $R_g = R = 0$ and $C = C_o$ the negative capacitance completely cancels the positive capacitance and Z_{ab} becomes infinite.

Now assume that a voltage source is inserted in series with the elements of Fig. 2.3. This corresponds to the case where the lossy negative capacitance is placed in series with the $R_g - C_o$ combination. Since both capacitors are linear the equivalent capacitance is $C_{eq} = -CC_o/(C_o - C)$. Note that if $C = KC_o$, $K > 1$, then $C_{eq} = KC_o/(K - 1)$. The effect of the negative capacitance is to make the equivalent capacitance larger than the positive capacitor, C_o. This capacitance multiplication becomes more pronounced as K approaches one, e.g., if $K = 1.1$ then $C_{eq} = 11\ C_o$. Again for low frequencies and a given voltage function the current in the circuit will have a greater amplitude with the negative capacitance than without it. Thus a type of current amplification is exhibited. The usefulness of this circuit is not current amplification as such but is capacitance multiplication. In microelectronic circuitry the practical deposited capacitance is on the order of picofarads, so a negative capacitance might be used to significantly increase the possible range of capacitor values.

2.3 Phase Plane Analysis--Switching Circuits

Considerable insight into the operation of a network containing one or more nonlinear elements may be acquired by means of phase plane analysis; unfortunately this technique is presently limited to second order systems. Consequently, only the twelve second order systems are considered in the following analysis. The cubic charge-voltage characteristic of the NNC will be replaced by the piecewise linear characteristic shown in Fig. 2.4. When the second order systems are represented on a phase plane three distinct cases are observed. An example illustrating each of these three cases follows.

Network 1R is shown redrawn in Fig. 2.5 with a DC voltage source included. The equation for the network is:

$$\frac{e-E}{R_g} + \frac{1}{L}\int e\,dt + \frac{e}{R} + i = 0,$$

or

$$\frac{1}{R_g}\frac{de}{dt} + \frac{e}{L} + \frac{1}{R}\frac{de}{dt} + \frac{di}{dt} = 0 \qquad (2.1)$$

However $e = f(q)$, so $\frac{de}{dt} = \frac{de}{dq}\frac{dq}{dt} = i\frac{de}{dq}$,

and $i = \frac{dq}{dt}$; therefore, Eq. (2.1) may be written

$$\left(\tfrac{1}{R} + \tfrac{1}{R_g}\right)\frac{de}{dq}\,i + \frac{e(q)}{L} + \frac{di}{dt} = 0,$$

and 1R is completely described by the following two equations:

$$\left.\begin{aligned} \frac{di}{dt} &= -\left(\tfrac{1}{R} + \tfrac{1}{R_g}\right)\frac{de}{dq}\,i - \frac{e(q)}{L}\,; \\ \frac{dq}{dt} &= i. \end{aligned}\right\} \qquad (2.2)$$

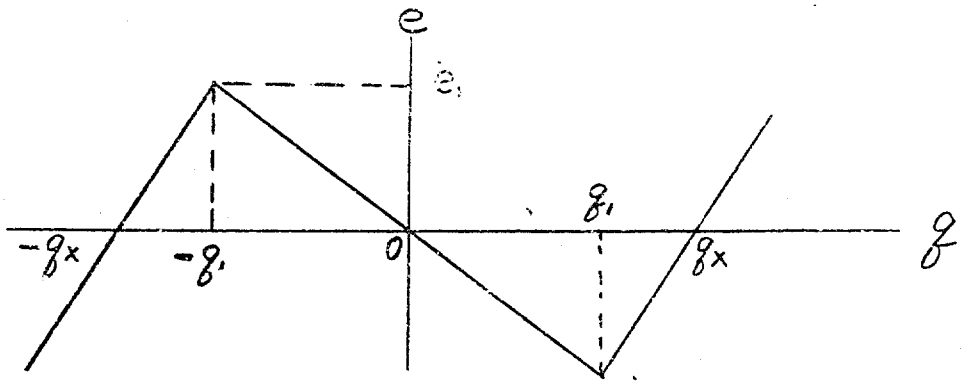

Fig. 2.4. Characteristic of Piecewise Linear Capacitance

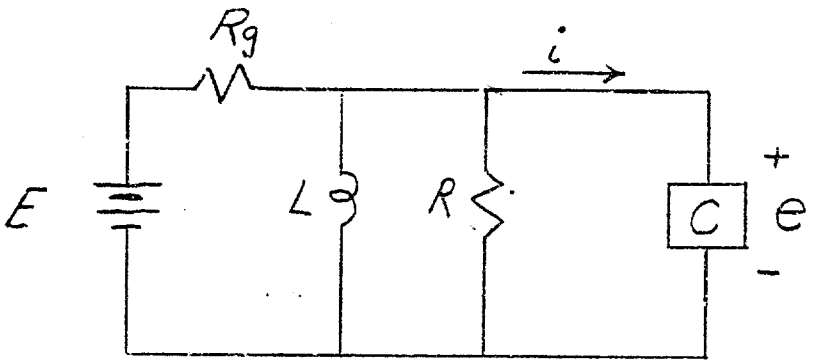

Fig. 2.5. Network IR Redrawn for Phase Plane Analysis

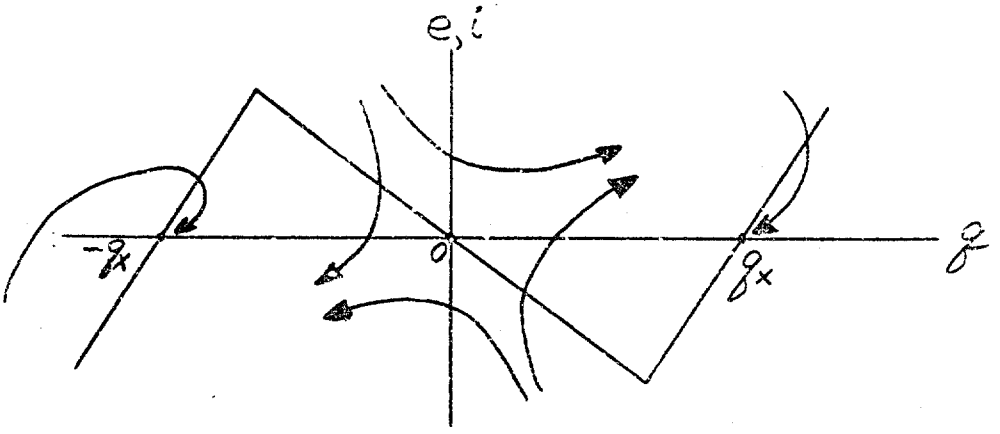

Fig. 2.6. Phase Plane Plot of IR

At the singular points $\frac{dq}{dt} = \frac{di}{dt} = 0$, consequently $i = 0$, $e = f(q) = 0$ are singular points of IR. From Fig. 2.4 it is seen that there are three points where $e = f(q) = 0$; these points are at $q = 0$, $q = \pm q_x$.

To find the types of singularities Eqs. (2.2) are combined:

$$\frac{di}{dq} = \frac{-(1/R + 1/R_g)\frac{de}{dq} i - \frac{e(q)}{L}}{i} \tag{2.3}$$

Near a singularity the phase plane variables can be written as $i = i_s + i_o$ and $q = q_s + q_o$ where i_s and q_s are the values of the variables at the singularity and i_o and q_o are small changes. In order to make the preceding substitution into Eq. (2.3) the first two terms of the Taylor's series expansion for $e(q)$ must be used, viz.,

$$e = f(q) = f(q_s) + \left.\frac{df(q)}{dq}\right|_{q_s} q_o . \tag{2.4}$$

also define $\left.\frac{df(q)}{dq}\right|_{q_s} = 1/C_s$,

so that

$$e = f(q) = f(q_s) + q_o/C_s . \tag{2.5}$$

This Taylor's series expansion and the definition of C_s will be used in all of the phase plane examples. With the aforementioned substitutions the system is described, in the vicinity of the singular points, by the relationship

$$\frac{di_o}{dq_o} = \frac{-(1/R + 1/R_g)\frac{1}{C_s} i_o - q_o/LC_s}{i_o} \qquad (2.6)$$

The characteristic roots are:

$$\lambda_{1,2} = \frac{1}{2}\left\{-(1/R + 1/R_g)1/C_s \pm \left[(1/R + 1/R_g)^2 \frac{1}{C_s^2} + 4(-1/LC_s)\right]^{1/2}\right\} \qquad (2.7)$$

The three singularities may be classified as follows:

1. At $q_s = \pm q_x$, $C_s > 0$; $Re[\lambda_1, \lambda_2] < 0$ so the points are stable nodes, or stable foci if $4/LC_s > (1/R + 1/R_g)^2 1/C_s^2$.
2. At $q_s = 0$, $C_s < 0$; $\lambda_{1,2}$ are real and of opposite sign so the point is a saddle.

A possible phase plane trajectory for IR is sketched in Fig. 2.6 superimposed on the assumed charge-voltage characteristic.

Note that, while IR always has two stable states separated by an unstable state, this circuit is of limited value as a switching circuit since there is no obvious way to cause the switching action to take place. The DC bias voltage, E, does not appear explicitly in Eq. (2.2) so it is not easy to say how much of a change in E would be required to cause i to change enough to effect a movement from one stable point to the other. If this switching were done only the initial and final values of the charge on the capacitor would be switched; the voltage, e, across the capacitor always becomes zero in the steady state. This would result in a pulse of current flowing

into or out of the capacitor. The other networks that exhibit this type of phase plane are 5R and 8R.

Another type of phase plane configuration is illustrated by network 3R, shown in Fig. 2.7. The equations for this network are:

$$\left.\begin{aligned} R_1 i_1 + L\frac{di_1}{dt} + e &= E \,, \\ i &= i_1 - e/R_2 \,; \end{aligned}\right\} \qquad (2.8)$$

or

$$\begin{aligned} \frac{di_1}{dt} &= \frac{1}{L}\left(E - R_1 i_1 - e(q)\right), \\ \frac{dq}{dt} &= i = i_1 - \frac{e(q)}{R_2} \,. \end{aligned} \qquad (2.9)$$

Singular points occur at

$$i_1 = \frac{e(q)}{R_2} = \frac{E}{(R_1 + R_2)} \qquad (2.10)$$

and

$$e(q) = \frac{R_2}{R_1 + R_2} E \,. \qquad (2.11)$$

Equation (2.11) may be drawn on the assumed e-q characteristic of Fig. 2.4 (redrawn in Fig. 2.8) and regarded as a loadline as far as the singularities of 3R are concerned, for the voltage, e, at the singularities is determined by Eq. (2.11), and the voltage across the capacitor at all times is determined by the piecewise linear charecteristic. By using the concept of the loadline the values of charge at the singularities may be found.

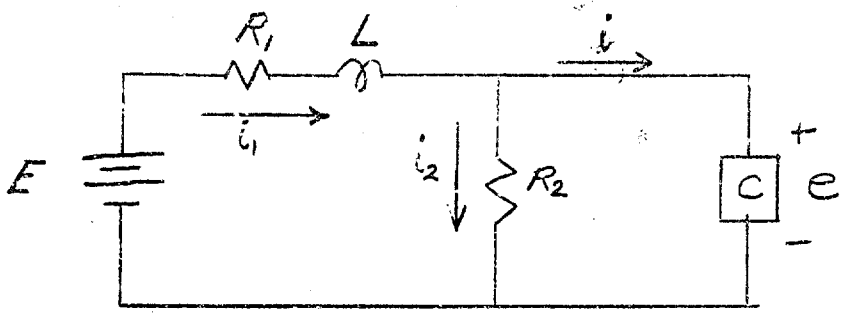

Fig. 2.7. Network 3R Redrawn for Phase Plane Analysis

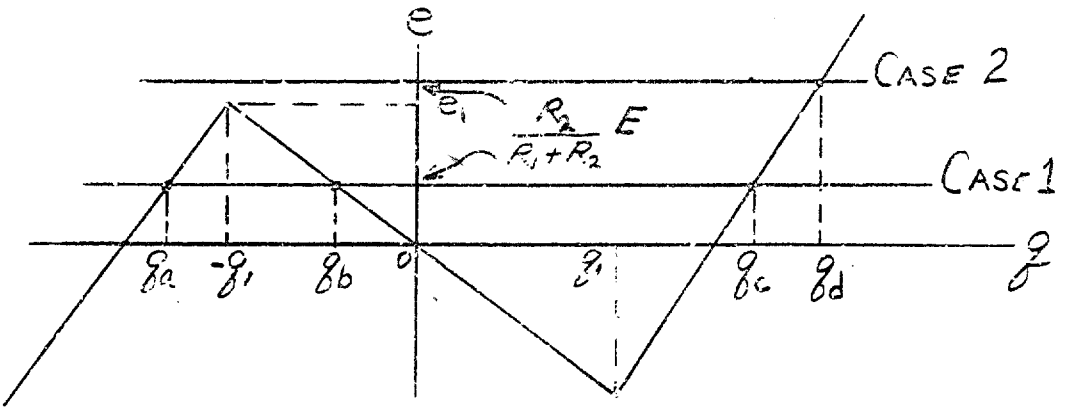

Fig. 2.8. Charge-Voltage Characteristic with Loadline for 3R

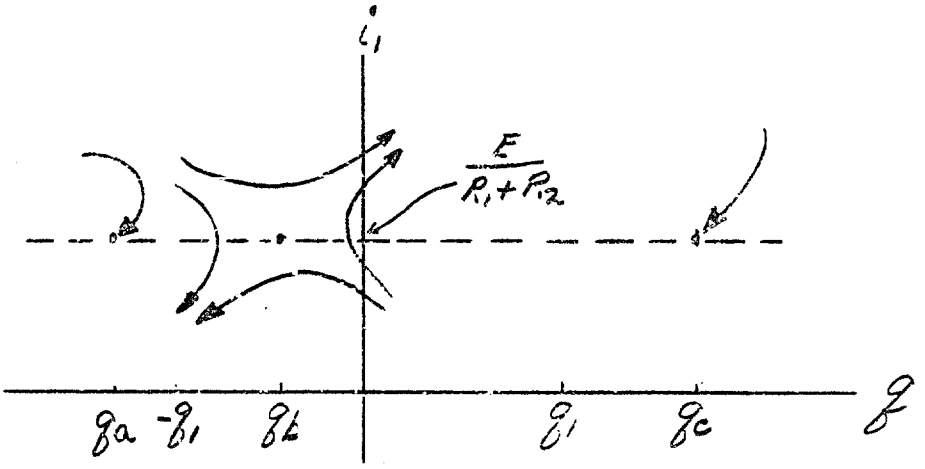

Fig. 2.9. Phase Portrait of 3R

Note that, in Fig. 2.8, two cases are indicated. If $\frac{R_2}{R_1+R_2}E < e_1$ then there are three intersections of the loadline and the e-q characteristic; hence, there are three singular points with values of charge q_a, q_b, q_c, as labeled in Fig. 2.8. On the other hand, if $\frac{R_2}{R_1+R_2}E > e_1$, then there is only one singular point with charge q_d.

For Case I (three singularities) the characteristic roots are:

$$\lambda_{1,2} = \frac{1}{2}\left\{-\left(\frac{R_1}{L}+\frac{1}{R_2C_s}\right) \pm \left[\left(\frac{R_1}{L}+\frac{1}{R_2C_s}\right)^2 - \frac{4}{LC_s}\left(1+\frac{R_1}{R_2}\right)\right]^{1/2}\right\}. \qquad (2.12)$$

With regard to Case I the following statements are true: (1) if $C_s > 0$ at a singularity then the singularity is either a stable node or a stable focus. (2) if $C_s < 0$ at a singularity then that singularity is a saddle point regardless of the relative values of R_1/L and $1/R_s|C_s|$.

For Case II the lone singularity with charge q_d has essentially the same properties that the singularity with charge q_c has in Case I. A possible phase portrait of 3R is shown in Fig. 2.9 for Case I. Several other networks exhibit the same type of loadline and phase portrait that 3R does; these networks are: 3L and 6R, with the phase plane variables being inductor current and capacitor charge, and 2R, 2L, 4R, and 7R, with the phase plane variables being capacitor current and charge.

Note that switching action could take place in a circuit of this type if the voltage E is variable. For example,

suppose the system were initially at the state identified by q_a (see Fig. 2.8), and the voltage E were increased so that $\frac{R_2}{R_1+R_2}E > e_1$; this would result in a system with only one singularity which might be the one identified by q_d in the figure. The operating point would move from the position on the left side of the characteristic to the point on the right side of the characteristic. This would result in an increase in the capacitor voltage, e, that could be considerably out of proportion to the increase in E, as well as an increase in the capacitor charge, q. This increase in charge will be accompanied by a pulse of current with magnitude depending on how fast the charge changes.

Finally, only networks 2C and 4C remain to be studied by phase plane analysis. As previously noted, these are the only two networks that could be made stable for possible small signal amplifiers. It will be seen that the loadlines for these two networks make them interesting as possible switching circuits also. Both 2C and 4C are redrawn in Fig. 2.10, although only the detailed analysis for 2C will be presented.

The equations for network 2C are:

$$E = Ri + L\frac{di}{dt} + q/C_o + e(q),$$

or

$$\frac{di}{dt} = \frac{1}{L}\left(E - Ri - q/C_o - e(q)\right) \qquad (2.13)$$

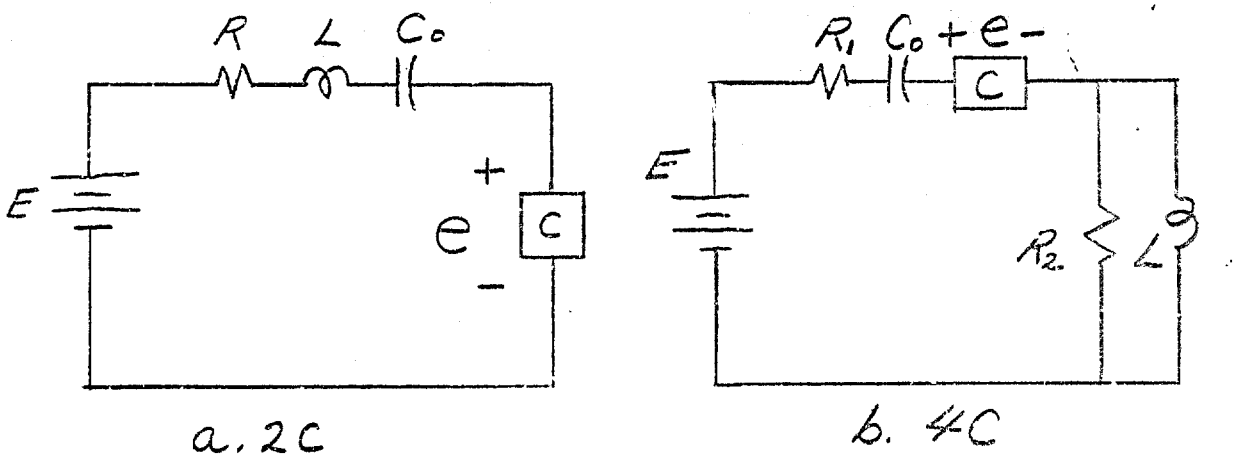

Fig. 2.10. Networks 2C and 4C

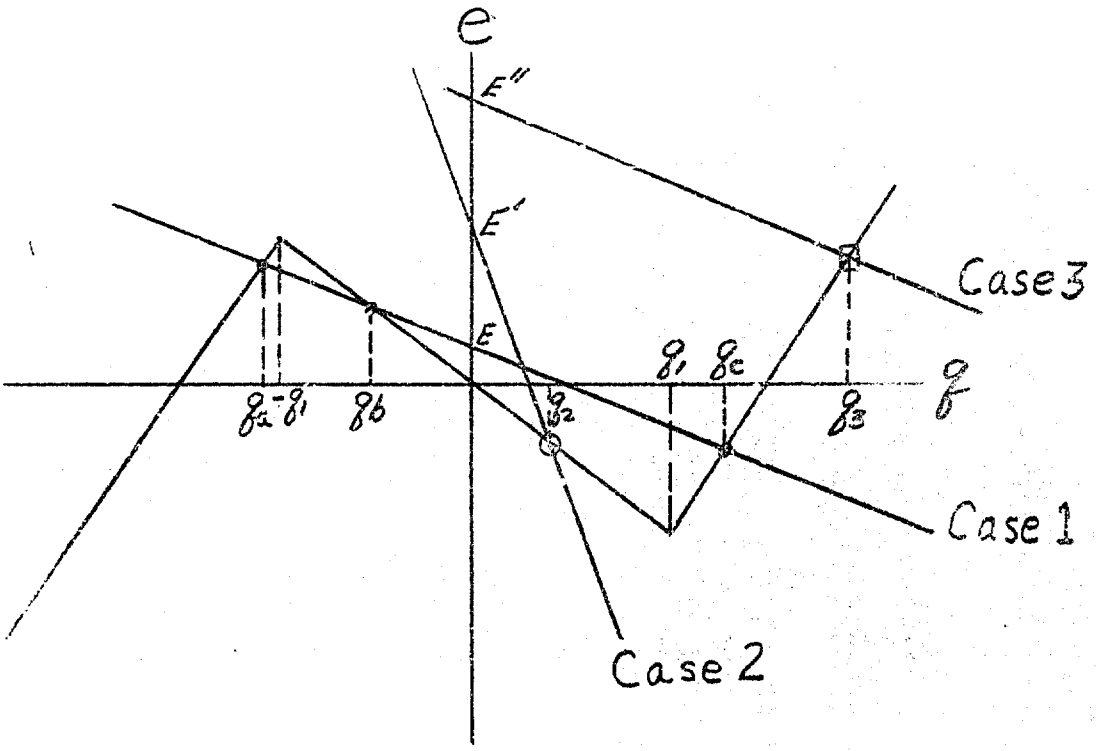

Fig. 2.11. Possible Loadlines for 2C

and

$$\frac{dq}{dt} = i \tag{2.14}$$

For 2C the singular points occur where $i = 0$ and $e(q) = E - q/C_o$. As before, the expression for $e(q)$ that partially defines the singular points may be viewed as a loadline on the e-q characteristic, except that, in this case, the slope of the loadline is not zero, but is $-1/C_o$. The singular points must be on the intersection of the e-q curve and the loadline (see Fig. 2.11). There are three possibilities depending on the values of E, e_1, and C_o.

Again the substitution is made that near each singularity $i = i_s + i_o$ and $q = q_s + q_o$; also $e(q) = e(q_s) + q_o/C_s$ where $1/C_s = \frac{de}{dq}\big|_{q_s}$. Then the ratio of Eq. (2.13) to Eq. (2.14) becomes

$$\frac{di_o}{dq_o} = \frac{\frac{1}{L}\left(-q_o/C_o - q_o/C_s - Ri_o\right)}{i_o} \tag{2.15}$$

and the characteristic roots are

$$\lambda_{1,2} = \frac{1}{2}\left\{-\frac{R}{L} \pm \left[\left(\frac{R}{L}\right)^2 - 4/L\left(1/C_o + 1/C_s\right)\right]^{1/2}\right\} \tag{2.16}$$

Equation (2.16) will be used to determine the types of singularities for each of the three cases indicated in Fig. 2.11.

Case I. Three Singularities

In order for this case to exist, it is necessary (but not sufficient) that $|E| < e_1$, and, in addition, it is necessary that $|1/C_s| > 1/C_o$ where this value of C_s is the negative value.

At q_a and $q_c, C_s > 0$ and Eq. (2.16) shows that the characteristic roots for both these cases will always have negative real parts; hence, these are either stable nodes or stable foci. At q_b, however, C_s is negative and must be less than C_o, so this point is a saddle. A phase portrait of 2C is shown in Fig. 2.12.

Case II. One Singularity on the Negative-Slope Portion of the e-q Curve

For this case to exist the values in the system must be adjusted so that $1/C_o > 1/|C_s|$, where C_s is again the negative value, and also so that $E < e_1\left[(|C_s|/C_o) - 1\right]$. The inequality is found by considering the values for which the loadline intersects the piecewise linear characteristic at the point $(q_1, -e_1)$ (see Fig. 2.11); at this point the equation for the negative-slope portion of the characteristic is $-e_1 = q_1/|C_s|$, and the equation of the loadline is $-e_1 = E - q_1/C_o$. If q_1 is eliminated from these two equations the value of E for which the intersection is $(q_1, -e_1)$ is given; obviously E must be smaller than this value or Case III will result. A similar inequality holds for $E < 0$. For this case $1/C_s$ is negative but less than $1/C_o$, so Eq. (2.16) reveals that this singularity is either a stable node or a stable focus.

Case III. One Singularity on the Positive-Slope Portion of the e-q Characteristic

Phase plane analysis reveals what might be expected here; i.e., the lone singular point may be either a stable node or a stable focus.

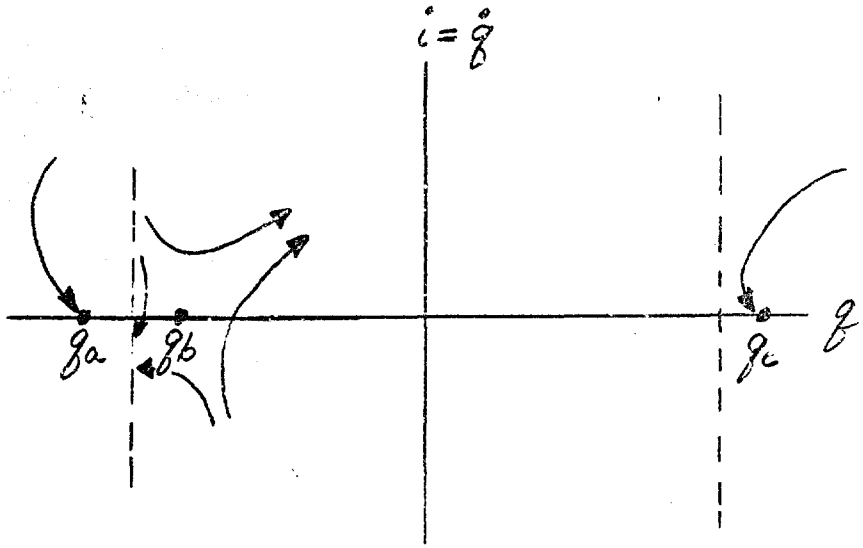

Fig. 2.12. Phase Portrait of 2C--Case I

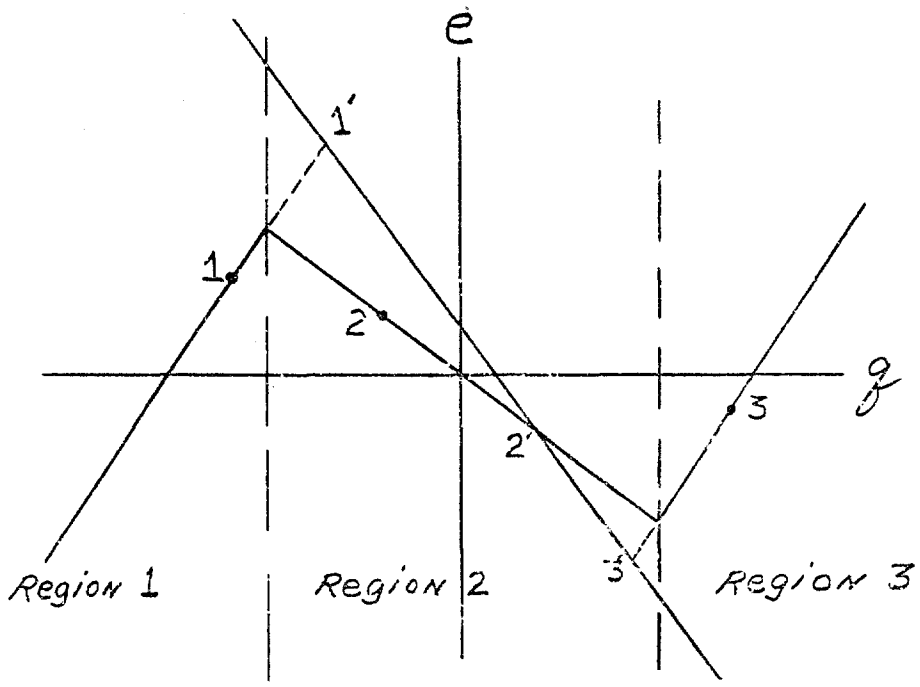

Fig. 2.13. Virtual Singularities
Network 2C, Case II

The preceding phase plane analysis for 2C was checked on an analog computer as well as by an isocline construction and found to be valid.

It should be pointed out here that the isocline construction of both Case II and Case III involves the concept of virtual singularity.[15] In each of these cases the loadline is situated so that there is only one real singularity; each of the other two singularities may be thought of as having moved into regions other than where they started in Case I, and, while they no longer exist as real singular points, they still influence the phase trajectory exactly as they did in Case I, when the trajectory is in their region of influence.

The foregoing statements are illustrated in Fig. 2.13 for Case II. The original singular points for Case I are numbered 1, 2, and 3; when the parameters are changed so that Case II results, singularity 2 is shifted some to 2', but singularities 1' and 3' are now virtual singularities located by extending the positive-slope portions of the e-q characteristic. Note that, although 1' and 3' are now in region 2, they still influence the phase trajectory in regions 1 and 3, respectively, in the same way as they did for Case I. Of course, these virtual singular points would be represented on the q axis in the phase plane.

---

[15] Cunningham, p. 112ff.

Networks 2C and 4C are obviously suitable as switching circuits; they may be induced to change states either by a momentary change of appropriate magnitude in E, or by varying the value of the capacitance C_o.

The switching action of network 2C has been demonstrated by means of an analog computer. The constants chosen for this study are (see Fig. 2.10) R = 1, L = 1, C_o = 1, and E = .25; for the piecewise linear characteristic the constants are (see Fig. 2.4) e_1 = 1, q_1 = .5, q_x = 1, and $|C_s|$ = .5. Selection of these constants results in three singular points which is Case I, Fig. 2.11.

A phase portrait of network 2C with E = .25 is shown in Fig. 2.14. From this portrait the location of the two stable foci and the saddle point may be noted. The next three figures show the results of momentarily changing the magnitude of E. In Fig. 2.15 a family of trajectories is shown for different values of E. These trajectories all start at the left hand focus obtained when E = .25; thus each curve represents a step of voltage added in series with E. Timing marks have been added to the trajectories so the duration of the pulse as well as the amplitude may be seen. In each case the time from the start to the first timing mark is .38 seconds, and the time between all other timing mark is .85 seconds. So for a given amplitude of pulse applied to the circuit one may estimate the time required for the switching action to take place. The

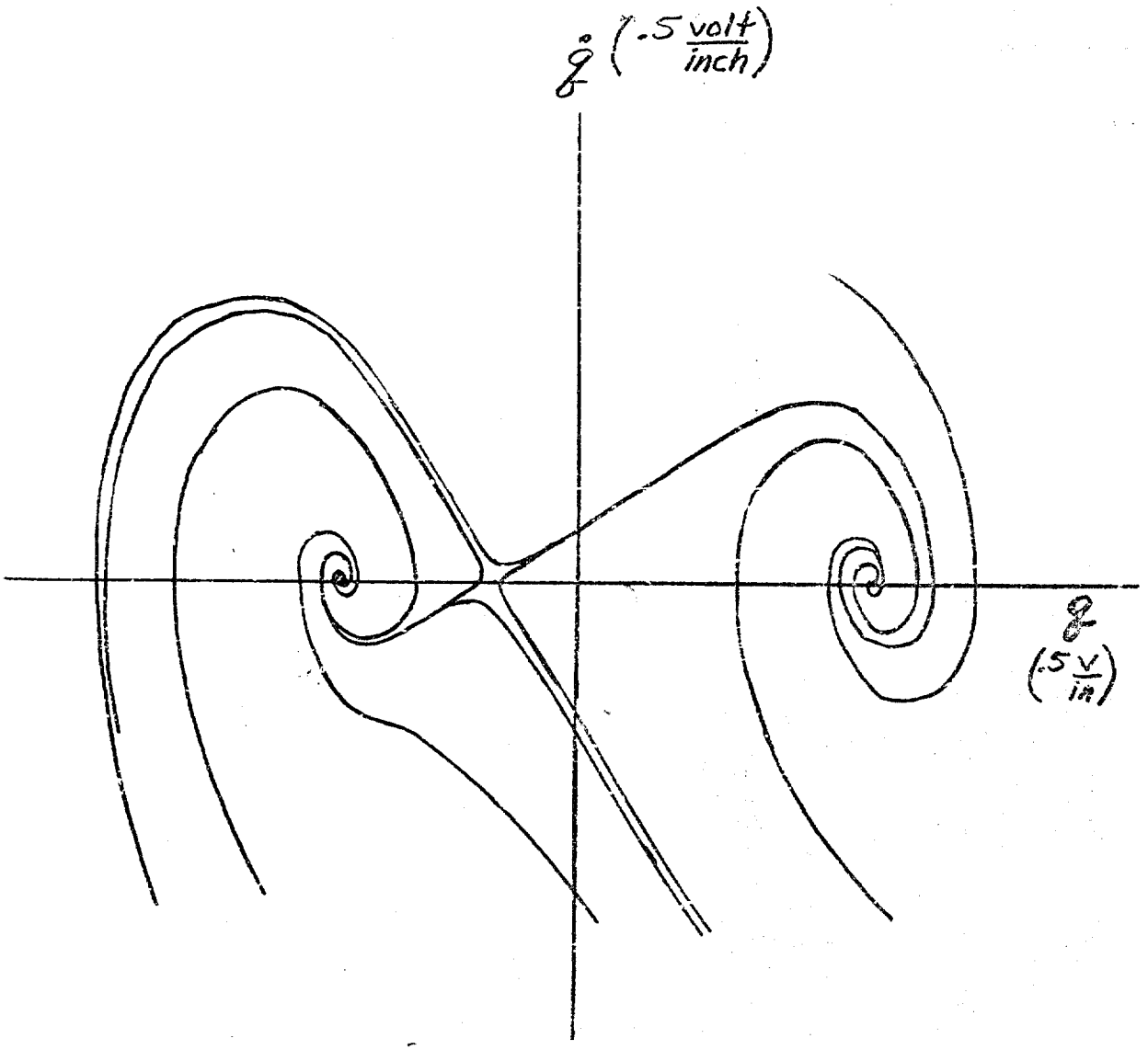

Fig. 2.14. Phase Portrait of Network 2C

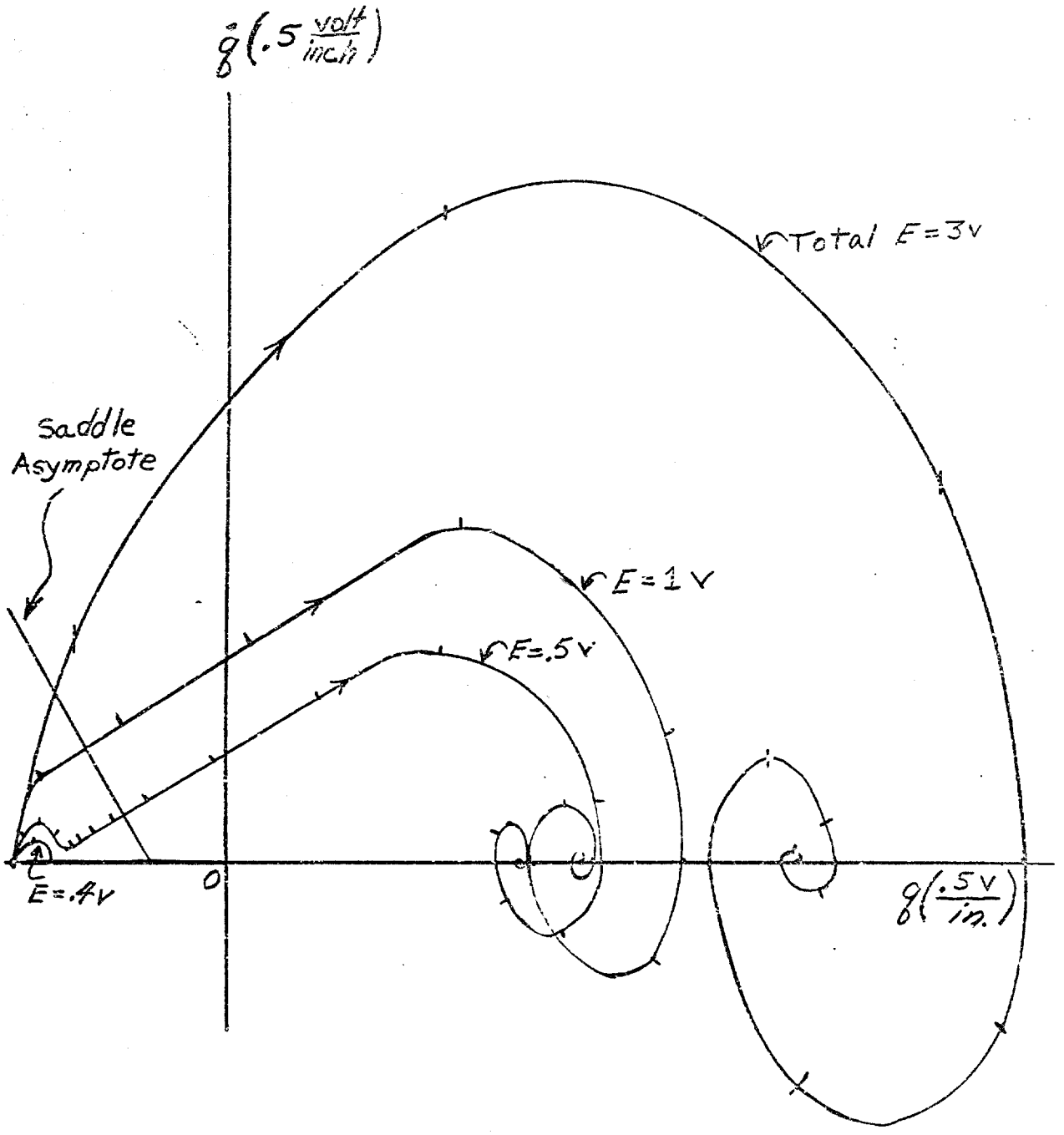

Fig. 2.15. Phase Trajectories for Network 2C for Various Positive Values of Voltage E

saddle asymptote has also been drawn on the figure to give an idea of how long a pulse of given amplitude must be applied for switching to take place. If a pulse of given amplitude is applied long enough for the trajectory to cross the saddle asymptote and then removed the trajectory will continue on to the right hand focus obtained when E = .25. This is illustrated in Fig. 2.17 by the curve labeled Positive Step. This curve starts at the left hand focus obtained when E = .25; a positive step of amplitude 1.25 is applied in series with E; at point A this step is removed and the curve splits into two curves, one labeled E = .25 and the other labeled Total E = 1.5. The curve labeled E = .25 is a trajectory of the original system; note that it ends at the right hand focus shown in Fig. 2.14. The other curve is included here to show the final state of the system if the positive pulse is not removed; this curve also has timing marks from which the duration of the pulse may be estimated.

The same general remarks made about Fig. 2.15 apply also to Fig. 2.16. This family of curves illustrates the results of applying negative pulses to the system when it is initially at the right hand focus obtained when E = .25. In Fig. 2.17 the curve labeled negative step shows the trajectory obtained when a negative pulse with amplitude equal to 1.25 is used to switch the system from the right hand focus to the left hand focus, the negative pulse being removed at point B. These

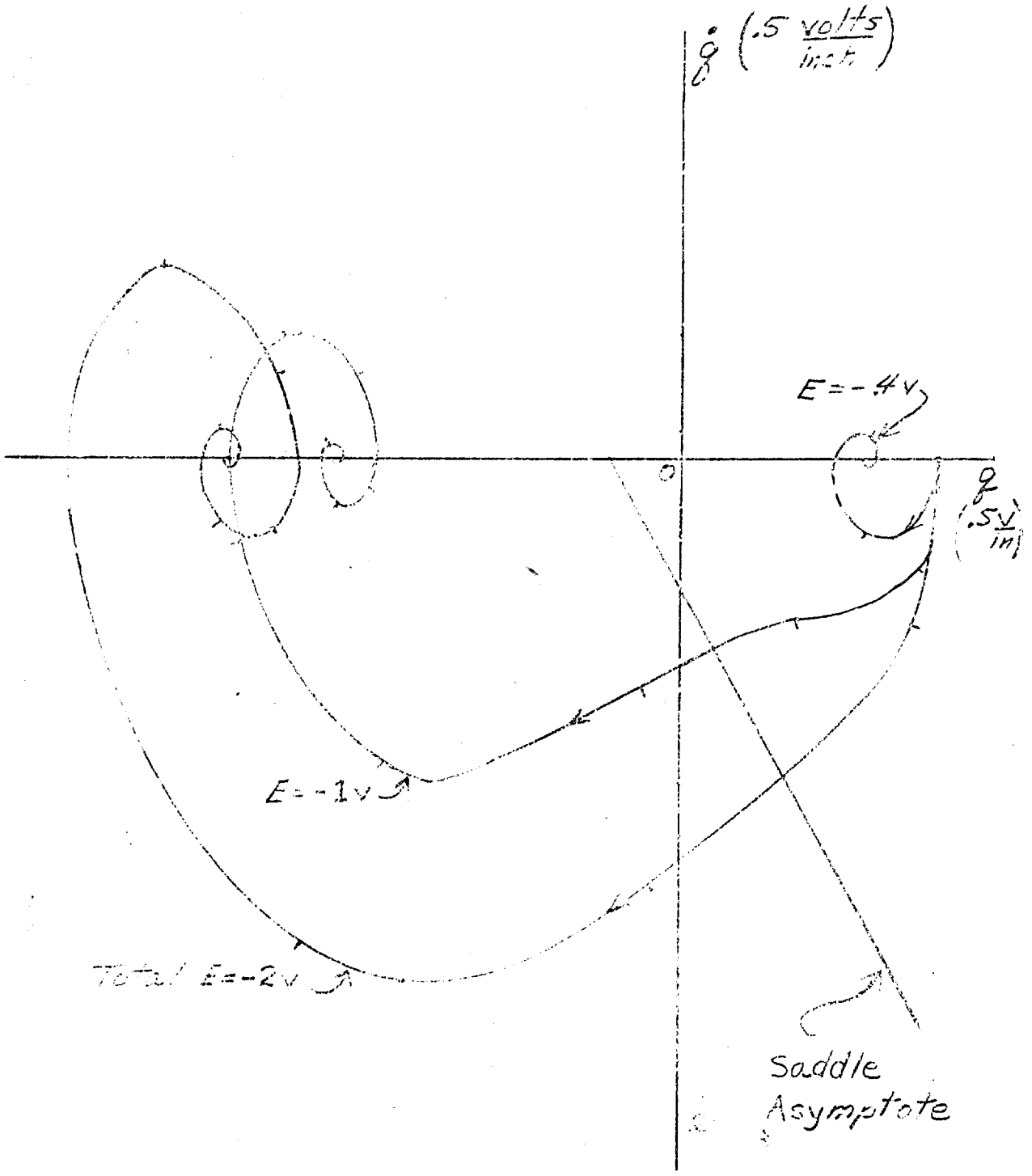

Fig. 2.16. Phase Trajectories for Network 2C for Various Negative Values of Voltage E

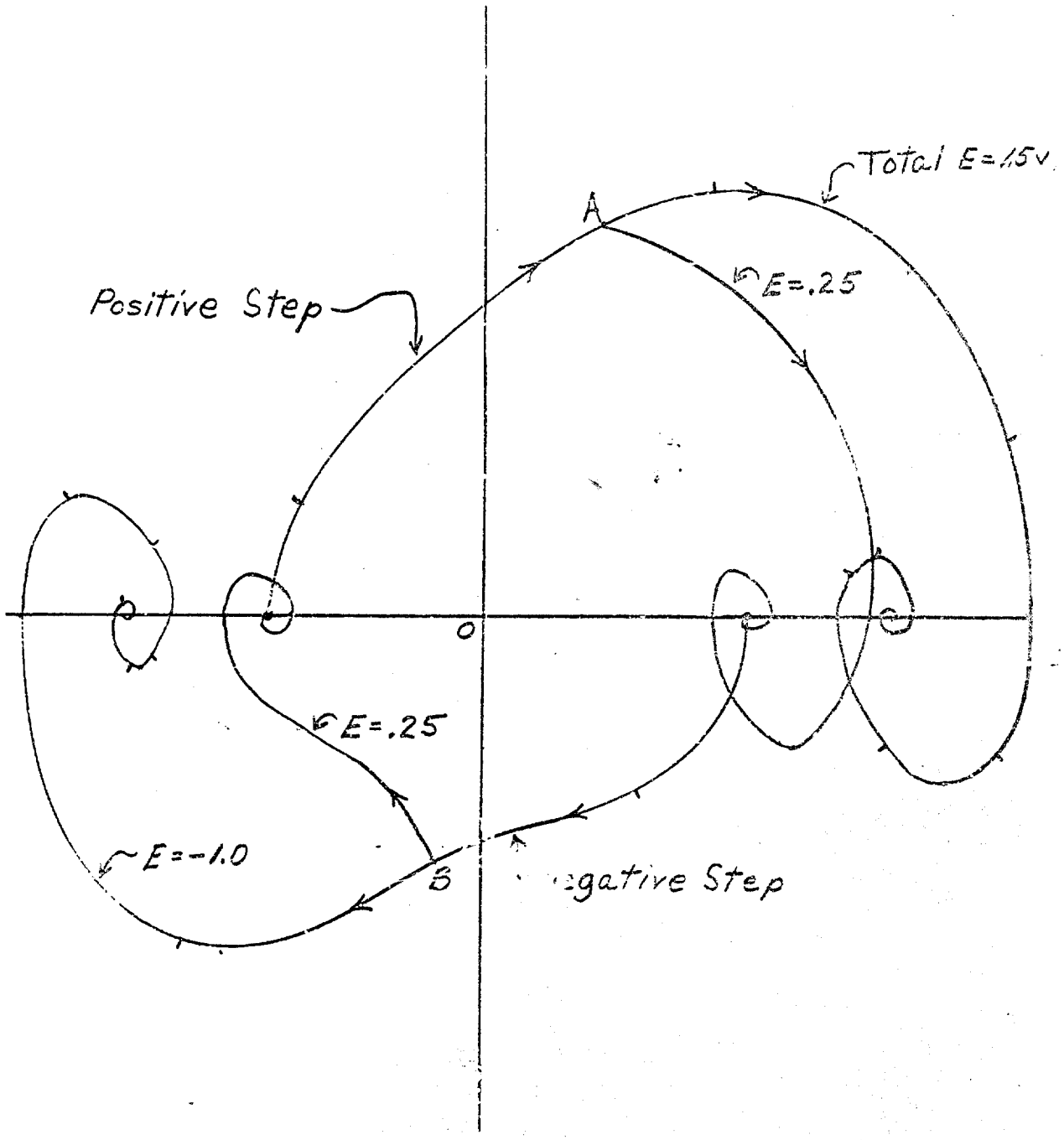

Fig. 2.17. Trajectories for Network 2C Illustrating Switching from Each Stable Singularity to the Other

curves clearly indicate that the system has two stable states and that switching from either state to the other one may be effected by a pulse of appropriate amplitude and duration.

Switching possibilities for the twelve second order networks have been determined by singular point analysis, and possible trajectories from one stable singular point to the other one have been shown by phase plane plots. The twelve third order networks may also be investigated for possible switching circuits. Singular point analysis reveals that all of the third order networks may have two stable singular points and one unstable singular point, or may have only one stable singular point, depending on the magnitude of the bias voltage. From this viewpoint alone any of these networks might be considered suitable as switching circuits; however, only networks 4L, 6L, and 7L would be practical switches since the equations for the charge on the nonlinear capacitor for these networks contain a term proportional to the voltage, E. This means that, for these three networks, not only the location of the singular points, but the number of singular points may be changed by varying E. The equations for these networks all have the same form, so only the singular point analysis for 4L is illustrated below.

The equation for 4L is

$$\dddot{q} + K\ddot{q} + \frac{R_1 R_2}{L_1 L_2}\dot{q} + \frac{1}{L_1}(-a+3bq^2)\dot{q} + \frac{R_2}{L_1 L_2}(-a+3bq^3) = \frac{R_2}{L_1 L_2}E \qquad (2.17)$$

where $K = \frac{R_2}{L_2} + \frac{R_1+R_2}{L_1}$. The parameter numbers are indicated in Fig. 2.18. The location of the singular point (or points) is defined by the following equations:

1. $\ddot{q} = 0.$
2. $\dot{q} = 0.$
3. $e = -aq + bq^3 = E$.

Equation (3) above is shown in Fig. 2.19 as a loadline to specify one possible location of the singular points on the e-q characteristic for $0 < |E| < e_1$. The characteristic equation of this network in the neighborhood of any of the three singular points is

$$\lambda^3 + K\lambda^2 + \left[\frac{R_1R_2}{L_1L_2} + \frac{3b}{L_1}\left(q_s^2 - \frac{a}{3b}\right)\right]\lambda + \frac{3bR_2}{L_1L_2}\left(q_s^2 - \frac{a}{3b}\right) = 0, \qquad (2.18)$$

with q_s equal to the value of charge at a given point. Let q_s in Eq. (2.18) equal q_b (Fig. 2.19); at this singular point $q_s^2 - a/3b < 0$, and there is one sign change of the coefficients of Eq. (2.18) for any values of the circuit elements. Therefore this singular point is unstable since at least one of the roots of this equation has a positive real part. When q_s is equal to either q_a or q_c, then $q_s^2 - a/3b > 0$ and all the coefficients of Eq. (2.18) have the same sign. Application of the Routh stability criterion indicates that both of these singular points are stable due to the characteristic roots at each singularity having negative real parts. The switching action of this network, as well as networks 6L and 7L, may be explained

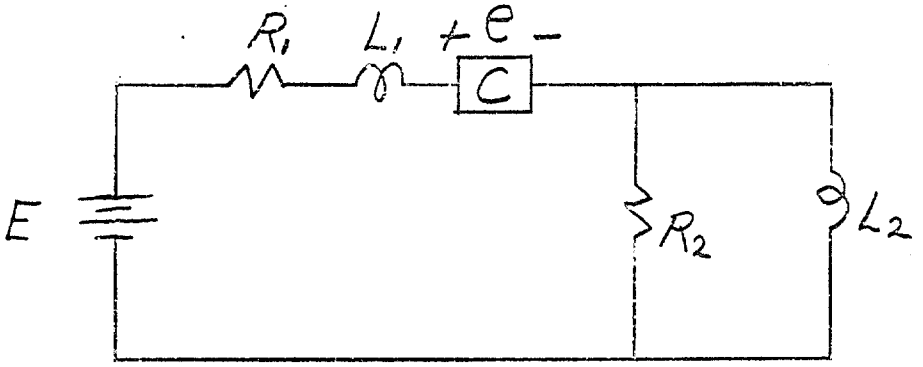

Fig. 2.18 Network 4L

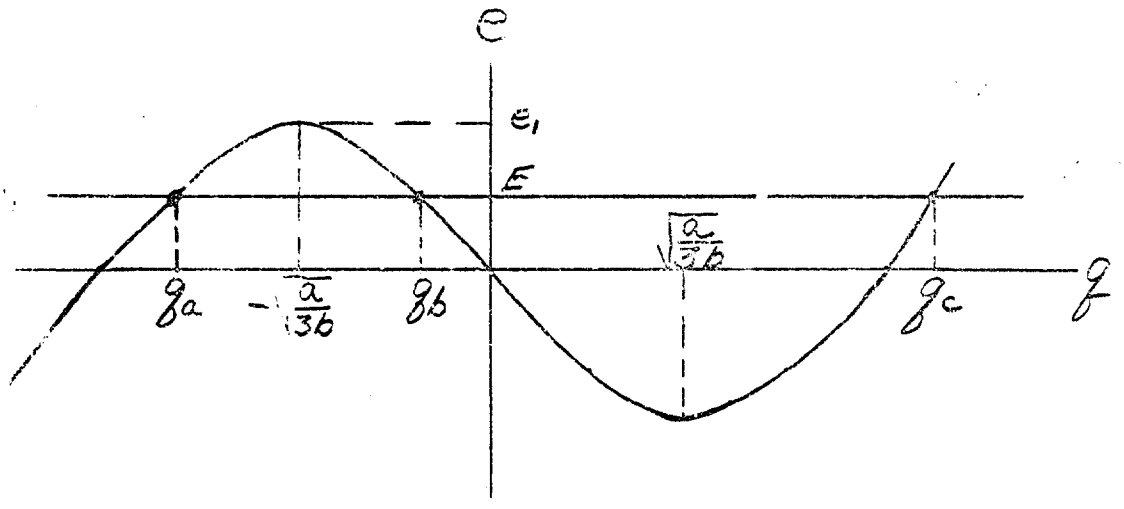

Fig. 2.19. Location of Singular Points for Network 4L

in an analogous manner to network 2C, which has been discussed in detail in the preceding paragraphs of this study.

2.4 Oscillation

Thus far the discussion has been primarily concerned with the stability of networks as small signal amplifiers and with their utility as switching circuits. The question of stability has been investigated by means of linear circuit theory, and the switching possibilities have been illustrated by means of phase plane analysis. The case for oscillation, however, is not nearly as straight forward as the cases for amplification and switching. There is no way to tell, in general, whether a limit cycle can exist for a nonlinear equation. While there are numerous theorems dealing with the existence of limit cycles (e.g., see Graham and McRuer, p. 345ff.), these are theorems for very special cases or theorems which give either sufficient conditions for a limit cycle or necessary conditions but not both.

It might be well to point out again that the question here concerning oscillation is whether a limit cycle can exist in any part of the phase plane; this is significantly different from the question that arises in control system design in which the search is for some region of the phase plane for which no oscillation can take place. Indeed, if the control system designer can find some region in which no limit cycle can exist, he will attempt to operate the control system "in this region"

and will be confident that no oscillation can occur. In other words, if the present problem were approached by the second method of Liapounoff, a Liapounoff function would have to be found that would promise stability of the whole phase plane in order to say whether oscillation could occur; part of the plane would not be enough to completely answer the propcsed question.

Formal proofs will be given to show that none of the second order networks can support a sustained oscillation; however, it can be intuitively argued that none of the networks which contain a resistance can have a variable that oscillates without decay. It has already been shown that the average power associated with the nonlinear capacitor is zero; this is signifi-cant here, since if the average DC input power to the capacitor is zero, and the average AC output power is zero, then no energy conversion from DC to AC can take place. That is, AC energy cannot be supplied to the network by the battery—NNC combination. The battery can deliver no AC power to the resistance in the network, so the AC power consumed by the resistance must come from the energy initially stored in the network. Therefore, the AC energy in the network must ultimately decrease with time. The LC network of Fig. 1.4(b) has been shown to have an oscillatory solution; this can be true because no energy is taken from the network. If a resistance were added anywhere in this network, power would be lost and the energy in the system would decrease to zero.

One theorem that is quite general (for second order networks) and that reveals some facts about the present problem is known as the negative criterion of Bendixson.[16] The theorem states that if the equations of the system are given by

$$\dot{x} = P(x, y)$$
$$\dot{y} = Q(x, y),$$

then no limit cycle exists in any region of the x-y phase plane for which the expression $\frac{\partial P}{\partial x} + \frac{\partial Q}{\partial y}$ has an invariant sign and is not identically zero. Note that the theorem gives a sufficient condition that prohibits the existence of a limit cycle; this is not a necessary condition. If the expression $\frac{\partial P}{\partial x} + \frac{\partial Q}{\partial y}$ changes sign in a region then a limit cycle may or may not exist in that region. Since partial derivatives are involved, the continuous relationship between charge and voltage, i.e., $e = -aq + bq^3$, will be used in the equations which describe each of the networks, rather than the piecewise linear characteristic that was actually used in the phase plane analysis.

The results of the application of Bendixson's Theorem to the twelve second order networks are shown in Table 2.1. The first case of Table 2.1 is self explanatory; for the four networks listed, $\frac{\partial P}{\partial x} + \frac{\partial Q}{\partial y}$ does not involve either of the phase plane variables; hence, the algebraic sign is invariant over the whole phase space. Cases 2 and 3 of Table 2.1 may be

---

[16] N. Minorsky, Nonlinear Oscillations (New York: D. Van Nostrand Company, Inc., 1962), p. 82ff.

LIMIT CYCLE CONDITIONS	NETWORKS
1. No limit cycle possible	2R, 2L, 2C, 7R
2. No limit cycle possible if $a < \frac{R_1 R_2}{L}$	3R, 3L, 4R, 6R, 8R
3. No limit cycle if $a < \frac{R_1 R_2}{L} + \frac{1}{C_o}$	4C
4. No limit cycle possible if $q^2 < \frac{a}{3b}$	1R, 5R

TABLE 2.1. LIMIT CYCLE CONDITIONS FOR THE SECOND ORDER NETWORKS OBTAINED BY MEANS OF A CONTINUOUS q-e CHARACTERISTIC

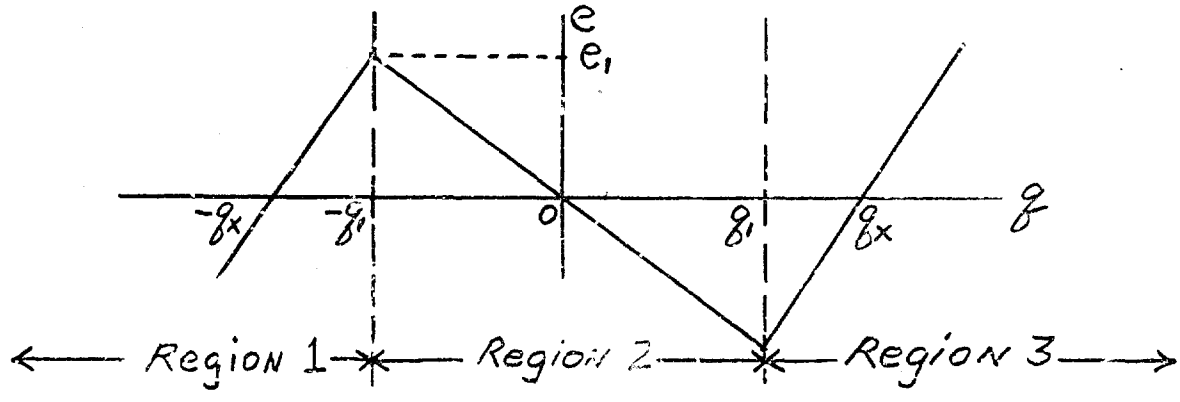

Fig. 2.20. Piecewise Linear Capacitor Characteristic

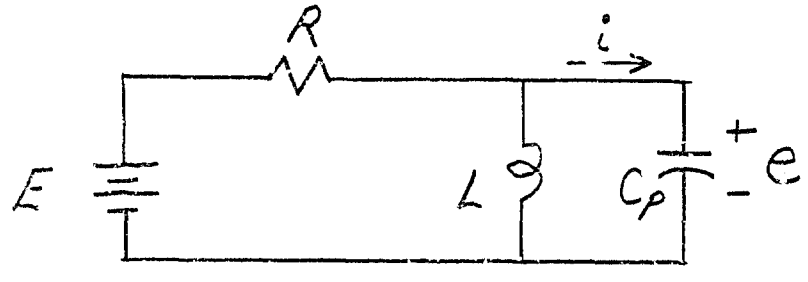

Fig. 2.21. Network 1R

considered together since these cases both give relationships between the circuit parameters and the coefficient a, which partially characterizes the NNC. For these two cases Bendixson's Theorem simply says that if the coefficient of the damping force is always positive there can be no oscillation. If the coefficient of the damping force is positive for some values of the variable and negative for other values, then oscillation is possible but not certain. Case 4 of Table 2.1 gives no new information about networks 1R and 5R. This says that there can be no limit cycle for which the capacitance is always negative. A consideration of Poincaré's index results in this same conclusion.

Thus Bendixson's Theorem is used to eliminate four of the networks as possible oscillators (Case 1, Table 2.1). The question of oscillation for the other eight networks will now be answered by means of a phase plane study. If the charge-voltage characteristic of the nonlinear capacitor is assumed to be piecewise linear then three regions may be defined as shown in Fig. 2.20. Phase plane trajectories may theoretically be calculated for any of the twelve second order networks by means of linear network theory, a given solution being obtained for each of the three linear regions, and then the three solutions being joined at the region boundaries. This approach will now be used for one of the second order networks to show that, regardless of where a given trajectory starts, it is impossible

for that trajectory to return to its starting point. The given trajectory will end up at one of the stable singular points for all values of the network parameters as well as for all values of q_1, q_x, and e_1. The network chosen for this analysis is 1R, redrawn in Fig. 2.21 with R and R_g combined into a single resistor, R. The piecewise linear capacitor is designated as C_p, where p takes on the values 1, 2, or 3 depending on the region under discussion. The value of C_p is obtained from the charge-voltage relationship for each region, which is:

Region 1. $$e = \frac{e_1}{g_x - g_1}(g + g_x) \quad ; \quad C_1 = \frac{g_x - g_1}{e_1} . \tag{2.19}$$

Region 2. $$e = -\frac{e_1}{g_1} g \quad ; \quad C_2 = -\frac{g_1}{e_1} . \tag{2.20}$$

Region 3. $$e = \frac{e_1}{g_x - g_1}(g - g_x) ; \quad C_3 = \frac{g_x - g_1}{e_1} = C_1 . \tag{2.21}$$

The network equations, valid for each region, are:

$$\frac{d^2 e}{dt^2} + \frac{1}{RC_p}\frac{de}{dt} + \frac{e}{LC_p} = 0, \tag{2.22}$$

$$i = C_p \frac{de}{dt} = \frac{dg}{dt} . \tag{2.23}$$

First the pertinent relationships for each region will be listed then the phase plane calculations will follow.

Region 1. $i(0) = I_0$, $q(0) = Q_0$

Characteristic roots: $$s_{1,2} = -\frac{1}{2RC_1} \pm \sqrt{\left(\frac{1}{2RC_1}\right)^2 - \frac{1}{LC_1}} ,$$

$$s_1 < 0 , \; s_2 < 0 ; \; |s_2| > |s_1| .$$

$$q = q_x + \left[\frac{s_2(q_x+Q_0)-I_0}{s_2-s_1}\right]e^{s_1 t} - \left[\frac{s_1(q_x+Q_0)-I_0}{s_2-s_1}\right]e^{s_2 t} \tag{2.24}$$

$$e = \frac{e_1}{q_x-q_1}\left\{\left[\frac{s_2(q_x+q_0)-I_0}{s_2-s_1}\right]e^{s_1 t} - \left[\frac{s_1(q_x+Q_0)-I_0}{s_2-s_1}\right]e^{s_2 t}\right\} \tag{2.25}$$

$$i = s_1\left[\frac{s_2(q_x+Q_0)-I_0}{s_2-s_1}\right]e^{s_1 t} - s_2\left[\frac{s_1(q_x+Q_0)-I_0}{s_2-s_1}\right]e^{s_2 t} \tag{2.26}$$

If the singularity at $(q = q_x,\ I = 0)$ is a node then the slope of the asymptote as $t \to -\infty$ is $s_2(q_x + q)$, and the slope of the asymptote at $t \to +\infty$ is $s_1(q_x + q)$.

Region 2. $q(0) = Q_0,\ I(0) = I_0$

Characteristic roots: $p_{1,2} = -\frac{1}{2RC_2} \pm \sqrt{\left(\frac{1}{2RC_2}\right)^2 - \frac{1}{LC_2}}$,

$p_1 > 0$ and real, $p_2 < 0$ and real; $|p_1| > |p_2|$.

$$q = \left[\frac{p_2 Q_0 - I_0}{-p_2-p_1}\right]e^{p_1 t} - \left[\frac{p_1 Q_0 - I_0}{p_2-p_1}\right]e^{p_2 t}. \tag{2.27}$$

$$e = \frac{-e_1}{q_1(p_2-p_1)}\left[(p_2 Q_0 - I_0)e^{p_1 t} - (p_1 Q_0 - I_0)e^{p_2 t}\right]. \tag{2.28}$$

$$i = \frac{p_1(p_2 Q_0 - I_0)}{p_2-p_1}e^{p_1 t} - \frac{p_2(p_1 Q_0 - I_0)}{p_2-p_1}e^{p_2 t}. \tag{2.29}$$

Asymptotes of saddle: $\dot{q} = p_1 q$ as $t \to +\infty$

$\dot{q} = p_2 q$ as $t \to -\infty$.

Region 3. $q(0) = Q_0$, $I(0) = I_0$

Characteristic roots: $s_{1,2} = -\frac{1}{2RC_3} \pm \sqrt{\left(\frac{1}{2RC_3}\right)^2 - \frac{1}{LC_3}}$,

but $C_3 = C_1$ so characteristic roots are same as for Region 1.

$$q = q_x + \left[\frac{s_2(Q_0 - q_x) - I_0}{s_2 - s_1}\right] e^{s_1 t} - \left[\frac{s_1(Q_0 - q_x) - I_0}{s_2 - s_1}\right] e^{s_2 t}. \qquad (2.30)$$

$$e = \frac{e_1}{(q_x - q_1)(s_2 - s_1)} \left\{ [s_2(Q_0 - q_x) - I_0] e^{s_1 t} - [s_1(Q_0 - q_x) - I_0] e^{s_2 t} \right\} \qquad (2.31)$$

$$i = s_1 \left[\frac{s_2(Q_0 - q_x) - I_0}{s_2 - s_1}\right] e^{s_1 t} - s_2 \left[\frac{s_1(Q_0 - q_x) - I_0}{s_2 - s_1}\right] e^{s_2 t}. \qquad (2.32)$$

If the singularity at ($q = q_x$, $I = 0$) is a node then the slopes of the asymptotes as t becomes large are the same as for R1.

The phase plane is shown in Fig. 2.22 along with the e-q characteristic of the capacitor. Also shown in this figure are possible asymptotes for the saddle point and the values of current at which these asymptotes intersect the boundaries of Region 2. Refer to this figure for the following discussion.

Assume first that initial conditions are such that the trajectory starts in R1 (Region 1). There are three possibilities:

1. q decays to $-q_x$, never leaving R1.
2. q enters R2 at some time t_1 but returns to R1 because $I(t_1) < -p_2 q_1$, the intersection of the saddle asymptote with the boundary between R1 and R2.

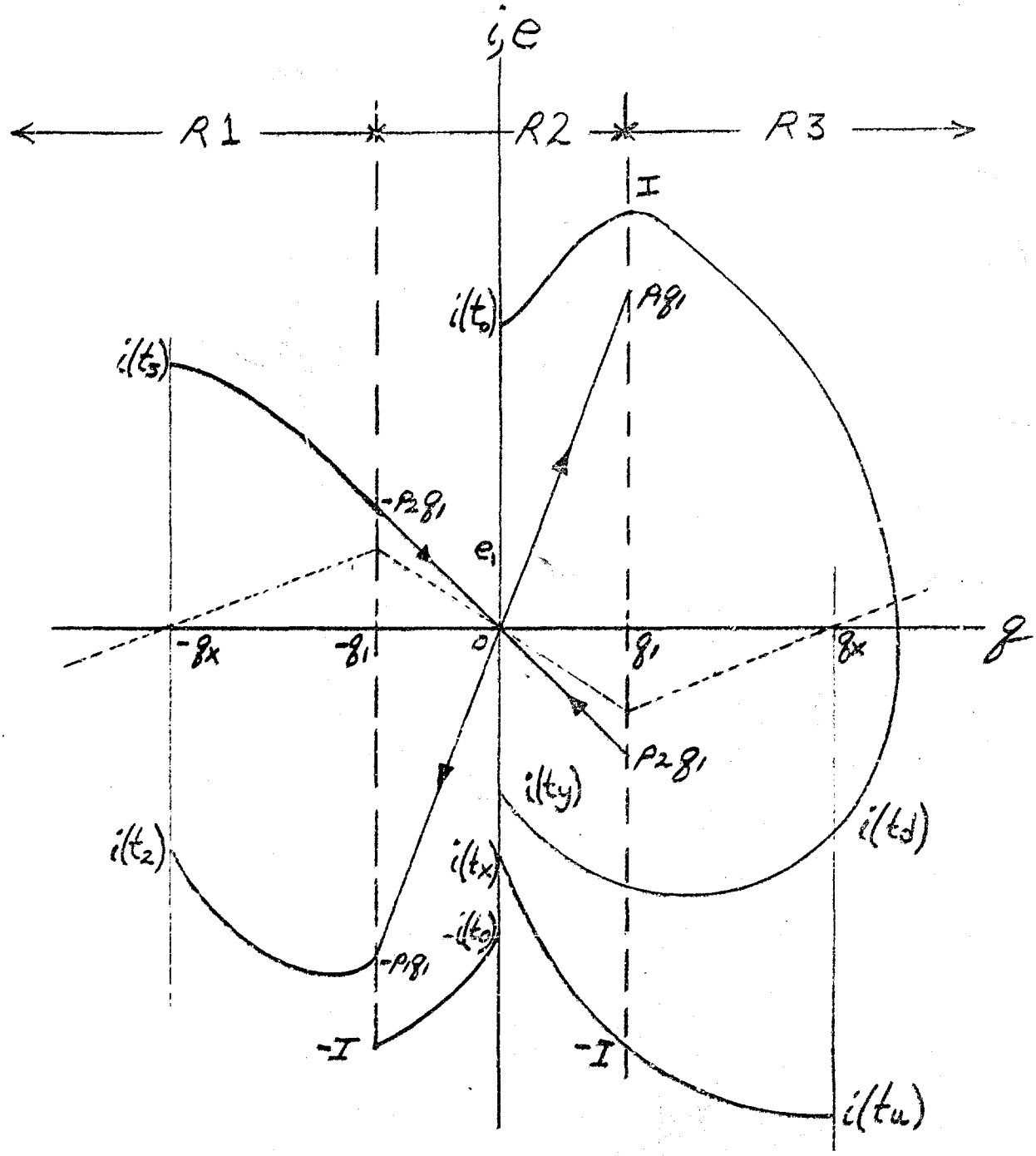

Fig. 2.22. Phase Plane Plot of Network 1R

3. q enters R2 and passes through to R3 if

$i(t_1) > - p_2 q_1$.

The singularity at ($q = - q_x$, $i = 0$) is either a stable node or a stable focus. Obviously if the trajectory never leaves R1 there can be no limit cycle around this singularity.

Assume that possibility 2 has occurred; the trajectory leaves R1, enters R2 and returns to R1. The minimum value that the current can have when re-entering R1 is $- p_1 q_1$; at this value of current $q = - q_1$. With these values as initial conditions it is desired to find the value of current when the charge reaches $- q_x$. This occurs in the time it takes for e to go from e_1 to zero. To find this time set Eq. (2.25) equal to zero at $t = t_2$;

$$t_2 = \frac{1}{s_2 - s_1} \ln \left[\frac{s_2 (q_x - q_1) + p_1 q_1}{s_1 (q_x - q_1) + p_1 q_1} \right] . \qquad (2.33)$$

Insert t_2 into Eq. (2.26) and get

$$i(t_2) = \frac{- \left[s_2 (q_x - q_1) + p_1 q_1 \right]^{\frac{s_2}{s_2 - s_1}}}{\left[s_1 (q_x - q_1) + p_1 q_1 \right]^{\frac{s_1}{s_2 - s_1}}} . \qquad (2.34)$$

Now suppose that the singularity at ($q = q_x$, $i = 0$) is a node; the following statements may be applied to Eq. (2.34)

1. $i(t_2)$ must be real
2. $s_2 (q_x - q_1) < 0$
3. $s_1 (q_x - q_1) < 0$

4. $p_1 q_1 > 0$

5. $s_2/(s_2-s_1)$ and $s_1/(s_2-s_1)$ are not integers, so

6. $\left.\begin{aligned} s_2(q_x-q_1) + p_1 q_1 &> 0 \\ s_1(q_x-q_1) + p_1 q_1 &> 0 \end{aligned}\right\}$ for $t(t_2)$ real

7. $s_2(q_x-q_1) < s_1(q_x-q_1)$

8. $s_2(q_x-q_1)$ is the intersection of the node asymptote and the boundary of R1 as $t \to -\infty$

   $s_1(q_x-q_1)$ is the intersection of the node asymptote and the boundary of R1 as $t \to +\infty$.

A possible trajectory satisfying Statements 1 through 7 is shown in Fig. 2.23. Also shown are the asymptotes with intersections specified by Statement 8. With reference to Fig. 2.23, note that if $s_2(q_x-q_1) < -p_1 q_1$ then the trajectory could reach the singular point only at $t_2 = \infty$; this condition is prevented by Statement 6 above. The important thing here is that the node asymptotes are solution curves which extend throughout R1, and, since no solution curves may cross, it is impossible for any trajectory which enters R1 to do anything but approach the singular point. Similar statements may be made about the singular point in R3; hence, the conclusion to be drawn is that there can be no limit cycle if the two stable singularities are nodes. For the remainder of this discussion it will be assumed that the phase plane contains two stable foci and one saddle point.

Equations (2.33) and (2.34) may be rewritten as

$$t_2 = \frac{\theta_1}{\beta} \qquad (2.35)$$

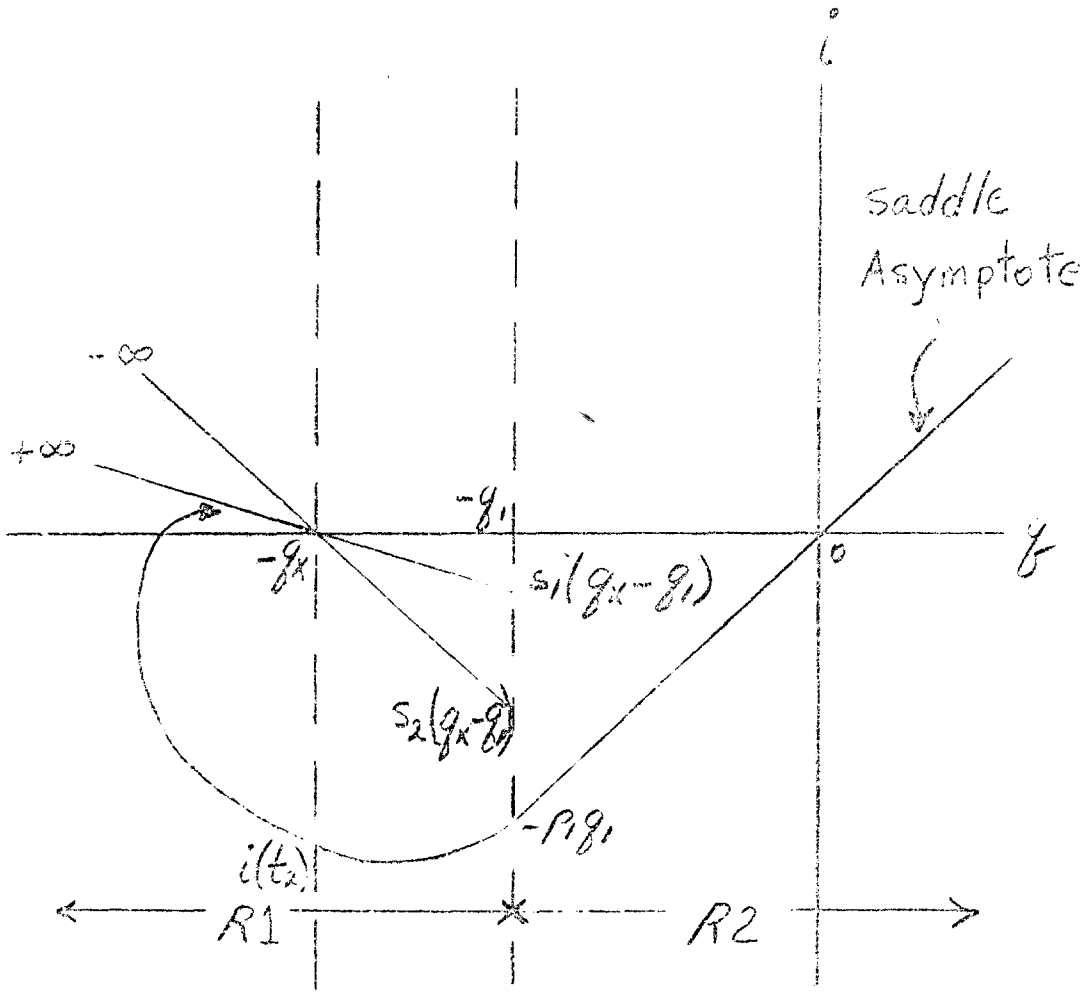

Fig. 2.23. Possible Trajectory for Stable Node

and

$$i(t_2) = -W e^{-\frac{\alpha}{\beta}\theta_1}, \qquad (2.36)$$

where $s_1 = -\alpha + j\beta$ and $s_2 = -\alpha - j\beta$

$$W = \left\{\left[-\alpha(g_x - g_1) + p_1 g_1\right]^2 + \beta^2(g_x - g_1)^2\right\}^{1/2},$$

and

$$\theta_1 = \tan^{-1}\frac{\beta(g_x - g_1)}{-\alpha(g_x - g_1) + p_1 g_1}$$

It is now desirable to find the maximum value of current that the trajectory may exhibit on the line $q = -q_x$ (chosen for convenience) and still have possibility 2 occur. This is $i(t_3)$ in Fig. 2.22. To find $i(t_3)$, it is necessary to write the equations for RI with time reversed so that the trajectory will move from right to left in the upper half of the phase plane. Then, with initial conditions $Q_0 = -q_1$, $I_0 = -p_2 q_1$, find the time, t_3, that it takes e to go to zero. Plug t_3 into the equation for i with time reversed. Note that the current obtained in this way is the negative of the actual current since, if $t = -t'$, then $\frac{dq}{dt} = -\frac{dq}{dt'}$. When this calculation is made it turns out that

$$i(t_3) = C e^{\frac{\alpha}{\beta}\delta_1} \qquad (2.37)$$

and

$$t_3 = \frac{\delta_1}{\beta} \qquad (2.38)$$

where again, $s_1 = -\alpha + j\beta$ and $s_2 = -\alpha - j\beta$ and

$$C = \left\{ [\alpha(g_x - g_{11}) - \beta_2 g_{11}]^2 + \beta^2 (g_x - g_{11})^2 \right\}^{1/2},$$

$$\delta_1 = \tan^{-1} \frac{\beta(g_x - g_{11})}{\alpha(g_x - g_{11}) - \beta_2 g_{11}} .$$

Now it can be shown that $C = W$, and, since $\delta_1 > 0$ and $\theta_1 > 0$ the conclusion is reached that

$$|i(t_3)| > |i(t_2)| \quad . \tag{2.39}$$

This conclusion demonstrates that there can be no limit cycle around the focus as well as that possibility 3 cannot result if possibility 2 exists initially. If initial conditions are such that the trajectory passes through the point $i(t_3)$, then the preceding analysis guarantees that when the trajectory has gone through 180 degrees it will be nearer the singular point than it was at $i(t_3)$. The trajectory can never retrace itself no matter how skewed the spiral is since the two points in question are 180 degrees apart. It may also be said that there can be no limit cycle around the singular point in R3 due to the symmetry of the problem.

Possibility 3 remains to be discussed, if a limit cycle exists for this possibility then it encircles all three singular points. The limit cycle will pass through the point $q = q_1$, $i = I > p_1 q_1$ (see Fig. 2.22). It will be shown that if a trajectory passes through the point I, encircles the three singular points and returns to intersect the line $q = q_1$, then the value of current at this intersection will be less

than the value I. It is actually not necessary to trace the trajectory through a complete revolution due to the symmetry of the capacitor characteristic. If a closed trajectory passes through the point $q = q_1$, $i = I$ then it must also pass through the point $q = -q_1$, $i = -I$. Project backwards from $i = I$, $q = q_1$ to the ordinate; the trajectory will intersect the ordinate at some $i(t_o)$. Project backwards from $i = -I$, $q = -q_1$ to the ordinate; the value of current at this intersection is $-i(t_o)$. The statement to be proven, then, if there is to be no limit cycle, is that if a trajectory pastes through the point $q = 0$, $i = i(t_o)$ then when the trajectory has gone through 180 degrees, $q = 0$ again but $i > -i(t_o)$. This proof is done by proving that if a given trajectory passes through the point $q = 0$, $i = i(t_o)$ then a second trajectory can be found that prevents the given trajectory from reaching the point $q = 0$, $i = -i(t_o)$ since trajectories cannot cross one another in the phase plane.

First, choose any value of $I > p_1 q_1$; with this value of initial current and $Q_c = q_1$ find $i(t_o)$ and $i(t_d)$ (Fig. 2.22). Find

$$t_d = \frac{2\pi - \mu}{\beta} \quad , \tag{2.40}$$

and

$$i(t_d) = -M e^{-\frac{\alpha}{\beta}(2\pi - \mu)} \quad , \tag{2.41}$$

where $s_1 = -\alpha + j\beta$, $s_2 = -\alpha - j\beta$, and

$$M = \left\{[-\alpha(q_x - q_1) - I]^2 + \beta^2(q_1 - q_x)^2\right\}^{1/2} ;$$

$$\mu = \tan^{-1}\frac{\beta(q_x - q_1)}{\alpha(q_x - q_1) - I} ,$$

also

$$i(t_0) = \frac{[I - p_2 q_1]^{\frac{p_2}{p_2 - p_1}}}{[I - p_1 q_1]^{\frac{p_1}{p_2 - p_1}}} \qquad (2.42)$$

Now a possible trajectory may be drawn through the points defined by I, $i(t_d)$ and $i(t_0)$.

Assume that a second trajectory is started at $q = q_1$; $i = -I$. This trajectory intersects the ordinate at $i(t_x)$ and intersects the line $q = q_x$ at $i(t_u)$ (see Fig. 2.22). These values are:

$$t_x = \frac{1}{p_2 - p_1}\ln\left[\frac{p_2 q_1 + I}{p_1 q_1 + I}\right] ; \qquad (2.43)$$

$$i(t_x) = \frac{-[p_2 q_1 + I]}{[p_1 q_1 + I]^{\frac{p_1}{p_2 - p_1}}} ; \qquad (2.44)$$

$$t_u = \frac{\pi - \lambda}{\beta} , \qquad (2.45)$$

and

$$i(t_u) = -G\, e^{\frac{\alpha}{\beta}(\pi - \lambda)} \qquad (2.46)$$

where, in R3, $s_1 = -\alpha + j\beta$, $s_2 = -\alpha - j\beta$ and

$$G = \left\{\left[-\alpha(g_x - g_{1,}) - I\right]^2 + \beta^2 (g_x - g_{1,})^2\right\}^{1/2} j$$

$$\lambda = \tan^{-1} \frac{\beta(g_x - g_{1,})}{-\alpha(g_x - g_{1,}) - I} .$$

Now it remains to be shown that $|i(t_x)| < |i(t_o)|$ and $|i(t_d)| < |i(t_u)|$; if this is true then the original trajectory must intersect the negative half of the ordinate at some $i(t_y)$ which is greater than $-i(t_o)$.

First, compare $|i(t_x)|$ [Eq. (2.44)] with $|i(t_o)|$ [Eq. (2.42)]

$$\frac{\left[g - g_1 + I\right]^{\frac{p_2}{p_2 - p_1}}}{\left[p_1 g_1 + I\right]^{\frac{p_1}{p_2 - p_1}}} \stackrel{?}{<} \frac{\left[I - p_2 g_1\right]^{\frac{p_2}{p_2 - p_1}}}{\left[I - p_1 g_1\right]^{\frac{p_1}{p_2 - p_1}}} . \qquad (2.47)$$

It has already been established that

$$I > p_1 q_1 \quad \text{and} \quad |p_1| > |p_2|, \quad \text{so}$$

$$I > |p_2 q_1| \ ; \ \text{also} \ \ p_1 q_1 > 0 \ \ \text{and} \ \ p_2 q_1 < 0$$

so for any value of I it is obvious that

$$I - |p_2 q_1| < I + |p_2 q_1|$$

and

$$I + p_1 q_1 > I - p_1 q_1 \ ;$$

so inequality Eq. (2.47) is indeed true. Then compare $|i(t_d)|$ [Eq. (2.41)] with $|i(t_u)|$ [Eq. (2.46)]

$$\left\{\left[-\alpha(g_1 - g_x) - I\right]^2 + \beta^2 (g_1 - g_x)^2\right\}^{1/2} e^{\frac{-\alpha}{\beta}(2\pi - \mu)}$$

$$< \left\{\left[-\alpha(g_x - g_{1,}) - I\right]^2 + \beta^2 (g_x - g_{1,})^2\right\}^{1/2} e^{\frac{\alpha}{\beta}(\pi - \lambda)} \qquad (2.48)$$

First consider the exponential terms of Eq. (2.49)

$$\frac{e^{\alpha/\beta(\pi-\lambda)}}{e^{-\alpha/\beta(2\pi-\mu)}} = e^{\frac{\alpha}{\beta}(3\pi-\lambda-\mu)},$$

but $0 < \lambda < \pi$ and $0 < \mu < \pi$ so $\lambda + \mu < 2\pi$ and $3\pi - (\lambda + \mu) > \pi$, therefore

$$\frac{e^{\alpha/\beta(\pi-\lambda)}}{e^{-\alpha/\beta(2\pi-\mu)}} > 1,$$

and

$$e^{\frac{\alpha}{\beta}(\pi-\lambda)} > e^{-\frac{\alpha}{\beta}(2\pi-\mu)}. \qquad (2.49)$$

In comparing the terms under the radicals in Eq. (2.48), it is only necessary to consider

$$[-\alpha(g_x - g_i) - I]^2 \gtrless [\alpha(g_x - g_i) - I]^2 \qquad (2.50)$$

Now I is considered positive for this example and $\alpha > 0$ $g_x - g_i > 0$ so inequality Eq. (2.50) is obviously true for any I. Inspection of Eqs. (2.48), (2.49), and (2.50) clearly indicates that $|I(t_d)| < |t_u)|$. Thus no limit cycle can exist for network 1R. This also applies to network 5R, which is essentially the same network as 1R.

Six second order networks remain to be considered as oscillators; of these, network 8R may be eliminated immediately since the equations for 8R for each linear region have the same form as the equations previously discussed for 1R. The equations for these two networks are listed below.

Network 1R.

$$R1:\ \ddot{\theta} + \tfrac{1}{RC_1}\dot{\theta} + \tfrac{1}{LC_1}\theta = -\tfrac{1}{LC_1}\theta_x \ . \qquad (2.51)$$

$$R2:\ \ddot{\theta} + \tfrac{1}{RC_2}\dot{\theta} + \tfrac{1}{LC_2}\theta = 0 \ . \qquad (2.52)$$

$$R3:\ \ddot{\theta} + \tfrac{1}{RC_3}\dot{\theta} + \tfrac{1}{LC_3}\theta = \tfrac{1}{LC_3}\theta_x \ . \qquad (2.53)$$

Network 8R. (The resistor in series with the source is R_1)

$$R1:\ \ddot{\theta} + \frac{R_1}{R_1+R_2}\left(\tfrac{1}{R_1C_1} + \frac{R_2}{L}\right)\dot{\theta} + \frac{R_1}{LC_1(R_1+R_2)}\theta = -\frac{R_1}{LC_1(R_1+R_2)}\theta_x \ . \qquad (2.54)$$

$$R2:\ \ddot{\theta} + \frac{R_1}{R_1+R_2}\left(\tfrac{1}{R_1C_2} + \frac{R_2}{L}\right)\dot{\theta} + \frac{R_1}{LC_2(R_1+R_2)}\theta = 0 \ . \qquad (2.55)$$

$$R3:\ \ddot{\theta} + \frac{R_1}{R_1+R_2}\left(\tfrac{1}{R_1C_3} + \frac{R_2}{L}\right)\dot{\theta} + \frac{R_1}{LC_3(R_1+R_2)}\theta = \frac{R_1}{LC_3(R_1+R_2)}\theta_x \ . \qquad (2.56)$$

Now if a set of numerical coefficients is chosen for the equations of 8R then the parameters of 1R may be selected so that corresponding equations of the two sets are identical. Note that $1/LC_p(1R)$ may be made equal to $R_1/LC_p(R_1 + R_2)(8R)$ and then R of 1R may be varied to make

$$\frac{1}{RC_p} = \left(\frac{R_1}{R_1+R_2}\right)\left(\frac{1}{R_1C_p} + \frac{R_2}{L}\right) \ .$$

The equations for each of the other five second order networks are similar to the equations for network 1R except for the inclusion of a constant term which is proportional to the applied voltage, E. It can be shown, however, that with a simple transformation of variables the analysis just completed for 1R applies to these networks also. The equations for

network 3R are presented as an example to illustrate this transformation. The equations for 3R are:

$$R1:\quad \ddot{q} + \left(\frac{R_1}{L} + \frac{1}{R_2 C_1}\right)\dot{q} + \frac{1}{LC_1}\left(1 + \frac{R_1}{R_2}\right)q = \frac{E}{L} - \frac{1}{LC_1}\left(1 + \frac{R_1}{R_2}\right)q_x . \tag{2.57}$$

$$R2:\quad \ddot{q} + \left(\frac{R_2}{L} + \frac{1}{R_2 C_2}\right)\dot{q} + \frac{1}{LC_2}\left(1 + \frac{R_2}{R_2}\right)q = \frac{E}{L} . \tag{2.58}$$

$$R3:\quad \ddot{q} + \left(\frac{R_1}{L} + \frac{1}{R_2 C_3}\right)\dot{q} + \frac{1}{LC_3}\left(1 + \frac{R_1}{R_2}\right)q = \frac{E}{L} + \frac{1}{LC_3}\left(1 + \frac{R_1}{R_2}\right)q_x . \tag{2.59}$$

Now let $q = \chi + \frac{E}{L}\left[\frac{1}{LC_p\left(1 + \frac{R_1}{R_2}\right)}\right]$; (2.60)

the preceding equations then become:

$$R1:\quad \ddot{\chi} + \left(\frac{R_1}{L} + \frac{1}{R_2 C_1}\right)\dot{\chi} + \frac{1}{LC_1}\left(1 + \frac{R_1}{R_2}\right)\chi = -\frac{1}{LC_1}\left(1 + \frac{R_1}{R_2}\right)q_x . \tag{2.61}$$

$$R2:\quad \ddot{\chi} + \left(\frac{R_2}{L} + \frac{1}{R_2 C_2}\right)\dot{\chi} + \frac{1}{LC_2}\left(1 + \frac{R_1}{R_2}\right)\chi = 0 . \tag{2.62}$$

$$R3:\quad \ddot{\chi} + \left(\frac{R_1}{L} + \frac{1}{R_2 C_3}\right)\dot{\chi} + \frac{1}{LC_3}\left(1 + \frac{R_1}{R_2}\right)\chi = \frac{1}{LC_3}\left(1 + \frac{R_1}{R_2}\right)q_x . \tag{2.63}$$

Note that each equation of network 3R may be made identical to one of the Eqs. (2.61), (2.62), or (2.63); thus the i-x phase plane can have no limit cycle. To go from the i-x plane to the i-q plane, however, each point of the i-x plane is displaced horizontally by an amount that is proportional to the voltage E [see Eq. (2.60)]. Since all of these displacements are horizontal and of the same magnitude it follows that if Eqs. (2.61), (2.62), and (2.63) cannot describe a closed trajectory then Eqs. (2.57), (2.58), and (2.59) cannot describe a closed trajectory either. In other words, the transformation

of variables indicated by Eq. (2.60) amounts to rescaling the abscissa of the system described by Eqs. (2.57), (2.58), and (2.59). Thus the conclusion reached here is that there can be no oscillatory solution of any of the second order networks for any values of the circuit parameters or for any values of q_1, q_x, or e_1.

It has not been proved rigorously whether a limit cycle exists for any of the third order systems; however, the intuitive argument based on the consumption of AC energy by the resistance of the system applies to the third order networks. That is, without a source of AC energy all oscillations in any of the networks must eventually die out.

Another argument concerning oscillation in the third order networks is as follows. Let the source resistance in all of these networks except 4L be initially infinite. Then network 3C becomes the RNNC circuit of Fig. 1.3(a) which will not oscillate; 5L and 5C become the LNNC circuit of Fig. 1.3(b) and will oscillate because they are lossless. The remaining networks become identical to second order networks for which oscillation has been shown to be impossible. Now, if the source resistance is allowed to become finite, a dissipative element is essentially added to each of these networks. Networks 5L and 5C will not oscillate since they will no longer be lossless; if the remaining networks will not oscillate without the source resistance then certainly the addition of this resistance will

not cause oscillation but will add to the damping that is already present. The same argument applies to network 4L except a different resistance is considered initially infinite.

The preceding arguments can be used to predict with reasonable certainty that no sustained oscillation can occur in any of the third order networks.

CHAPTER III

TRANSISTOR NEGATIVE IMPEDANCE CONVERTER CIRCUIT

In this chapter data taken from a transistor negative impedance converter (NIC) will be presented. The NIC is designed so that, ideally, the lumped model seen at its terminals is a negative capacitance. Of course, this ideal model cannot be obtained; some dissipation is expected to be associated with the model as well as shunt positive capacitance. It is the purpose of this part of the study to investigate the parasitic elements that must accompany the practical capacitance. One objective is to obtain the charge-voltage characteristic of this capacitance for comparison with the theoretical characteristic previously assumed.

3.1 The Basic NIC

The NIC circuit chosen for this study of nonlinear reactance was suggested by Linvill.[17] The basic circuit,

---

[17] Linvill, "Transistor Negative Impedance Converters," p. 725.

complete with biasing network, is shown in Fig 3.1, and the AC portion of the circuit is shown in Fig. 3.2

The network of Fig. 3.2 may be simplified somewhat before the qualitative operation of the circuit is discussed. C_2 and C_5 can be made large enough so that their reactance is negligible at all frequencies of interest, which places R_3, Z_L, and R_7 in parallel. Since the input impedance, Z_{in}, is to be equal to $(-Z_L)$, neither R_3 nor R_7 need be present in the expression for Z_{in}. One might consider, then, the possibility of making the parallel combination of R_3 and R_7 much larger than the impedance of Z_L, thus assuring that Z_{in} is independent of R_3 or R_7. There are practical limitations to the maximum resistance of both R_3 and R_7. From Fig. 3.1 it can be seen that increasing R_3 or R_8 increases the necessary DC supply voltage. The maximum resistance of R_7, as well as R_3, is limited by stability considerations; since R_7 and R_3 are in the base circuits of the transistors these resistors are preferably kept very low for bias point stability purposes. Emitter resistors R_1 and R_6 are chosen as large as the supply voltage will permit in order to improve stability. Notice that C_1 produces regenerative feedback so the circuit would almost certainly oscillate were it not for the degeneration provided by R_1 and R_6. The upshot of the preceding discussion is that it is not practical to make any of the resistances so large that they may be neglected in analysis.

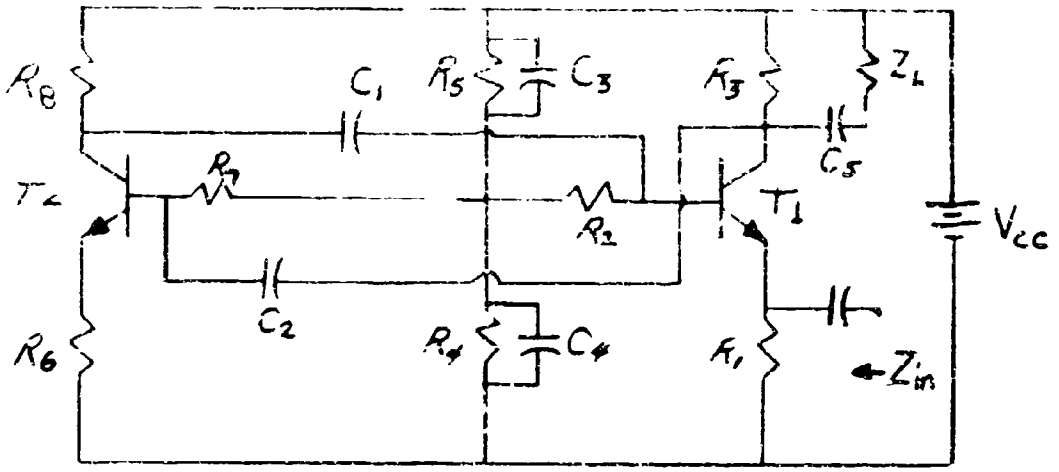

Fig. 3.1. Complete Basic NIC Circuit

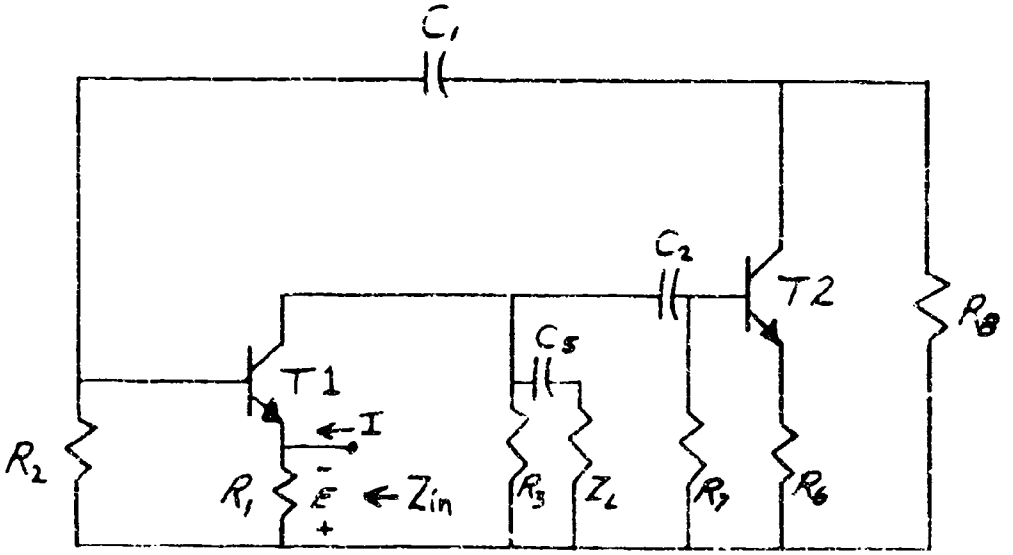

Fig. 3.2. AC Portion of the Basic NIC

A brief discussion of the operation of the circuit follows (see Fig. 3.2). A current I flows into the input terminals of the network; this causes current to flow out of the collector of T_1, resulting in a rise in collector voltage. This rise is coupled to the base of T_2 by capacitor C_2 causing the collector voltage of T_2 to decrease. This decrease is coupled to the base of T_1, and current flows up through R_1 resulting in a voltage, E, across R_1 with the polarity shown in Fig. 3.2. Thus $Z_{in} = E/I$ is negative. The network parameters are adjusted so that $Z_{in} = -KZ_L$. Hence the positive impedance Z_L is "converted" to a constant K times $-Z_L$ over some range of frequencies.

3.2 Analysis and Design of the NIC

A circuit analysis based on the simplest possible model of the transistor [fig. 3.3(a)] very quickly predicts the possibility of negative Z_{in} but does not yield enough information to choose values of all resistors. The transistor model actually used in the analysis is the h-parameter-small signal-low frequency model shown in Fig. 3.3(b); this model can be simplified [see Fig. 3.3(c)] since for practical transistors h_{re} is very small and its effect can be neglected, also h_{oe} is large enough that its effect can be neglected. Transistors with an α cutoff of 8 mc (Texas Instruments 2N118A) are used in the experimental NIC, so for frequencies below about 75 KC h_{ie} and h_{fe} are essentially real.

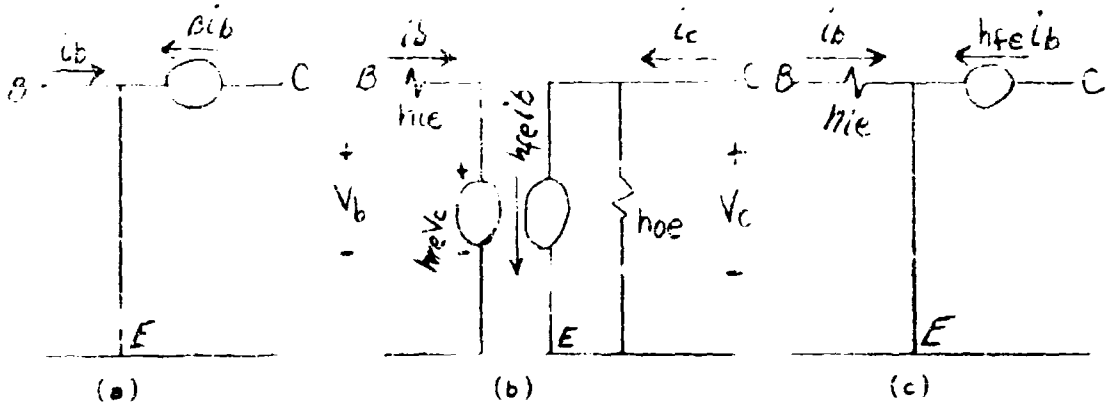

Fig. 3.3. Transistor Models Used for Analysis and Design of NIC

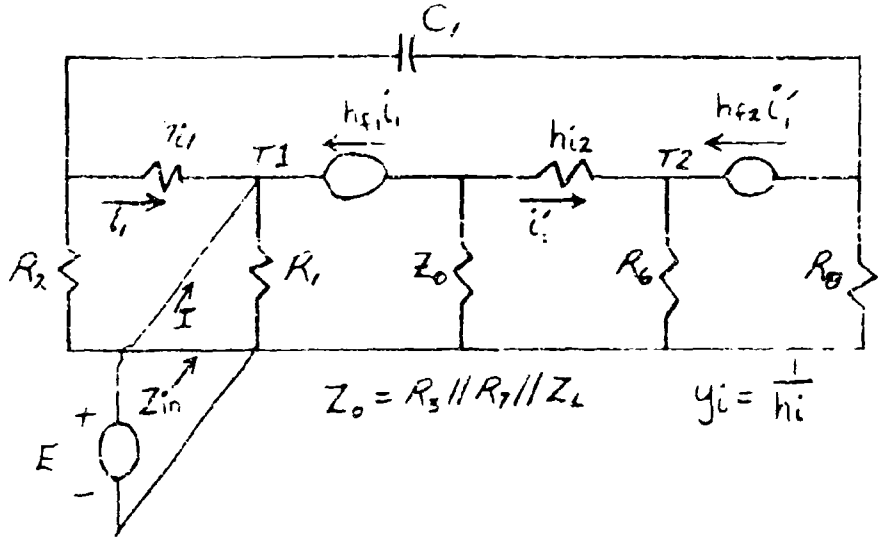

Fig. 3.4. NIC Circuit

R_1	R_2	R_3	R_6	R_7	R_8	h_{11}	h_{12}	h_{f1}	h_{f2}	R_4	R_5
3.3^K	2.2^K	6.8^K	3.3^K	2.2^K	6.8^K	1.33^K	1.5^K	30	36	5.1^K	27.3^K

TABLE 3.1. NIC CIRCUIT PARAMETERS

The NIC network is redrawn in Fig. 3.4 with the assumption that all capacitors except C_1 are large enough that their effects are negligible at the lowest frequency of operation (which is to be determined). Routine nodal analysis yields the following expression for Z_{in}:

$$Z_{in} = \frac{\cdots + sC_1(Y_8 + Y_2 + y_{fc_1} - y_{fc_1}h_{f_1}Z_0Y_6)}{Y_1Y_8(Y_2 + y_{fc_1}) + y_{fc_1}h_{f_1}Y_8Y_2 + sC_1\left[Y_2(Y_8 + Y_2 + y_{fc_1}) - Y_1y_{fc_1}h_{f_1}Z_0Y_6 + y_{fc_1}h_{f_1}(Y_8 + Y_2)\right]} \qquad (3.1)$$

The only previously unmentioned assumption necessary to arrive at Eq. (3.1) is

$$y_{fc_2}h_{f_2}|Y_0| \gg y_{fc_2}Y_0 + |Y_0|(y_{fc_2} + Y_6) . \qquad (3.2)$$

It should be noted here that, as long as the assumption of Eq. (3.2) is true, Z_{in} contains no terms dependent on transistor 2; hence, no transistor matching is required. However, Y_0 will contain a capacitance, so the inequality sets a low frequency limitation on the circuit. With $C_0 = 1$ μf it turns out that this inequality will be true even for zero frequency so in this case no low-frequency limit is imposed by Eq. (3.2). As C_0 is decreased in value the lower frequency limit increases.

It is possible to choose the circuit resistances so that only the terms in Eq. (3.1) which are multiplied by sC_1 are significant. This, of course, allows one to cancel sC_1 and make Z_{in} independent of C_1. Table 3.1 shows the values of

resistances that were chosen as well as the significant parameters of T1 and T2. The h parameters were measured with a Tektronix Type 576 curve tracer and are for 2N1184A transistors with I_C = 1.0 ma and V_{CE} = 20 V. With the values from Table 3.1 it turns out that Z_{in} may be simplified still furtner, since with these values

$$(Y_b + Y_c + g_{i1} - g_{i1} h_{f1} Z_o Y_b) \ll g_{i1} h_{f1} (Y_c + Y_e) . \qquad (3.3)$$

So Z_{in} is finally simplified to:

$$Z_{in} = \frac{Y_b + Y_c + g_{i1} - g_{i1} h_{f1} Z_o Y_b}{g_{i1} h_{f1} (Y_c + Y_e)} \qquad (3.4)$$

Some characteristics of Z_{in} [Eq. (3.4)] are:

1. The nonlinearities of h_{i1} and h_{f1} are present in Z_{in}, hence any attempt to achieve large voltage or current swings at the terminals of the NIC will be accompanied by nonlineer behavior of Z_{in}, also, the choice of Q point can affect Z_{in}.

2. As long as the transistor h parameters are real the only frequency dependent term in Z_{in} is Z_o. The reason that Z_o is assumed frequency dependent is that Z_L is a capacitor in this study.

3. Assuming h_{f1} and h_{i1} reasonably constant, Z_{in} has the form

$$Z_{in} = K_1 - K_2 Z_o , \qquad (3.5)$$

or a resistive term appears in series with the converted impedance. This suggests that one might use some type of compensating network to cancel out the parasitic resistance

4. Equation (3.5) indicates that Z_o (see Fig. 3.1) rather than Z_L, is converted to a negative impedance; therefore, it is necessary to consider Z_{in} as a function of Z_L before any compensating network can be incorporated into the system.

Consider Z_L as a pure capacitive reactance attributable to a capacitance C_o; then $Z_o = R_3 || R_7 || X_{C_o}$. For brevity let the parallel combination of R_3 and R_7 be called R_p. With Z_o written in terms of C_o and R_p, Z_{in} becomes

$$Z_{in} = \frac{\{(Y_8+Y_2+y_{fi})[1+(\omega R_p C_o)^2] - y_{fi} h_{fi} Y_o R_p\} + j\omega R_p^2 y_{fi} h_{fi} Y_6 C_o}{y_{fi} h_{fi} (Y_2+Y_8)[1+(\omega R_p C_o)^2]} \qquad (3.6)$$

or

$$Z_{in} = \frac{K_1 + K_2\omega^2 + j\omega K_3 C_o}{K_4 + K_5\omega^2} \quad ; K_1 < 0 \qquad (3.7)$$

Equation (3.7) indicates that both the real part and the imaginary part of Z_{in} are sensitive to frequency changes, at least throughout some frequency range. The theoretical locus of Z_{in} (C_o = 1 μf) is shown in Fig. 3.5, along with the locus of an ideal negative capacitance and also the locus of a positive resistance in series with a negative capacitance. Thus this Z_{in} does exhibit a negative capacitance effect, but the parasitic resistance associated with the capacitance and the low frequency limitation make some sort of compensating network desirable if this impedance is to be used as a circuit element.

A plot of the impedance of the actual NIC (uncompensated) is shown in Fig. 3.8. This plot differs from the

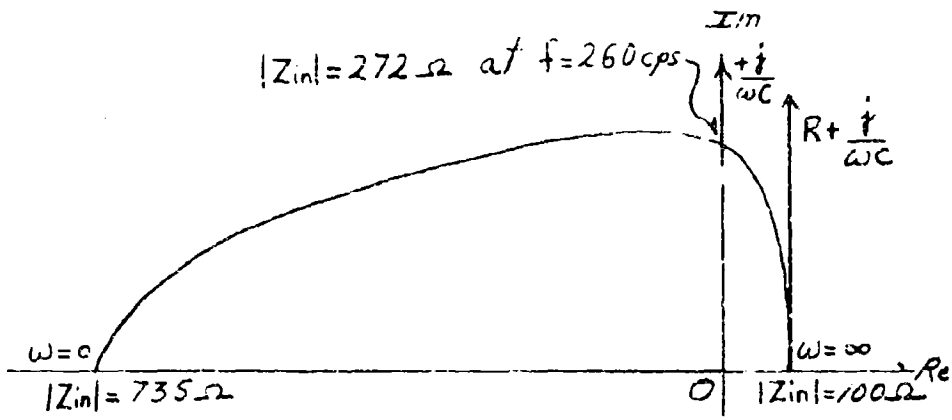

Fig. 3.5. Locus of the Phasor Z_{in} with C_o = 1 μf

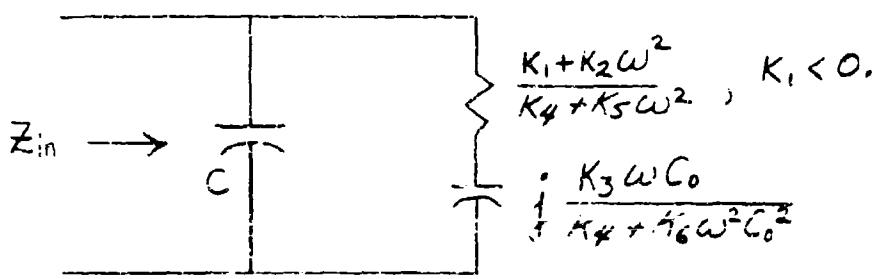

Fig. 3.6. Complete NIC Model

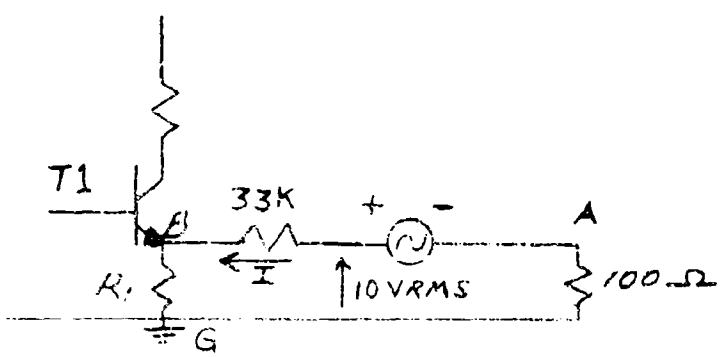

Fig. 3.7. Measurement of Phasor Impedance, Z_{in}

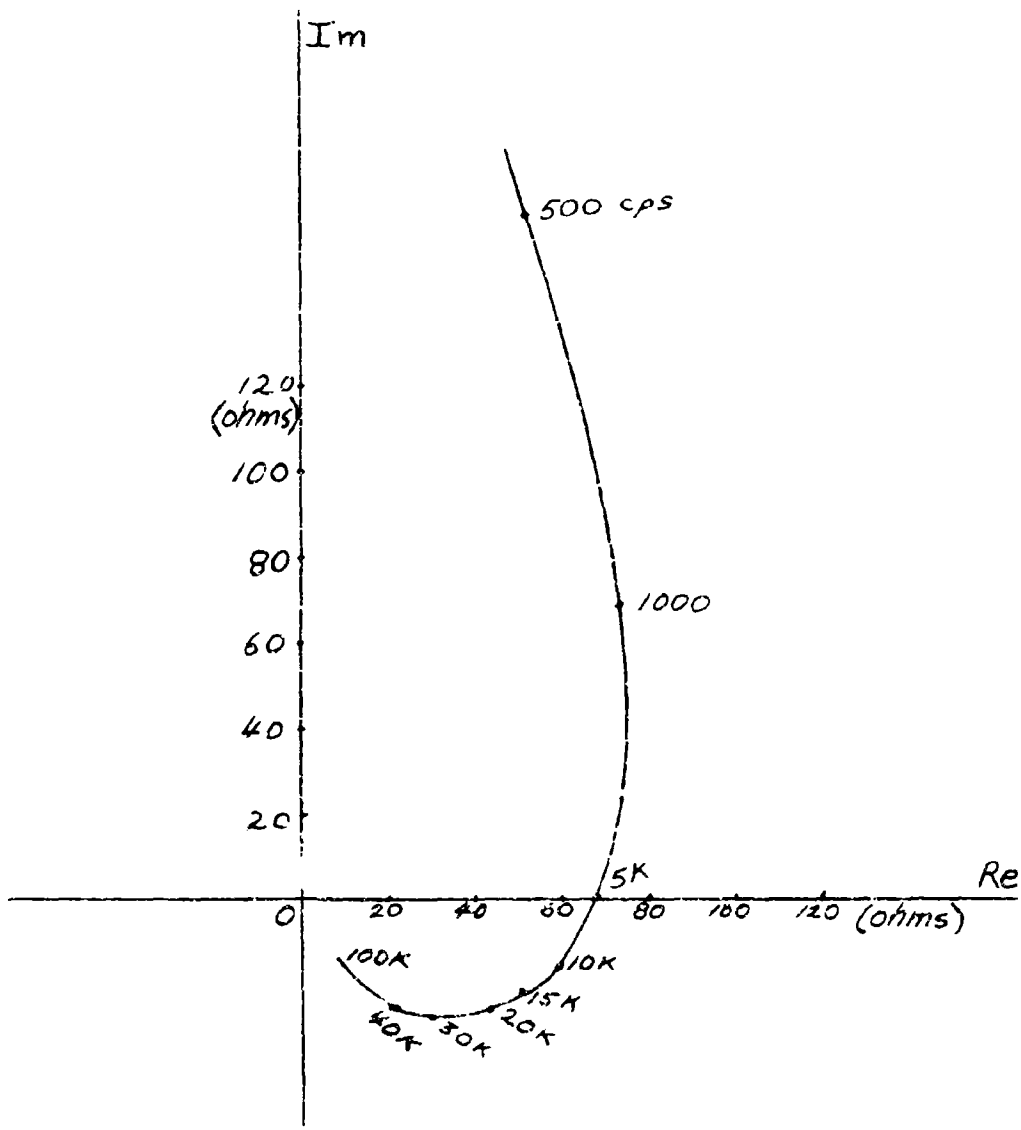

Fig. 3.8. Input Impedance Plot of the NIC
(C_0 = 1 μf)

theoretical impedance locus in that the effects of unavoidable shunt capacitance are present in the actual plot. The actual locus compares favorably with the theoretical locus for frequencies from about 200 cps to 2 KC; at this frequency the shunt capacitance begins noticeably to shift the phase of current with respect to voltage and the two plots begin to differ. The complete NIC model is shown in Fig. 3.6.

For the experimental NIC (C_o = 1 μf), the constants of Fig. 3.6 are as follows:

$$K_1 = Y_8 + Y_2 + y_{i_1} - y_{i_1} h_{f_1} Y_6 R_p = -9.7 \times 10^{-3}$$

$$K_2 = (Y_8 + Y_2 + y_{i_1})(R_p C_o)^2 = 4.1 \times 10^{-7}$$

$$K_3 = R_p^2 y_{i_1} h_{f_1} Y_6 = 18.5$$

$$K_4 = y_{i_1} h_{f_1} (Y_2 + Y_8) = 13.3 \times 10^{-6}$$

$$K_5 = y_{i_1} h_{f_1} (Y_2 + Y_8)(R_p C_o)^2 = 37 \times 10^{-12}$$

$$K_6 = K_5 / C_o^2 = 37$$

Now consider the frequencies for which $K_2\omega^2 >> |K_1|$ and $K_5\omega^2 >> K_4$. The first inequality is true for $f > 770$ cps, and the second inequality is true for $f > 300$ cps; therefore, for $f > 770$ cps:

$$Z_{in} = \frac{K_2}{K_5} + j\frac{1}{\omega C_o \frac{K_5}{K_3}} \qquad (3.8)$$

$$= 110 + j\frac{1}{\omega 2 C_o} \qquad (3.9)$$

Equations (3.8) and (3.9) indicate that, excluding the effects of shunt capacitance and assuming that the h parameters remain real and constant, Z_{in} looks like a 110 ohm resistor in series with a negative capacitance equal to $2C_o$.

The circuit used to measure the phasor impedance Z_{in} is shown in Fig. 3.7. The terminal voltage of the negative capacitance is V_{BG} and the current is $-V_{AG}/100$; the phase angle between current and voltage is measured with a dual-trace oscilloscope.

3.3 Compensating Networks

Although not directly pertinent to this study, a brief discussion of possible compensation is presented here. This compensation is based on an inspection of the expression for Z_{in} [Eq. (3.6)]. For a more theoretical approach to compensation of negative impedance converters the reader is referred to the literature.[18]

The first step in improving the locus of Z_{in} will be to put a resistance in series with C_o, resulting in Z_o shown in Fig. 3.9. The inclusion of R_o will result in a negative-resistance term in Z_{in} as well as a positive-resistance term. The value of R_o will be chosen so that the real part of Z_{in} will be reduced. With R_o included,

---

[18] Larky, p. 124.

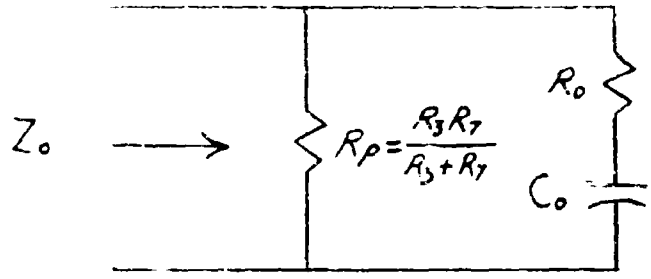

Fig. 3.9. Z_o with Compensating Resistor

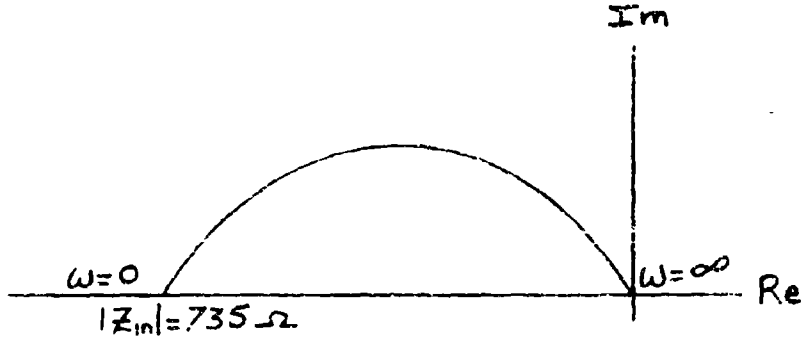

Fig. 3.10. Locus of Z_{in} with R_o included

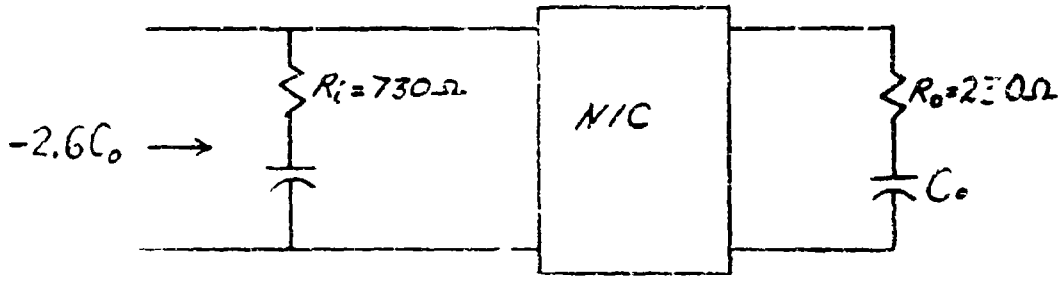

Fig. 3.11. Compensated NIC

$$Z_{in} = \frac{Y_a - Y_c R_p + \omega^2 C_o^2 (R_o + R_p)[Y_a (R_o + R_p) - Y_c R_p R_o] + j\omega Y_c R_p^2 C_o}{Y_d [\omega^2 C_o^2 (R_o + R_p)^2 + 1]} \qquad (3.10)$$

where

$Y_a = Y_8 + Y_2 + y_{i1}$ mhos.

$Y_c = y_{i1} h_{f1} Y_6$ mhos squared.

$Y_d = y_{i1} h_{f1} (Y_2 + Y_8)$ mhos squared.

Now if R_o is chosen so that

$$Y_a (R_o + R_p) = Y_c R_p R_o ,$$

or

$$R_o = \frac{Y_a R_p}{Y_c R_p - Y_a} ,$$

for this value of R_o

$$Z_{in} = \frac{(Y_a - Y_c R_p)^3 + j\omega Y_c R_p^2 (Y_a - Y_c R_p)^2 C_o}{Y_d [\omega^2 C_o^2 Y_c^2 R_p^4 + (Y_a - Y_c R_p)^2]} \qquad (3.11)$$

With the parameter values given in Table 3.1, $Y_a - Y_c R_p < 0$ so Z_{in} has the form

$$Z_{in} = \frac{-K_1}{f(\omega^2)} + \frac{j\omega K_2 C_o}{f(\omega^2)} \; ; K_1 > 0, K_2 > 0 . \qquad (3.12)$$

The locus of this Z_{in} is shown in Fig. 3.10. Note that, with R_o included, the locus of Z_{in} is similar to the locus of a constant (-R) in parallel with a constant (-C). Furthermore, the value of R_o is independent of C_o, but depends on the transistor parameters h_{f1} and h_{i1}.

Now refer to Eq. (3.11) and investigate the frequencies for which $\omega^2 C_o^2 Y_c^2 R_p^4 >> (Y_a - Y_c R_p)^2$. For this NIC the inequality above is valid for $f > 260$ cps, so this frequency

limitation will be placed on the NIC and Z_{in} will be simplified again:

$$Z_{in} = \frac{(Y_a - Y_c R_p)^3}{\omega^2 Y_d C_o^2 Y_c^2 R_p^4} + j \frac{(Y_a - Y_c R_p)^2}{\omega C_o Y_d Y_c R_p^2} \quad , \tag{3.13}$$

or

$$Z_{in} = \frac{-K_3}{\omega^2} + j \frac{K_4}{\omega C_o} \quad ; K_3 > 0, K_4 > 0. \tag{3.14}$$

It was mentioned earlier that the locus of Z_{in} with R_o looks like (-R) in parallel with (-C). This prompts one to examine Y_{in} in order to remove the parasitic resistance. For f > 260 cps,

$$Y_{in} = \frac{Y_d}{(Y_a - Y_c R_p)} - j \frac{\omega C_o Y_d Y_c R_p^2}{(Y_a - Y_c R_p)^2} \tag{3.15}$$

Since $Y_a - Y_c R_p$ is negative the real part of Y_{in} will be negative. Obviously, if a positive resistance, R_1, equal to $|Y_a - Y_c R_p|/Y_d$ is placed across the input terminals of the NIC, the parasitic resistance will be canceled out and

$$Z_{in} = j \frac{1}{\omega C_o \frac{Y_d Y_c R_p^2}{(Y_a - Y_c R_p)^2}} \quad . \tag{3.16}$$

Figure 3.11 displays the compensated NIC with the values of resistances needed to effect the impedance conversion. Note that neither compensating resistor depends on C_o. A capacitor is included in series with the 730 ohm resistor, R_1, so the DC biasing of the transistor will not be upset. Equation (3.16) implies that the compensating resistors will cause the

terminals of the NIC to look like an ideal negative capacitor; of course, this will not be true for two reasons: first, a very simple low frequency, linear modal of the transistors was used in the analysis and design of the NIC; second, both R_i and R_o are dependent (at least) on the transistor parameters h_f and h_i, so Q point, magnitude of driving source, and frequency affect the optimum values for R_i and R_o. The effect of compensation (for a fixed Q point and driving-source magnitude) is sketched in Fig. 3.12. Note the frequencies at which Z_{in} is purely capacitive and at which Z_{in} is real, both with and without compensation, and with R_o only. Several points can be made concerning compensation of the NIC. First consider the intersection of the three loci of Fig. 3.12 with the real axis; not only is the resistive part of Z_{in} reduced considerably by compensation, but the useful frequency range of the negative capacitor is increased by a factor of three. Second, the reduction in the real part of Z_{in} is in evidence at the intersections of the loci with the imaginary axis; although the capacitive reactance is different for each of the loci, the frequency is also different so that at this intersection each of the loci represent a capacitance of approximately the same value (3.5 μf). Finally, note that the largest part of the compensation is accomplished by R_o. The measurements for Fig. 3.12 were made with R_o = 220 ohms and R_i = 780 ohms (680 + 100), since these were readily available in standard resistor values in the lab; it is presumed that this compensation might be improved if desired.

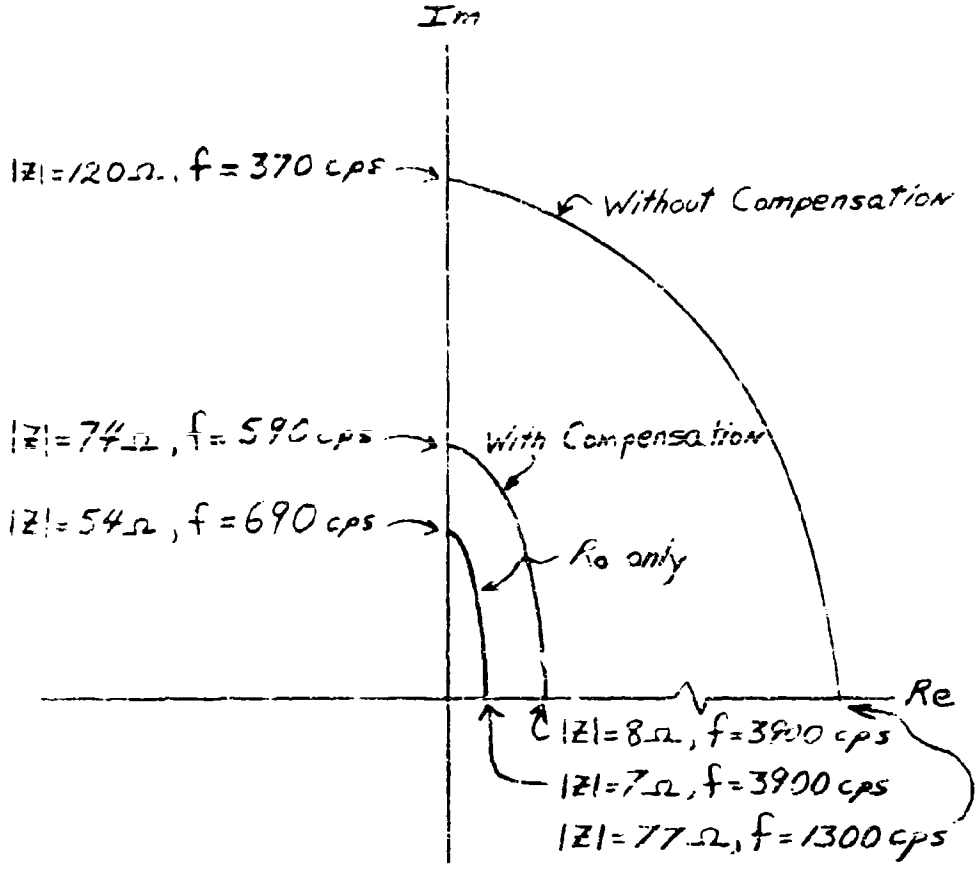

Fig. 3.12. Locus of Z_{in} with and without Compensation

3.4 The NIC Used As a Circuit Element

The data presented in this section are intended to demonstrate the use of the NIC as a circuit element. The NIC is placed in the circuit shown in Fig. 3.13 and the driving point impedance is measured as a function of frequency. This circuit is chosen to illustrate that it is possible to effect capacitance cancellation by using the NIC. If $R_1 = R_2 = R$ and $C_1 = C_2 = C$ then the impedance of the RC circuit is real at all frequencies and is

$$Z_{in}' = \frac{R}{2} - \frac{1}{2R\omega^2C^2} \qquad (3.17)$$

The impedance of the NIC is measured and plotted in Fig. 3.13. From approximately 1 kc to 3 kc the NIC looks like a resistor with value slightly less than 100 ohms in series with a negative capacitor with value of 2.5 μf. Therefore, values of R_1 and C_1 are chosen as 94 ohms and 2.5 μf, respectively. The impedance of this series R_1C_1 is also plotted on Fig. 3.13. These values are used to plot Eq. (3.17).

Then the NIC is placed in parallel with the series R_1C_1, and this impedance is measured and plotted. It can be seen from the figure that the reactive component of the impedance is indeed small throughout the frequency range considered. Obviously, neither the two capacitors nor the two resistors are exactly equal at all these frequencies, but the cancellation effect can be seen. Furthermore, since the measured curve agrees fairly well with the theoretical plot of Z_{in}' [Eq. (3.17)],

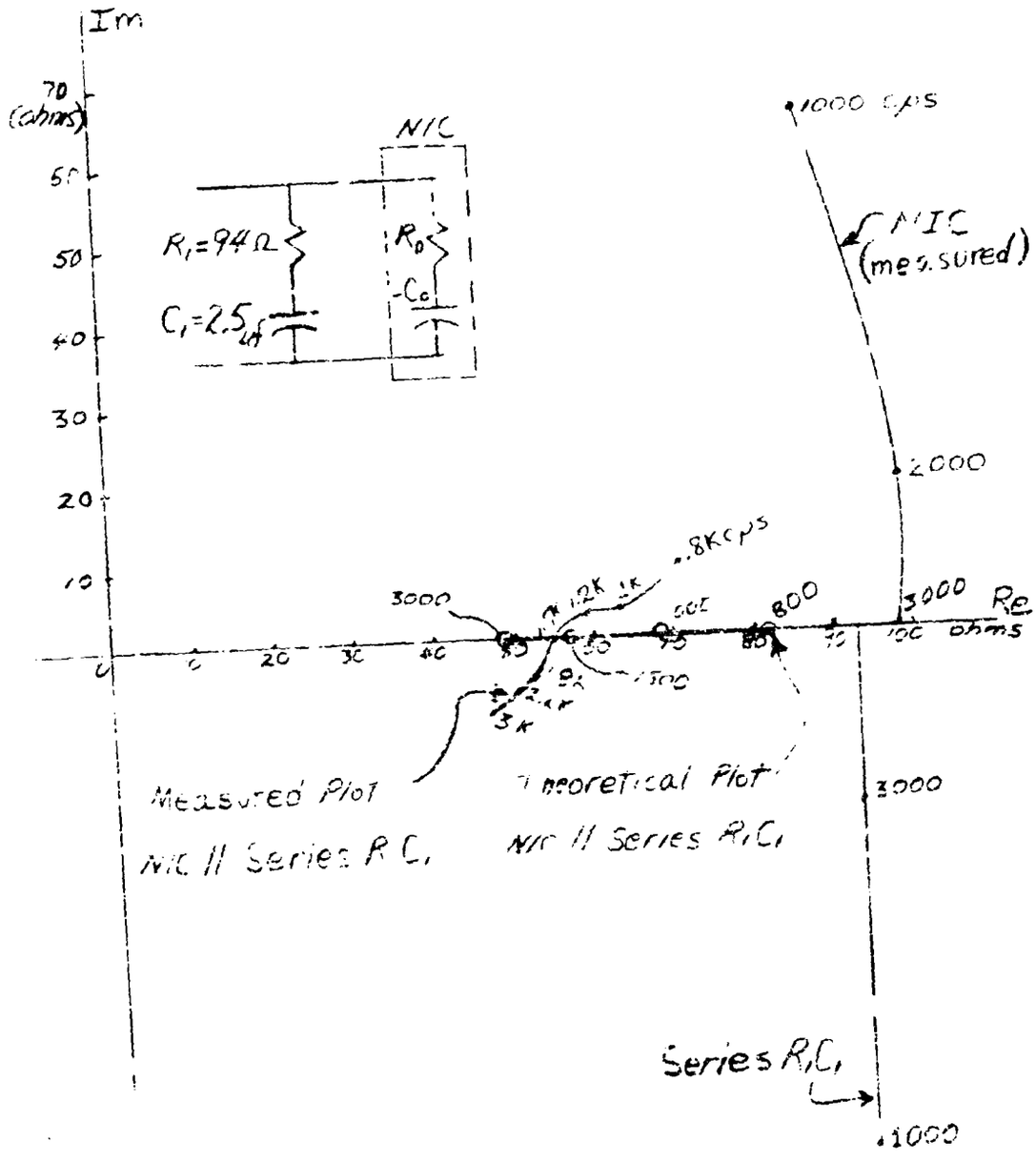

Fig. 3.13. Impedance Plots

the assumption that the NIC is a circuit element which consists of a constant resistance in series with a constant negative capacitance [see Eq. (3.9)] is reasonably good.

3.5 Square Wave Measurements

A lumped model of the NNC has been predicted from analysis of the NIC, and this model has been verified throughout a certain range of frequencies by means of AC steady state measurements. This model will now be used to calculate the transient response of a circuit which contains the NNC. Values for these calculations will be obtained from measurements made on the circuit.

A square wave oscillator is applied to the NIC, as shown in Figs. 3.14(a),(b); some response waveforms are shown in Figs. 3.14(c),(d). With the amplitudes implied in Fig. 3.14 the circuit is operating in a reasonably linear mode; if the driving-source magnitude is increased the mode of operation naturally becomes nonlinear and distortion results; this will be discussed later.

The presence of negative capacitance at this square wave frequency (2 KC) may be seen from Figs. 3.14(c),(d). Note that while the source voltage is a positive constant the current is positive and is not quite constant but is increasing very slightly. Throughout this half period, however, the NIC terminal voltage is decreasing almost linearly.

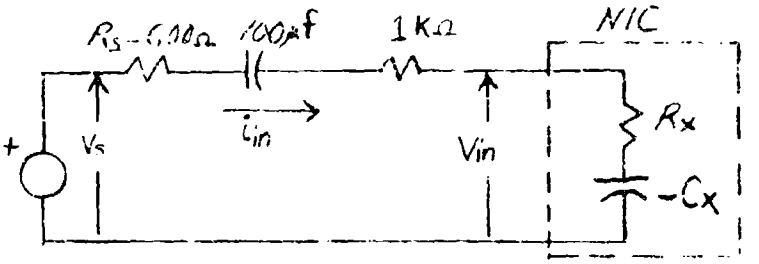

(a) Square Wave Oscillator Applied to the NIC (f = 2 KC)

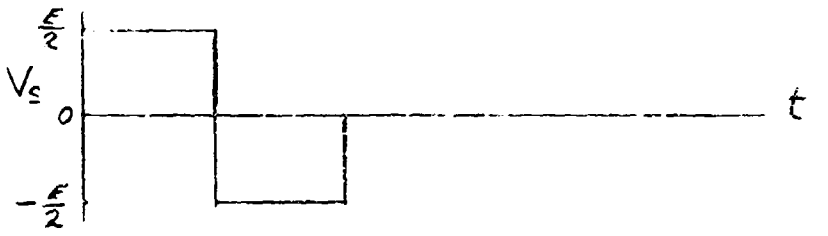

(b) Source Voltage (one cycle)

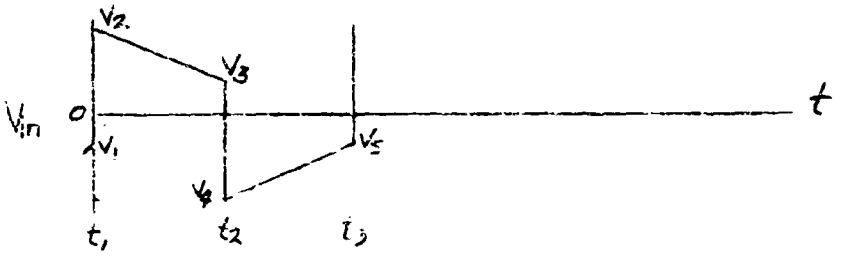

(c) Voltage Across Terminals of the NIC

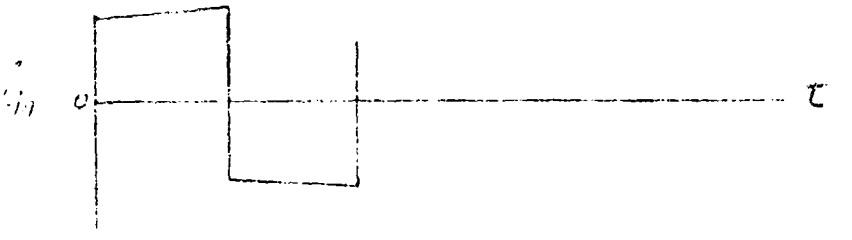

(d) Current into the NIC

Fig. 3.14. Transient Study of the NIC

The purpose of this section of the discussion is to interpret these waveforms in terms of the lumped model of the NIC; i.e., R_x in series with C_x; the shunt capacitance is neglected here. The values of R_x and C_x are assumed to be constant although this is not strictly true since the transistor parameters will vary some even in the small-signal case.

With this magnitude of driving voltage the current and voltage waveforms exhibit half-wave symmetry, so it will only be necessary to discuss the half cycle for which the source voltage is $+V/2$. At this time it is also convenient to indicate the solution for v_{in} of Fig. 3.15(a) which is the circuit of Fig. 3.14(a) with the external resistances combined and with the 100 μf capacitor omitted since its only purpose is to block DC current. The source is also considered a step function of voltage. The initial voltage across the negative capacitor is V_c, as shown. This network is easily solved by standard techniques to yield:

$$i(t) = \frac{(V_o - V_c)}{R + R_g} e^{\frac{t}{(R+R_g)C}}, \qquad (3.18)$$

and

$$V_{in}(t) = V_o - \frac{(V_o - V_c)R_g}{R + R_g} e^{\frac{t}{(R+R_g)C}}. \qquad (3.19)$$

Equation (3.18) indicates that if a very short time is considered then current might be considered as increasing linearly. Equation (3.19) indicates that for a very short time the voltage will decrease approximately linearly. Equations (3.18) and

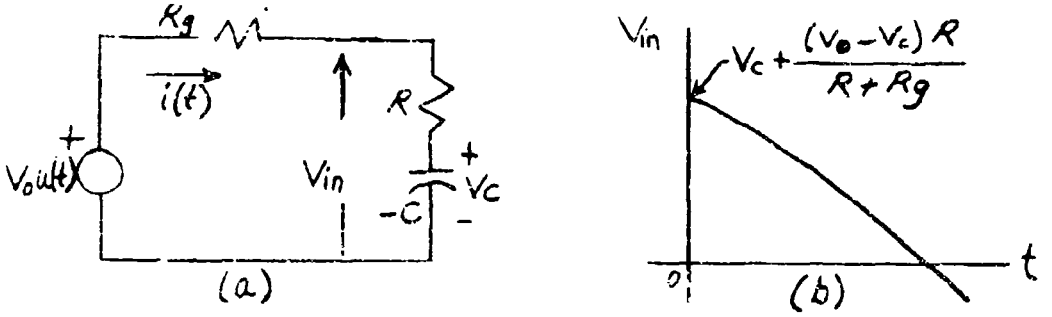

Fig. 3.15. Circuit Used for Calculations

Source Volt. Open Circuit Peak to Peak	Current (ma) Peak to Peak	V_1 volts	V_2 volts	V_3 volts	V_4 volts	R_x ohms	$-C_x$ μf	Comments on V_{in}
1. 5	2.5	-.1	.25	.1	-.25	120	4.5	All Straight Lines
2. 6	3.0	-.15	.3	.2	-.35	130	8.5	V_2 to V_3 is Slight Exponential
3. 6.5	3.5	-.25	.35	.35	-.4	163	∞	$V_2 = V_3$

Calculations Are from the Positive Half Cycle
V_1, V_2, V_3, V_4 Do Not Include DC Bias Voltage

TABLE 3.2. SOME EXPERIMENTAL RESULTS INDICATING NON-LINEARITY (f = 2 KC , T = .5 msec.)

(3.19) denote the responses measured from a time $t = 0$, which is the instant that the step is applied to the circuit. The present problem, however, involves a square wave of applied voltage rather than just a step. Consequently, it will be necessary to consider the response at some time t_1 [see Fig. (3.14(c))] when the circuit is operating in the steady state in order to relate the waveforms to R_x and C_x. Refer to Fig. 3.14 for the following discussion:

at $t_1(-)$, $V_s = \frac{-E}{2}$; $V_{in} = V_1$ let $V_{cx} = V_a$

at $t_1(+)$; $V_s = \frac{E}{2}$; $V_{in} = V_2$; $V_{cx} = V_a$

let $\Delta V_{in} = \Delta V_{Rx} = V_2 - V_1$ and $\Delta E = \frac{E}{2} - \left(-\frac{E}{2}\right) = E$,

so, $\Delta V_{Rx} = \frac{\Delta E R_x}{R_x + R}$, where R = all series resistance except R_x, or,

$$R_x = \frac{\Delta V_{Rx} R}{\Delta E - \Delta V_{Rx}} = \frac{(V_2 - V_1) R}{E - (V_2 - V_1)} \quad . \tag{3.20}$$

Thus Eq. (3.20) gives an expression for R_x that contains quantities which can be measured externally to the NIC.

An expression for C_x is derived as follows: as before,

at $t_1(-)$, $V_{in} = V_1$; $V_{cx} = V_a$; $V_s = -\frac{E}{2}$ and $V_{Rx} = V_1 - V_a$;

at $t_1(+)$, $V_{in} = V_2$; $V_{cx} = V_a$; $V_s = \frac{E}{2}$ and $V_{Rx} = \frac{(E_2 - V_a) R_x}{R + R_x}$,

so at $t_1(+)$,

$$V_2 = V_{Rx} + V_a = \frac{(E/2 - V_a)R_x}{R + R_x} + V_a = \frac{E/2\, R_x}{R + R_x} + \frac{V_a R}{R + R_x}$$

and at $t_1(+)$,

$$V_a = \frac{V_2 (R + R_x)}{R} - \frac{E R_x}{2R} \quad . \tag{3.21}$$

Equation (3.21) gives the voltage across the negative capacitance at the end of a negative half cycle of the source V_s. Now between $t_1(+)$ and $t_2(-)$ the source looks like a step of voltage, and Eq. (3.19) may be used to describe the decrease in V_{in} during this interval of time. Thus, for $t_1 < t < t_2$,

$$V_{in} = E/2 - \frac{(E/2 - V_a)R}{R + R_x}\, e^{\frac{t - t_1}{(R + R_x)C_x}} \quad . \tag{3.22}$$

Equation (3.22) contains V_a, which cannot be conveniently measured, so substitute Eq. (3.21) into Eq. (3.22). This yields, still for $t_1 < t < t_2$,

$$V_{in} = \left(\frac{E}{2} - V_a\right)\left(\frac{R + R_x}{R} - e^{\frac{t - t_1}{(R + R_x)C_x}}\right) + \frac{V_2 (R + R_x)}{R} - \frac{E}{2}\frac{R_x}{R} \quad . \tag{3.23}$$

Finally, at $t = t_2(-)$, $t_2 - t_1$ = one-half period = $T/2$, and Eq. (3.23) becomes

$$V_{in} = V_3 = \left(\frac{E}{2} - V_2\right)\left(\frac{R + R_x}{R} - e^{\frac{T/2}{(R + R_x)C_x}}\right) + \frac{V_2 (R + R_x)}{R} - \frac{E}{2}\frac{R_x}{R} \quad . \tag{3.24}$$

Equations (3.20) and (3.24) together may be used to obtain experimental values for R_x and C_x for any given source frequency and amplitude. These expressions are as good as the assumption that R_x and C_x are constants. For example, using the circuit

of Fig. 3.14(a) with open circuit source magnitude of 1 volt peak-t -peak and C_o = 1 μf, one finds R_x = 102 ohms and C_x = 2.98 μf: this is good agreement with the values predicted in Eq. (3.9); viz., R_x = 110 ohms and C_x = - 2 μf, where neither magnitude nor frequency of the driving source was considered explicitly.

Table 3.2 shows some additional measurements that were made along with R_x and C_x as calculated from Eqs. (3.20) and (3.24). Items 2 and 3 of Table 3.2 are in error since there is obviously some significant nonlinearity due to transistor action. The comments accompanying these two items indicate that the assumptions made in the derivation of Eqs. (3.22) and (3.24) are not satisfied here; i.e., that R_x and C_x are constant. This can be seen from the fact that v_{in} does not exhibit half-wave symmetry with these magnitudes of driving sources. However, it is surely true that the parasitic resistance, R_x, as well as the negative capacitance, C_x, increase in value with an increase in the amplitude of the driving source at least up to some point. The difficulty encountered in measuring the variation of R_x and C_x with changes in current and/or voltage will be dealt with in the next section.

3.6 Attempt to Measure Charge-Voltage Characteristic

One objective of this experimental work is to determine the nonlinear relationship between the charge and voltage associated with a practical negative capacitance. In the first

part of this paper a number of calculations were based on the assumption of a piecewise linear relationship between charge and voltage. It is desirable to compare the actual q-v characteristic with the assumed characteristic as well as to determine which of the lumped circuits of Fig. 2.1 most closely approximate the actual NNC. The lumped model of the actual NNC has been clearly shown to be a nonlinear, frequency-dependent resistance in series with a nonlinear, frequency dependent negative capacitance, the series combination being shunted by a positive parasitic capacitance. While the shunt capacitance can be neglected in some instances, the series resistance cannot be neglected, and it is the nonlinearity of this series resistance which prevents a complete measurement of the q-v characteristic. The basic difficulty in this measurement is getting at the terminals of the capacitor. It is certainly impossible to get at the junction connecting R_x and C_x for obviously this clearly defined junction exists only in the model, not the NIC. Therefore, indirect methods must be used; Fig. 3.16 shows a scheme used to measure the voltage across the capacitor based on the series R-C model and to obtain the charge on the capacitor by integrating a voltage that is proportional to the current through the capacitor. If the output of the subtractor (1) is fed to the vertical amplifier of an oscilloscope and the output of the integrator (3) is fed to the horizontal amplifier of the oscilloscope, then the q-v characteristic should appear on

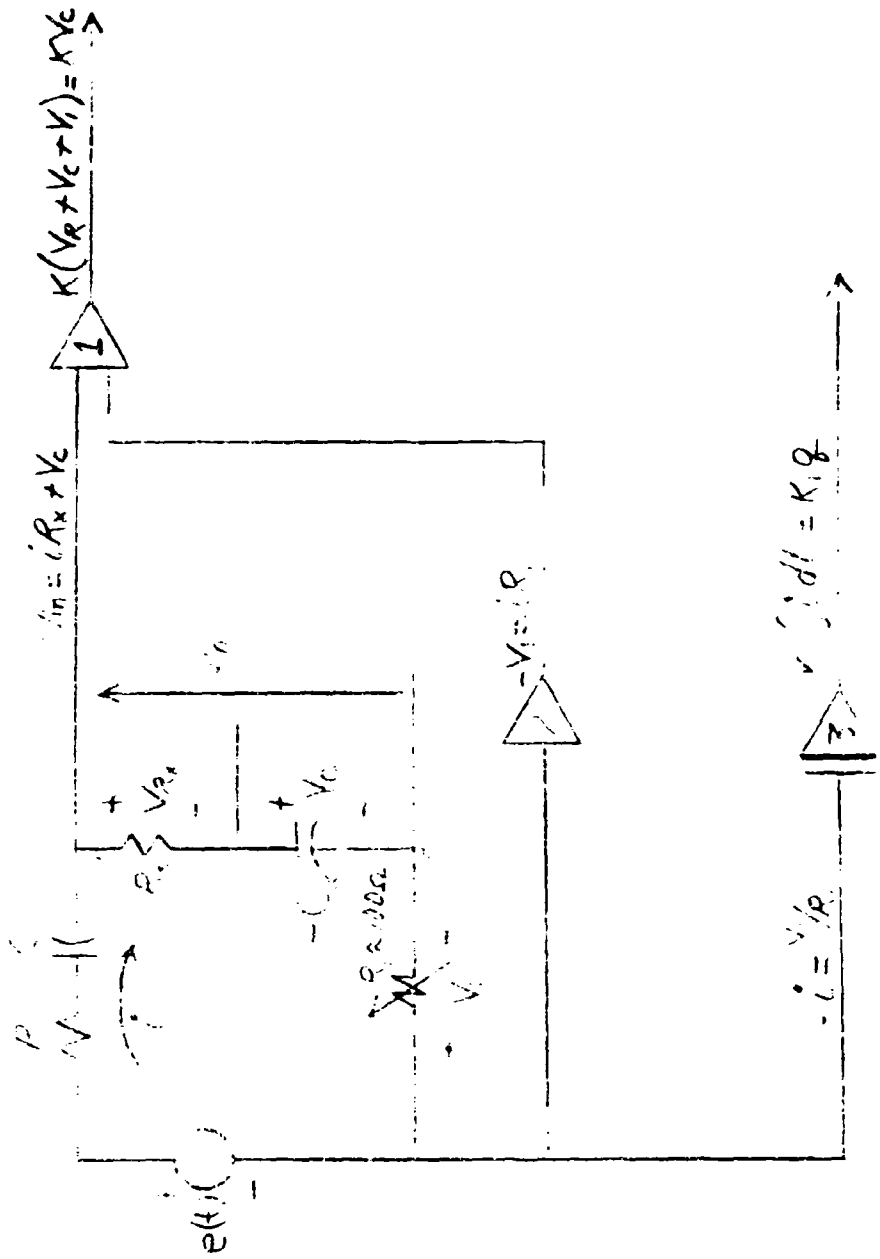

Fig. 3.16. Setup Used to Display q-v Characteristic on An Oscilloscope

the face of the scope. As previously mentioned, a voltage proportional to the charge on the NNC may be obtained by integrating a voltage proportional to the current through the NNC. Since the current i flows through the NNC and R_1 (neglecting shunt capacitance), the voltage $V_1 = -iR_1$ is integrated and inverted to give a voltage proportional to charge; viz., $K_1 q$. To obtain a voltage proportional to the voltage across the capacitor it is necessary to subtract from the input voltage, v_{in}, a voltage in phase with and equal to V_R; now $v_{in} = iR_x + v_c$ and $v_1 = -iR_1$, and the output of the inverter (2) is $+iR_1$; therefore, if R_1 is adjusted so that it is equal to R_x, then the output of the subtractor (1) is $+Kv_c$. Indeed, this can be shown experimentally to be the case as long as the amplitude of the driving source is small enough that R_x is reasonably constant and linear. When $e(t)$ is a square wave the output of the inverter (2) is a square wave [see Fig. 3.18(b)], as it should be, since the current is essentially a square wave. Under these conditions v_c is triangular [see Fig. 3.18(c)]. When $e(t)$ is sinusoidal the picture on the scope is a conventional Lissajous figure which indicates a 180 degree phase difference between v_c and q_c. When the driving voltage is increased in order to study the large signal q-v characteristic; however, the waveform iR_x no longer assumes the same form as the current because of the nonlinear characteristics of R_x. Since the voltage iR_1 does have the same waveform as the current, it is

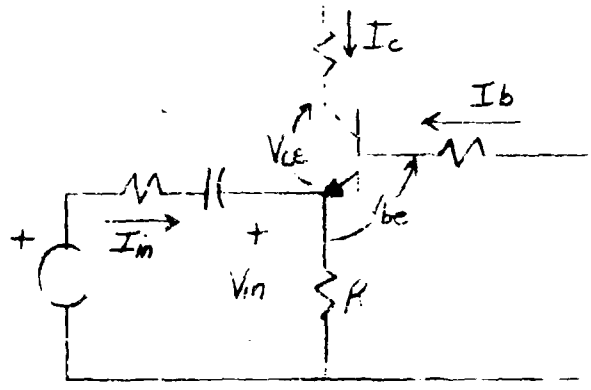

(a) Partial N:C Circuit

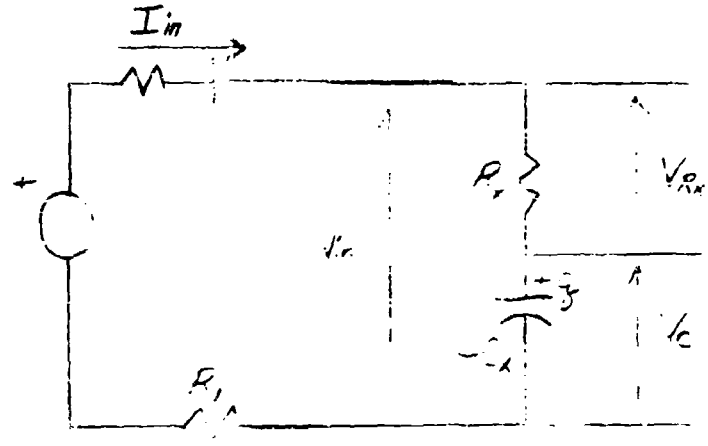

(b) Model of NNC

Fig. 3.17. Definition of Voltages and Currents

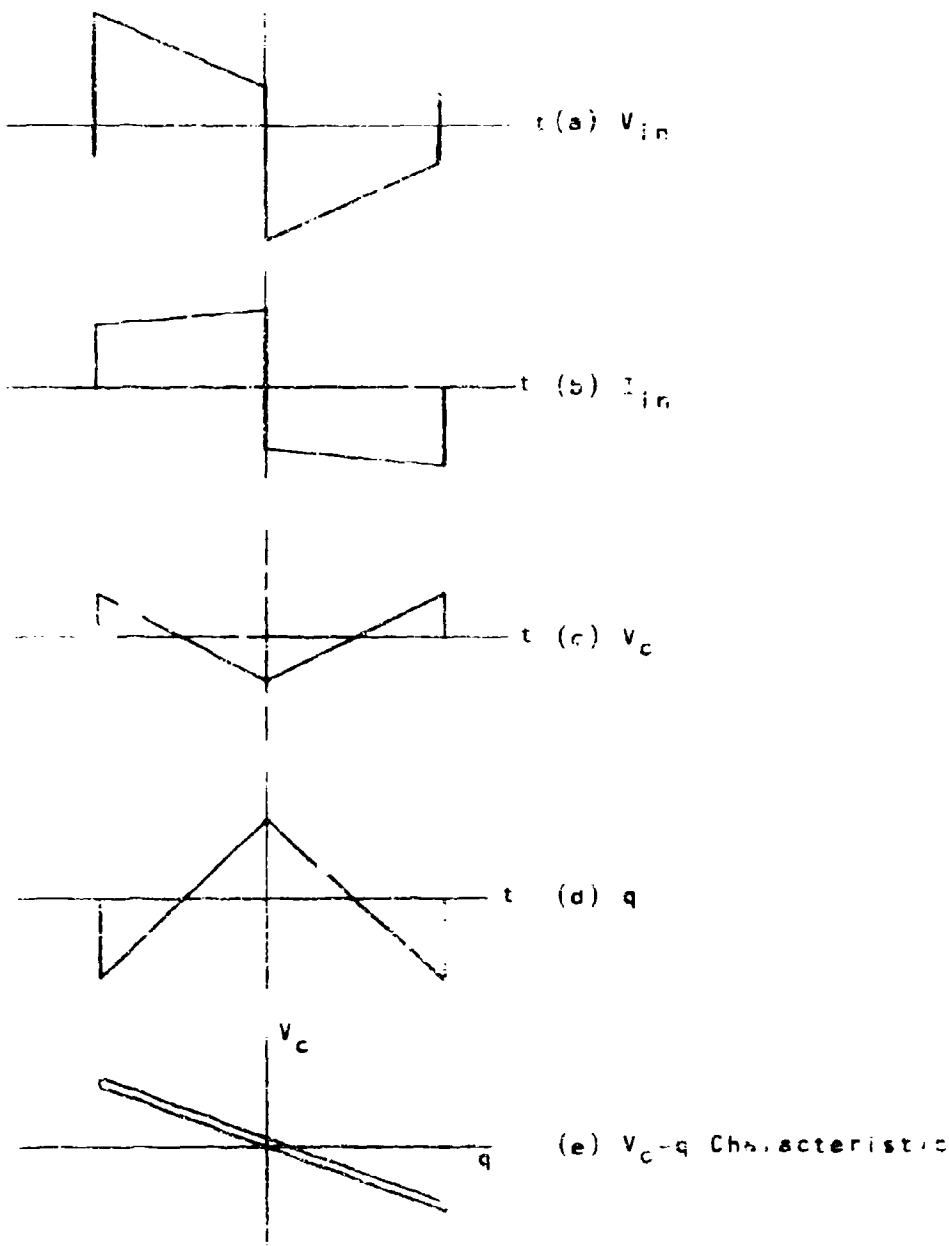

Fig. 3.18. Waveforms--Small Signal

impossible to "cancel" the v_R part of v_{in} with v_I and the output of the subtractor (1) is no longer $+Kv_c$ but is $+Kv_c + K(v_R + v_I)$[see Fig. 3.20(c)].

The inverter (2) and the integrator (3) for this part of the experiment were made with Philbrick operational amplifiers (Model K2-XA); the subtractor (1) was the differential input of a Tektronix 503 oscilloscope.

3.7 N:C Waveforms

The nonlinearities present in the N:C have been referred to previously. This section presents direct oscilloscope observations of their effects. The only elements of the N:C circuit that are considered nonlinear are the transistors. If an analytical approach is tried, then, even for the simple transistor model that has been used, the variation of h_{fe} and h_{ie} with transistor currents or voltage must be approximated analytically; since there are two transistors in the N:C, the resulting nonlinear differential equation is quite complex and requires that an approximate solution be made. No useful approximate solutions have been found in this work. Various waveforms of the N:C can be shown, however, for different values of driving voltage, and some insight into the mechanism that causes the nonlinearities can be obtained.

Two sets of waveforms are presented in Figs. 3.18 through 3.21. The first set consists of various N:C voltages obtained when the amplitude of the driving source is of such a

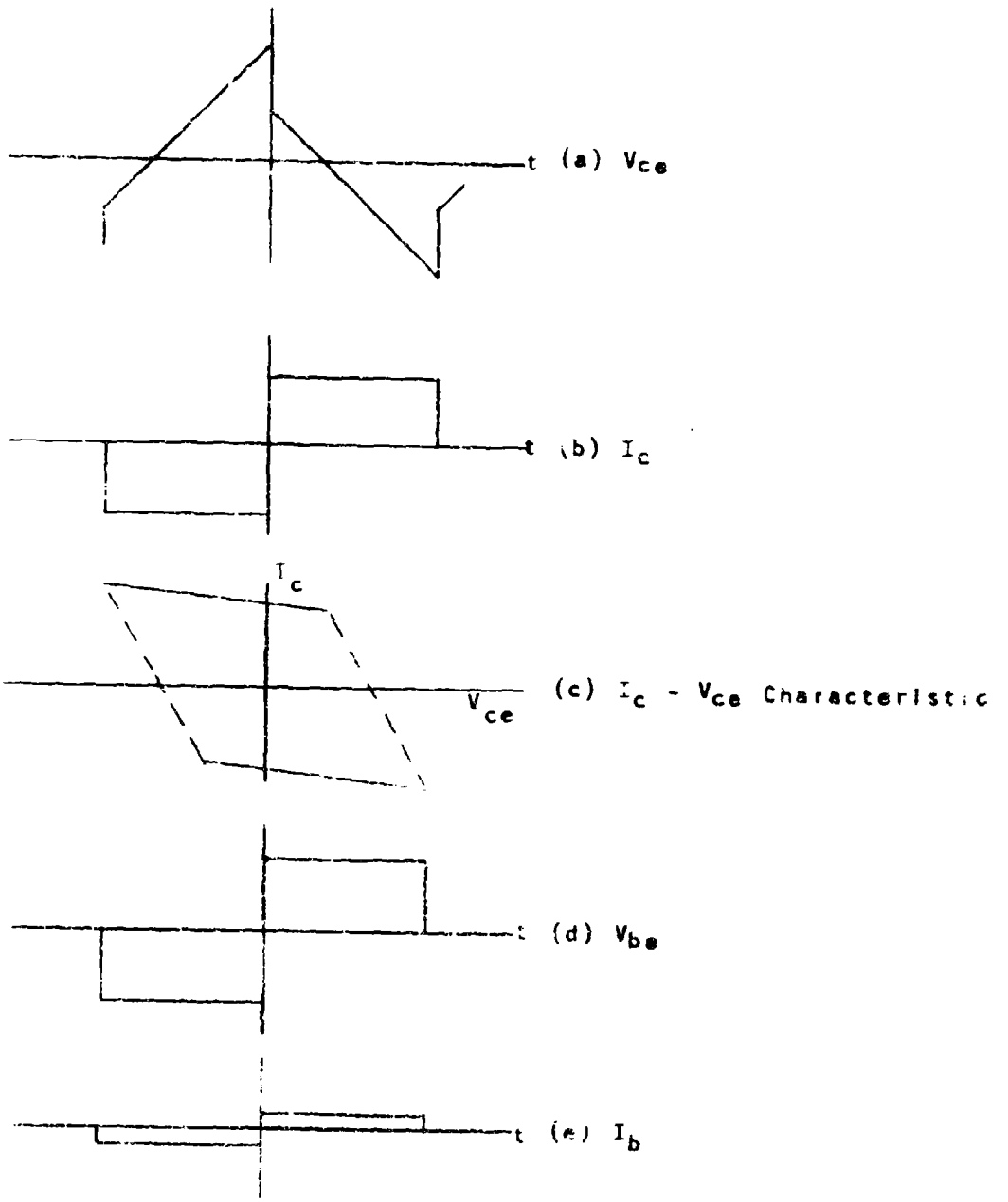

Fig. 3.19. Small Signal Operation

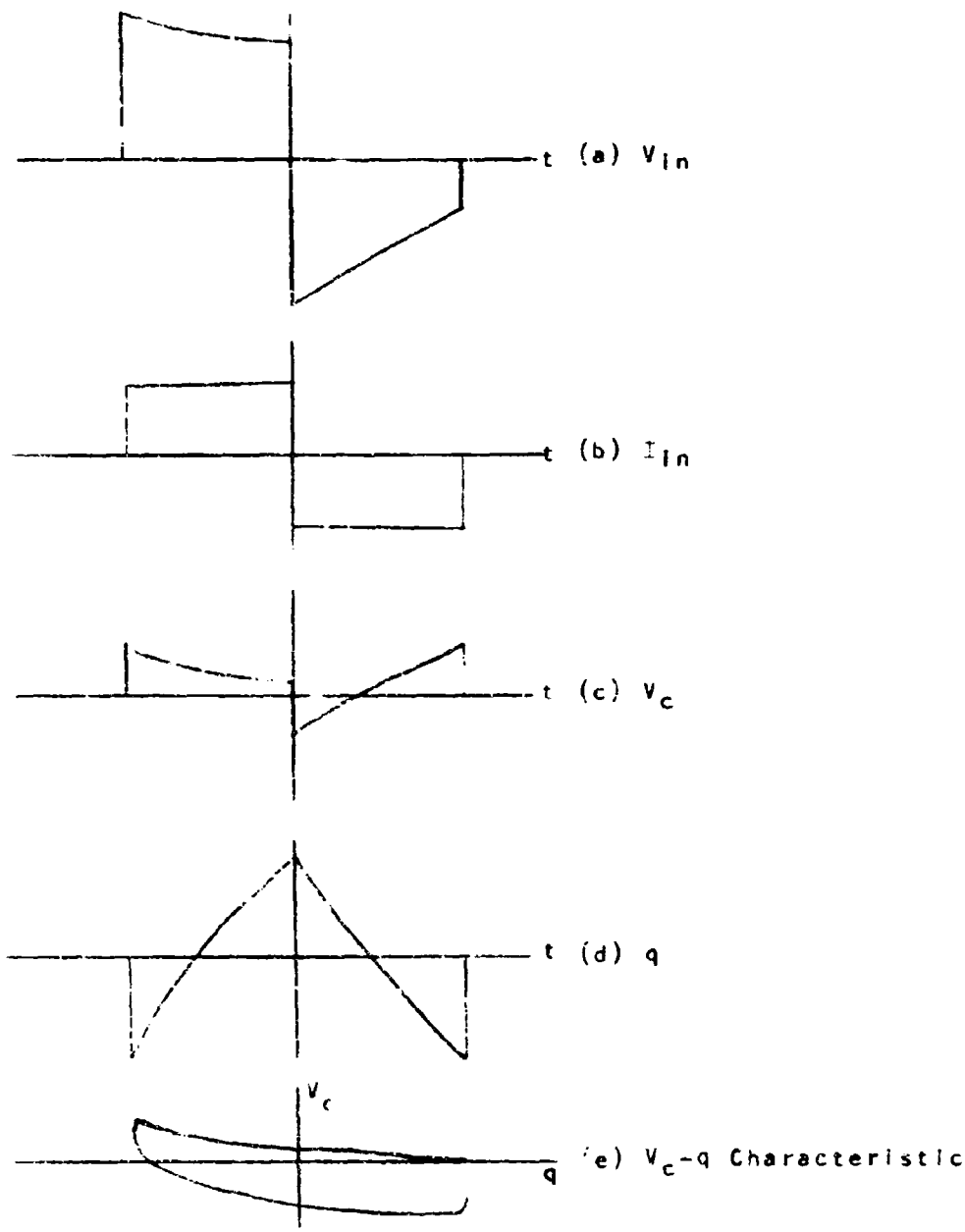

Fig. 3.20. Waveforms--Large Signal

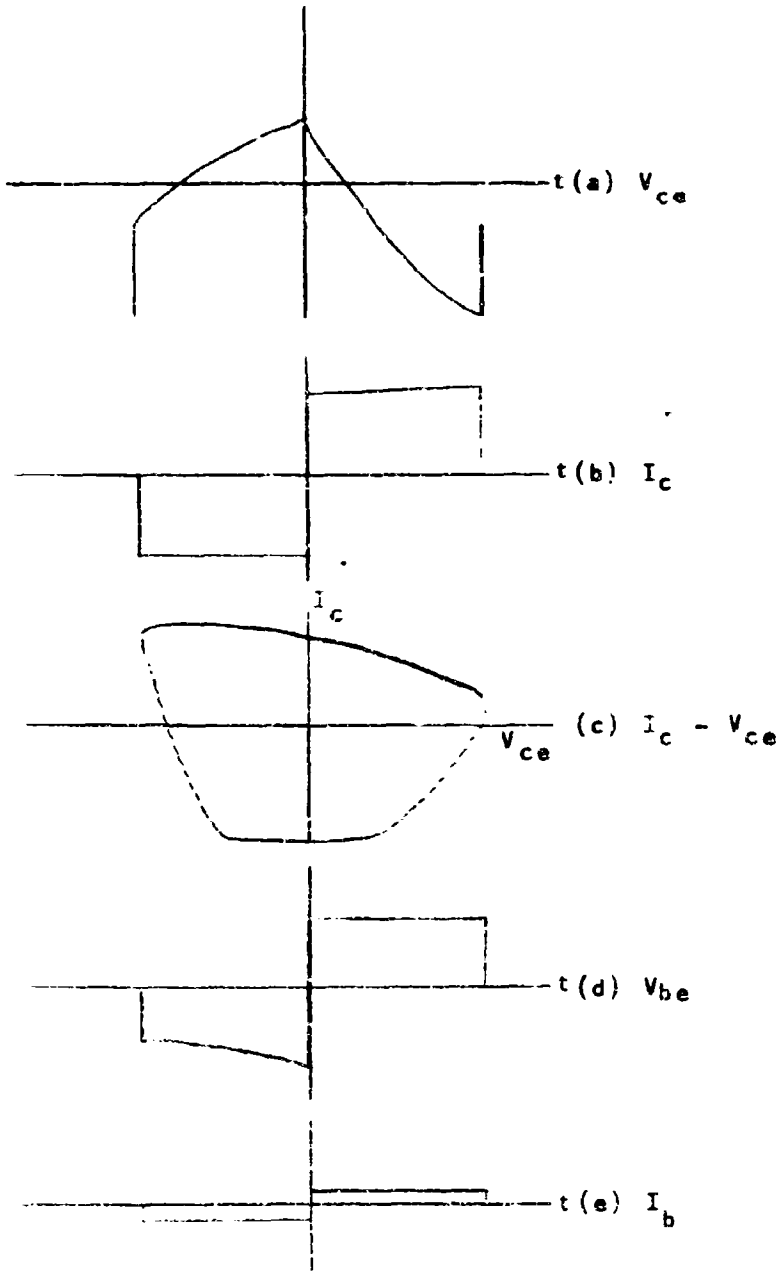

Fig. 3.21. Large Signal Operation

magnitude that the transistor operation is essentially linear. For the second set of waveforms the source amplitude has been increased until a high level of distortion is present.

A square wave source was chosen for this part of the study since it was decided that the waveforms would be more easily interpreted than if the source were sinusoidal. The following data apply to Figs. 3.18 through 3.21 also:

Square wave frequency: 2 KC

Q point (2N118A transistors): I_c = 1.5 ma ; v_{ce} = 20 V

Small-signal open circuit source voltage: 2.3 v_{ptp}

Large-signal open circuit source voltage: 7.2 v_{ptp}

Waveforms of the voltages listed below are given for each of the two case . For convenience these voltages are defined in Fig. 3.17. The waveforms are presented only for the input transistor, T-1 (see Fig. 3.2), since this transistor begins to operate in a nonlinear fashion before the other transistor does. The waveforms shown are:

1. Input voltage, v_{in}
2. Input current, I_{in} (Presented as voltage across 100Ω)
3. Capacitor voltage, v_c
4. Capacitor charge, q
5. q-v_c characteristic
6. Collector voltage, v_{ce}
7. Collector current, I_c (Presented voltage across 150Ω)
8. Base-emitter voltage, v_{be}

9. Base current, I_b (Presented as voltage across 100Ω)

10. $I_c - v_{ce}$ characteristic.

Only the AC portion of these waveforms are given. Knowledge of the Q point and the oscilloscope sensitivity can be used in most cases to determine total voltages and or currents.

Figures 3.18(a),(b),(c),(d) show the relationship between input voltage and current and the negative-capacitance voltage and charge under small-signal operation. Note that during the half cycle when current is positive charge is increasing, however, v_{in} and the voltage across the capacitance, v_c, are decreasing. This indicates that the capacitance is indeed negative. Figure 3.18(e) indicates that the capacitance is not only negative but is essentially constant for this amplitude of driving force.

Figure 3.19 shows transistor voltage and current waveforms under the same conditions as Fig. 3.18. From Fig. 3.18(c) it is seen that the total collector-emitter voltage swing about the Q point is approximately .25 volt while the collector-current varies about 6 ma above and below the Q point. This is a rather large current swing but practically no voltage swing at all. This the loadline for transistor T-1 is almost a vertical line.

The waveforms in Fig. 3.20 are for large signal operation. Figure 3.20(a) shows the distortion that is present in the input voltage. Figures 3.20(b) and (d) indicate that the

current and the charge are reasonably undistorted. However, Fig. 3.20(c) obviously does not reveal a triangular voltage across the capacitance. Actually Fig. 3.20(c) is not strictly the capacitance voltage since the effects of the nonlinear resistor, R_x, are present in this waveform as well as the nonlinearity of the capacitance, C_x. For this same reason Fig. 3.20(c) is not truly the q-v_c characteristic, although the negative slopes of this plot do indicate that the capacitance is still negative.

Figure 3.21 shows transistor currents and voltages under large signal operation. The principal cause of distortion can be seen from either Fig. 3.21(b) or Fig. 3.21(c); i.e., on the negative half cycle of collector current, the collector current goes to zero. Although not obvious from Fig. 3.21(a), the base current is also driven to zero at the same time that the collector current is zero.

3.8 Conclusions

A theoretical investigation has been made of the class of circuits which contains lumped models of a potentially realizable nonlinear negative capacitance in series with resistive, capacitive and inductive loads. This series combination is driven by a voltage source with nonzero internal resistance. The lumped models of the realizable NNC consist of all combinations of one positive linear resistor, one positive linear inductor and a hypothetical nonlinear capacitor. Two of these

networks are found to be stable on a small signal basis, i.e., when the amplitude of signal variations are assumed to be small enough that the nonlinear capacitor actually appears to be negative and linear.

When the model of the negative capacitance in each of these two networks is assumed to contain no inductance the networks become identical. When the resultant network is driven from a soldering iron entry it is capable of voltage amplification, and it is also capable of capacitance cancellation; that is, the negative capacitance can be used to cancel the effect of capacitive reactance due to a positive capacitor. When this RC network is driven from a pliers entry it is capable of current amplification as well as capacitance multiplication. The phenomenon of capacitance multiplication may be practically significant in microelectronic circuitry, since, in the present state of the art, the values of deposited capacitors are on the order of picofarads. A negative capacitance might be used to increase significantly the effective deposited capacitance, thus allowing the circuit designer to work with a much wider range of capacitor values.

Both phase plane analysis and Bendixson's negative criterion have been used to prove that none of the second order networks can be made to support an undamped oscillation due to the inclusion of the nonlinear capacitance. These proofs and energy considerations have been used to show that none of the third order networks are capable of oscillation.

Singular point analysis indicates that all of these networks have two stable singularities; hence, all are potential switching circuits; however, it is pointed out that some of the networks would make more practical switches than other networks due to the fact that the location of the singular points can be changed by varying the constant voltage applied to the network. One of these circuits has been simulated on an analog computer, and switching action from each stable singularity to the other one has been demonstrated. The amplitude of the switching pulse as well as its duration has been onsidered in this study. Such a capacitance should be quite useful as a lossless storage device, for when the capacitor is in either of its stable states no current flows, hence no power is dissipated.

Nonlinear negative capacitance has been produced in the laboratory by means of a negative impedance converter circuit. This NNC has the expected dissipative element associated with it as well as parasitic positive shunt capacitance. The lumped model predicted analytically has been verified by both AC steady state and transient measurements. At the frequencies used for testing no inductive effect is expected or noted in measurements. Use of this realizable negative capacitance as a circuit element has been demonstrated by measurements made to confirm capacitance cancellation and multiplication.

Waveforms of the various transistor voltages and currents are presented under both small signal and large signal operation to point out the nonlinear effect of the transistors in the NIC circuit.

B I B L I O G R A P H Y

Barbiere, R. G. "A Graphical Analysis of a Nonlinear RC Phase Shift Feedback Circuit," Proc. IRE, Vol. 43 (June, 1955), pp. 679-683.

Cote and Oaks. Linear Vacuum Tube and Transistor Circuits. New York: McGraw-Hill Book Company, Inc.

Cunningham, W. J. Introduction to Nonlinear Analysis. New York: McGraw-Hill Book Company, Inc., 1958.

Dewitt and Rossoff. Transistor Electronics. New York: McGraw-Hill Book Company, Inc., 1957.

Grahm D. and McRuer, D. Analysis of Nonlinear Control Systems. New York: John Wylie and Sons, Inc., 1961.

Kyhl, R. L., et al. "Negative L and C in Solid State Masers," Proc. IRE, Vol. 50 (July, 1962), pp. 1608-1623.

Larky, A. I. "Negative Impedance Converters," Trans. IRE on Circuit Theory, Vol. (Sept., 1957), pp. 124-131.

Levinson, N. and Smith, O. K. "A General Equation for Relaxation Oscillations," Duke Math. Journal, Vol. 9 (1942), pp. 382-403.

Linvill, J. G. "Transistor Negative Impedance Converters," Proc. IRE, Vol. 41 (June, 1953), pp. 725-729.

_____. "RC Active Filters in Which the N:C Uses Transistors," Proc. IRE, Vol. 42 (March, 1954), pp. 555-564

Lundry, W. R. "Negative Impedance Circuits--Some Basic Relations and Limitations," Trans. IRE PGCT, (Sept., 1957), pp. 132-139.

Manly, J. M. and Rowe, H. E. "Some General Properties of Nonlinear Elements," Proc. IRE, Vol. 44 (July, 1956), p. 904.

McDonald, J. R. and Brachman, M. K. "The Charging and Discharging of Nonlinear Capacitors," Proc. IRE, Vol. 43 (Jan., 1955), p. 71 and Correction Proc. IRE, Vol. 43 (June, 1955), p. 741.

Merrill, J. L. "Theory of Negative Impedance Converters," Bell System Technical Journal, Vol. 30 (Jan., 1951), pp. 88-109.

Minorsky, N. Nonlinear Oscillations. New York: D. Van Nostrand Company, Inc., 1962, p. 82ff.

Rowe, H. E. "Some General Properties of Nonlinear Elements II, Small Signal Theory," Proc. IRE, Vol. 46 (May, 1958), pp. 850-860.

Thomsen, J. S. and Schlesinger, S. P. "Analysis of Nonlinear Circuits Using Impedance Concepts," Trans. IRE, PGCT, CT2 (Sept., 1955), p. 271ff.

BLANK PAGE

Security Classification

DOCUMENT CONTROL DATA - R&D

(Security classification of title, body of abstract and indexing annotation must be entered when the overall report is classified)

1 ORIGINATING ACTIVITY (Corporate author)	2a REPORT SECURITY CLASSIFICATION
Laboratories for Electronics and Related Science Research The University of Texas, Austin	Unclassified 2b GROUP

3 REPORT TITLE

A STUDY OF NONLINEAR NEGATIVE CAPACITANCE

4 DESCRIPTIVE NOTES (Type of report and inclusive dates)

Technical Report No. 5, August 16, 1965

5 AUTHOR(S) (Last name, first name, initial)

Wright, Charles Lester, Graduate Student, Candidate for Ph.D. degree in Electrical Engineering, Ford Foundation Fellow

Harbourt, Cyrus O. Associate Professor of Electrical Engineering

6 REPORT DATE	7a TOTAL NO. OF PAGES	7b NO. OF REFS
August 16, 1965	110	18

8a CONTRACT OR GRANT NO.	9a ORIGINATOR'S REPORT NUMBER(S)
AF-AFOSR 766-65 b PROJECT NO.	JSEP, Technical Report No. 5
c d	9b OTHER REPORT NO(S) (Any other numbers that may be assigned this report)

10 AVAILABILITY/LIMITATION NOTICES

Qualified requesters may obtain copies of this report from DDC

11 SUPPLEMENTARY NOTES	12 SPONSORING MILITARY ACTIVITY
Includes research monitored by the Dept. of Defense's Joint Services Electronics Program through the Tech. Advisory Committee (U.S. Army, Navy, and Air Force.)	U. S. Air Force Office of Scientific Research, Washington, D. C. 20333, and others.

13 ABSTRACT An analytical study is made of the behavior of a certain class of RLC networks which contain a theoretical nonlinear negative capacitance along with various possible combinations of constant parasitic elements that are certain to be present in any physical realization of this type of capacitance. The theoretical capacitor is defined in terms of its charge-voltage relationship, i.e., $e = -aq + bq^3$, where e is the voltage across the terminals of the capacitor, q is the charge associated with the capacitor, and a and b are arbitrary, positive, real constants.

This study is directed toward an evaluation of the usefulness of a nonlinear negative capacitance in a network to accomplish either amplification or oscillation or switching.

In order for a network to be useful as an amplifier, its small-signal model must be stable. Therefore, for this part of the study the nonlinear capacitor is represented by a linear, negative capacitance. Of the 24 networks defined for this study only 2 are found to be possibly stable. Both of these networks, and only these networks, have a positive capacitor in series with the assumed negative capacitor.

Singular point analysis discloses that any of the defined networks may have 2 stable equilibrium points. This is the basic criterion for a bistable device, so the conclusion is that nonlinear capacitance, like nonlinear resistance, can be used effectively to construct a switching circuit. Phase plane plots of one of the second order networks are included to illustrate switching from each stable singularity to the other.

It is proven by phase plane methods that none of the second order systems can support a sustained oscillation. An argument based on energy relationships and on the nonoscillatory nature of the second order networks is presented to show that none of the third order networks can serve as oscillators. Hence, the results here indicate that, unlike negative resistance, negative capacitance cannot be used as the mechanism by which oscillation is induced in a passive network which contains dissipative elements.

A nonlinear negative capacitance has been realized by means of a transistor negative impedance converter circuit. From analysis of the negative impedance converter, the lumped model of the negative capacitance is predicted to be a nonlinear, frequency-dependent resistor in series with a nonlinear, frequency-dependent negative capacitance. The locus of the tip of the complex impedance, as a function of frequency, is predicted in this analysis; this locus was subsequently verified by steady state measurements in the laboratory. Although not considered in the analytical study, the effect of unavoidable stray capacitance was seen in the experimental results.

The square wave response of the negative impedance converter is also obtained, and a relationship between the steady state square wave response and the values of the model is derived.

DD FORM 1 JAN 64 1473

Security Classification

Security Classification

14 KEY WORDS	LINK A		LINK B		LINK C	
	ROLE	WT	ROLE	WT	ROLE	WT
CAPACITANCE CANCELLATION						
CAPACITANCE MULTIPLICATION						
CURRENT AMPLIFICATION						
LOSSLESS STORAGE DEVICE						
LUMPED MODELS (positive linear resistor, positive linear inductor, hypothetical nonlinear capacitor)						
MICROELECTRONIC CIRCUITRY						
NEGATIVE IMPEDANCE CONVERTER						
OSCILLATION						
SWITCHING ACTION						
NONLINEAR NEGATIVE CAPACITANCE						
VOLTAGE AMPLIFICATION						
WAVE FORMS (negative capacitance)						

INSTRUCTIONS

1. ORIGINATING ACTIVITY: Enter the name and address of the contractor, subcontractor, grantee, Department of Defense activity or other organization *(corporate author)* issuing the report.

2a. REPORT SECURITY CLASSIFICATION: Enter the overall security classification of the report. Indicate whether "Restricted Data" is included. Marking is to be in accordance with appropriate security regulations.

2b. GROUP: Automatic downgrading is specified in DoD Directive 5200.10 and Armed Forces Industrial Manual. Enter the group number. Also, when applicable, show that optional markings have been used for Group 3 and Group 4 as authorized.

3. REPORT TITLE: Enter the complete report title in all capital letters. Titles in all cases should be unclassified. If a meaningful title cannot be selected without classification, show title classification in all capitals in parenthesis immediately following the title.

4. DESCRIPTIVE NOTES: If appropriate, enter the type of report, e.g., interim, progress, summary, annual, or final. Give the inclusive dates when a specific reporting period is covered.

5. AUTHOR(S): Enter the name(s) of author(s) as shown on or in the report. Enter last name, first name, middle initial. If military, show rank and branch of service. The name of the principal author is an absolute minimum requirement.

6. REPORT DATE: Enter the date of the report as day, month, year, or month, year. If more than one date appears on the report, use date of publication.

7a. TOTAL NUMBER OF PAGES: The total page count should follow normal pagination procedures, i.e., enter the number of pages containing information.

7b. NUMBER OF REFERENCES: Enter the total number of references cited in the report.

8a. CONTRACT OR GRANT NUMBER: If appropriate, enter the applicable number of the contract or grant under which the report was written.

8b, 8c, & 8d. PROJECT NUMBER: Enter the appropriate military department identification, such as project number, subproject number, system numbers, task number, etc.

9a. ORIGINATOR'S REPORT NUMBER(S): Enter the official report number by which the document will be identified and controlled by the originating activity. This number must be unique to this report.

9b. OTHER REPORT NUMBER(S): If the report has been assigned any other report numbers *(either by the originator or by the sponsor)*, also enter this number(s).

10. AVAILABILITY/LIMITATION NOTICES: Enter any limitations on further dissemination of the report, other than those imposed by security classification, using standard statements such as:

(1) "Qualified requesters may obtain copies of this report from DDC."

(2) "Foreign announcement and dissemination of this report by DDC is not authorized."

(3) "U. S. Government agencies may obtain copies of this report directly from DDC. Other qualified DDC users shall request through _____."

(4) "U. S. military agencies may obtain copies of this report directly from DDC. Other qualified users shall request through _____."

(5) "All distribution of this report is controlled. Qualified DDC users shall request through _____."

If the report has been furnished to the Office of Technical Services, Department of Commerce, for sale to the public, indicate this fact and enter the price, if known.

11. SUPPLEMENTARY NOTES: Use for additional explanatory notes.

12. SPONSORING MILITARY ACTIVITY: Enter the name of the departmental project office or laboratory sponsoring *(paying for)* the research and development. Include address.

13. ABSTRACT: Enter an abstract giving a brief and factual summary of the document indicative of the report, even though it may also appear elsewhere in the body of the technical report. If additional space is required, a continuation sheet shall be attached.

It is highly desirable that the abstract of classified reports be unclassified. Each paragraph of the abstract shall end with an indication of the military security classification of the information in the paragraph, represented as *(TS)*, *(S)*, *(C)*, or *(U)*.

There is no limitation on the length of the abstract. However, the suggested length is from 150 to 225 words.

14. KEY WORDS: Key words are technically meaningful terms or short phrases that characterize a report and may be used as index entries for cataloging the report. Key words must be selected so that no security classification is required. Identifiers, such as equipment model designation, trade name, military project code name, geographic location, may be used as key words but will be followed by an indication of technical context. The assignment of links, rules, and weights is optional.